Generating hair follicle inductive dermal papillae cells from adipose derived mesenchymal stem cells

Dr Alice Clare Brown

Supervisors:

Prof. S. Kidson

Dr R. Ballo

Presented in fulfilment of the requirements for the degree of

Master of Science in Medicine

Division of Cell Biology

Department of Human Biology

Faculty of Health Sciences

University of Cape Town

October 2017

Declaration

I, Alice Clare Brown, hereby declare that the work on which this dissertation/thesis is based is my original work (except where acknowledgements indicate otherwise) and that neither the whole work nor any part of it has been, is being, or is to be submitted for another degree in this or any other university.
I empower the university to reproduce for the purpose of research either the whole or any portion of the contents in any manner whatsoever.

Signature: Signed by candidate Date: 25.06.2018

Acknowledgments

The thought of trying to express in words how grateful and appreciative I am to all the people who have carried me through to submitting this thesis today is very daunting. Hopefully I can try and do justice to the contribution of each one of you.

To my mother, thank you for your unconditional love and for the selfless work you do for your children every day of your life. You have always been my greatest supporter. You have picked me up when I have fallen and put me back together again more times than I can count. You have listened with interest to the stories of my day and you have pushed me to become the best version of myself by seeing that version in me before even I can. My enquiring mind and thirst for knowledge comes from you. Everything you do, as a mother, as a wife and as a friend and as a business woman you do with excellence and I am immeasurably proud to be your daughter.

To my father, you have always set the most incredible example for me. Your limitless compassion, tireless hard work, commitment to learning and providing the best possible standard of care to your patients have inspired me since I was a little girl. Thank you for everything you have done and continue to do for me. I try every day to fill your shoes, both as a doctor and as a person, and I hope one day to come somewhere close.

My sister Sara, needs special mention for all the effort, time and skill she has put into helping me to format and edit this thesis. She has accomplished this, as she does everything, with excellence and with grace. I am so deeply grateful for your help, I truly don't know what I would have done without you.

To my husband, Brandon, this thesis is as much mine as it is yours. Thank you for always making me feel that there is no limit to what I can achieve. Thank you for smoothing my journey in every possible way and for all the ways you support me and even carry me. Thank you for your love and for giving me the bright future that we are both working towards. Your wisdom, tolerance and the love you show to every single person in your life are an example to me. Every day I love you more and every day I feel luckier to have met you.

This work would not have been possible without the funding generously provided by the Medical Research Council through the Flagship Grant that was awarded to Professor Michael Pepper and Professor Sue Kidson as well as the National Research Foundation grant that was awarded to Prof Sue Kidson. I hope to be able in the years to come to do justice, both as a scientist and a doctor to the opportunity and learning these funds have afforded me.

Thank you also to Prof Michael Pepper, not only for his invaluable donation of adipose derived stem cells, but also for all the resources and advice he so willingly shared with us.

To the members of the Kidson lab. Dimakatso, I am deeply grateful for your endless sunshiny presence, warm and nurturing nature and selflessness in constantly helping me with all the things I could not do. Dennis, I am not sure what I would have done with your technical assistance, generous help with getting papers and constant affirmation and advice. Thuli, you were and are such a vital member of the Kidson lab – you taught me more than you will know and all your hard work, efficiency and positivity form the basis of the functioning of this lab. Austin, it was such a pleasure to have you join our lab. Your quiet hard work, endless good humour

and intelligence are an example to us all. Claire, thank you for patiently and effortlessly doing all that you do for our lab, we are so lucky to have you. To each and every one of you I would like to take this opportunity to tell you how much I admire and respect you. I feel so grateful to have worked with you and I feel so lucky to call you all my friends.

To Robes. Every single thing that happens in the Kidson lab happens under your watchful eye, endless dedication and caring direction. Thank you for teaching me, with endless patience, the molecular techniques in a cell biologist's armament – I cannot imagine that I could have taught by anyone with more technical excellence. Thank you for your kindness and support, for always being available and having time to help me with the smallest and the biggest query. Thank you for your tireless effort in the running of every single facet of the lab. The students who pass through the Kidson Lab are incredibly blessed to have you.

To Sue. Thank you for welcoming me into your lab from the first day I contacted you. The nurturing, enquiring atmosphere of the Kidson lab comes from you. To me your intellect, endless hunger for new knowledge and relentless pursuit of the truth are the epitome of what a scientist should be. To add to that you are kind, you are wise and you are fair. Thank you for creating an environment in the Kidson lab where everybody's opinion is equal, no question is too stupid or small to be asked and the contribution of every member is valued. With your guidance and teaching, a whole new dimension has been added to my view of human biology, my ability to interrogate data and my capacity to learn and understand. I know that this addition will be an invaluable addition to my work as a doctor. I am grateful for every minute that I was able to spend with you, discussing not only my thesis, but exciting new developments in the world of science and life in general and I hope that there will be many more such moments in the future. You are truly an example of the person, and academic that I would like to be

Table of Contents

List of Figures

List of Tables

Abstract

Current management options for cutaneous burn wounds, including split thickness skin grafts and cultured epithelial autografts, generate an epithelial barrier which lacks a dermal layer and skin adnexae including hair follicles and sebaceous glands. This results in a loss of pliability and contractures that cause functional and cosmetic impairment. Embryological hair follicle morphogenesis results from a complex series of mesenchymal-epithelial interactions and to date a method of generating de novo folliculogenesis from human cells has yet to be accomplished. Existing models rely on combining 'inductive' dermal and 'receptive' epithelial components and placing them within a suitable model. Epithelial cells are easily obtainable from skin biopsies therefore obtaining sufficient quantities of 'trichogenic' dermal cells remains the most significant challenge of this approach. The main aim of this project is to contribute to the achievement of de novo folliculogenesis by generating dermal papillae (DP) like-spheroids using adipose derived mesenchymal stem cells (ASCs) that, when combined with responsive epithelial cells, would be capable of inducing hair follicle formation.

ASCs were directed towards a hair follicle DP-like fate by culture using the hanging drop method and exposure to Wnt, mimicking signalling and mesenchymal condensation in embryological hair follicle induction. Gene expression analysis using RT-PCR showed that the DP-cell marker Versican is expressed at high levels in ASCs under routine culture conditions and the exposure of ASCs to Wnt results in a more than threefold increase in this expression. These results suggest that Wnt/β-catenin signalling may regulate DP cell aggregative growth through modifying versican expression possibly through binding of β-catenin to the TCF transcription factor complex. Culture of ASCs using the hanging drop method produces spheroids similar in size to human hair follicle DP. Histology of these spheroids demonstrates viable cells that flatten around the outside. The spheroids grow out when replated onto Matrigel in a 3D culture model and exhibit a morphology similar to that of primary hair follicle DP cells. Analysis of mRNA expression demonstrates that Versican expression is significantly upregulated in DP-like spheroids in the absence or presence of Wnt demonstrating that Versican may be responsible for both induction and maintenance of mesenchymal cell condensates. Alpha smooth muscle actin is expressed in low levels in ASC spheroids compared to ASCs in a monolayer and this may reflect a 'migratory' myofibroblast like phenotype of ASCs in a monolayer similar to cells with the hair follicle dermal sheath. The addition of Wnt to ASC spheroids has no additional effect on Versican expression possibly reflecting a negative feedback loop resulting from high local concentrations of endogenous Wnt expression from ASCs. The results of this study show that spheroid cell culture and exposure to Wnt of ASCs results in cell clusters with similar morphology and gene expression to hair follicle DP cells. The novel method of DP-like cell generation described in this study makes use of cells that are readily obtainable from patients and require minimal time and manipulation in culture and therefore could potentially be rapidly translatable to clinical trials

Chapter 1: Introduction, Literature Review and Aims

1.1. The problem statement

In South Africa, 3.2 % of the population sustain cutaneous burn wounds annually. Fifty percent of these burn victims are younger than 20 years of age (Albertyn et al., 2006). Poverty, mass illiteracy and urbanization with the development of shanty towns are all factors that have led to an increase in burns in South Africa in the past decade (Albertyn et al., 2006). Deep partial thickness and full thickness burns result in the destruction of the entire epidermis and dermis and, due to the absence of epithelial stem cells in the stratum basale and the hair follicle bulge, these structures have no capacity for healing (Figure 1.1). Full thickness skin grafting is a viable option for small burn wounds but is limited by donor site shortage. The standard for efficient and permanent closure of deeper burns is a split-thickness skin graft from an uninjured donor site on the same patient (autograft)(Cramer et al., 1962). In a split-thickness skin graft, sections of skin containing the epidermis and a portion of the dermis are harvested, meshed to increase the coverage area and then placed over the debrided wound bed.

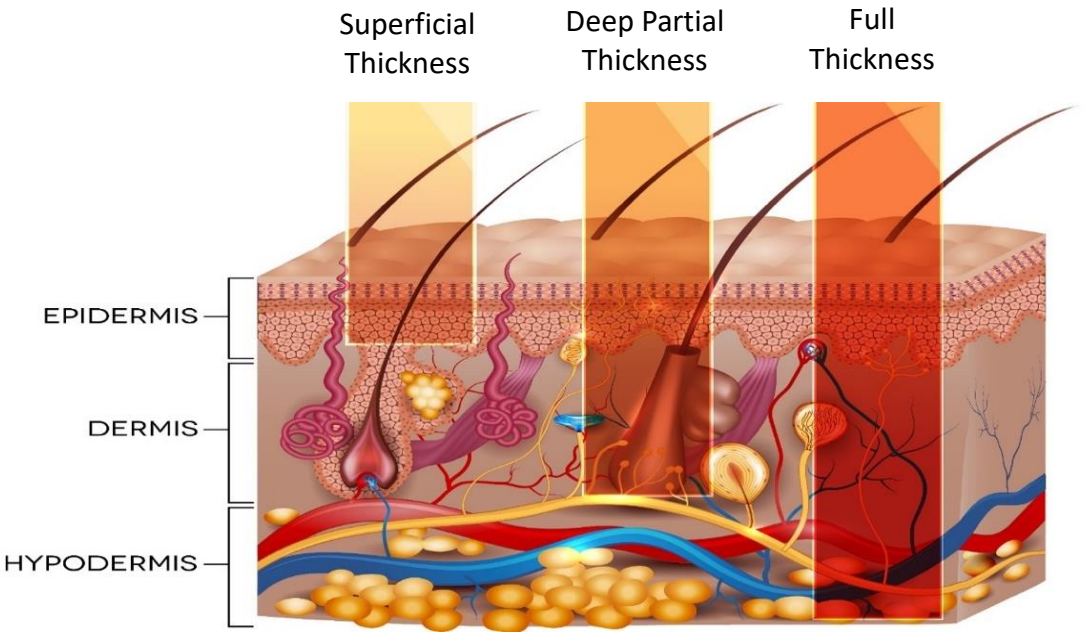

Figure 1.1: Classification of burn wounds based on injury depth. Schematic showing the layers of the skin and their involvement in various burn wounds. Superficial wounds are limited to the epidermis. Superficial partial thickness burns, involving the entire dermis and the top third of the dermis are not shown. Deep partial thickness wounds involve the entire epidermis and the majority of the dermis. Full thickness burns involve complete destruction of the epidermis and dermis and may extend to the underlying structures including muscle, tendon and bone. Both deep partial thickness and full thickness burns require excision and grafting as epithelial stem cells from the stratum basale and hair follicle have been destroyed preventing re-epithelialization and wound closure. (Image used under licence from Shutterstock.com)

Treatment of burn wounds with split thickness skin grafts results in severe scarring and functional limitation (Forjuoh, 2006). Due to the poor cosmetic and functional results of current management options, non-fatal burn wounds from full and partial thickness burns are a leading cause of disability-adjusted life-years (DALYs) lost in low and middle income countries. This results from prolonged hospitalisation, disfigurement and physical disability with resulting stigma and rejection (Peck, 2011).

One of the main reasons for the poor cosmetic and functional results of current cutaneous burn wound management options is that although split-skin grafts result in the generation of an epidermal barrier, they are limited by the absence of a functional dermis and the skin appendages that reside within it. The dermis conveys the durability and elasticity of skin while hair follicles and their associated sebaceous glands are a repository of epithelial and melanocyte stem cells and confer the lubrication and pliability that are vital components of the cosmetics and functionality of normal skin.

1.2. Biology and function of the hair follicle

Hair follicles have important roles in thermoregulation, physical insulation, sensitivity to noxious stimuli and social communication (Schneider et al., 2009). In addition, the associated pilosebaceous unit provides the lubrication that confers the flexibility and suppleness of normal skin (Niemann and Horsley, 2012). The importance of the hair follicle in skin biology does not rest solely with its ability to produce hair. In 1945, the neuroanatomist Bishop self-inflicted cutaneous wounds on his forearm and observed the vital role played by hair follicles in wound healing, including the fact that re-epithelialization starts around hair follicles and that scar formation only occurs in cutaneous wounds when the depth of the wound is such that the bases of hair follicles are destroyed (Bishop, 1945). Multiple different mechanisms are currently recognised for the contribution of hair follicles to wound healing. Hair follicles are self-renewing and contain reservoirs of multipotent stem cells that are capable of regenerating the epidermis (Millar, 2002). Stem cells from the hair follicle bulge respond to wound healing by migrating upwards from the lower isthmus to the interfollicular epidermis of the wound site surface and recruiting and mobilising stem cell progeny for acute repair (Ito et al., 2005). As epidermal appendages, hair follicles are highly vascularised and innervated and promote angiogenesis and re-innervation of the wounded area through paracrine signalling and cell precursors (Plikus et al., 2012). Mesenchymal precursors from the dermal papilla and dermal sheath are recruited at later stages of wound healing to aid in dermal and extracellular matrix remodelling (Jimenez et al., 2015).

In view of the critical contribution of hair follicles in successful cutaneous wound healing and in the functioning and aesthetics of normal human skin, it is evident that the absence of hair follicles represents a major stumbling block in current burn wound management. However, despite the challenge of *de novo* hair follicle generation being a target of a significant proportion of ongoing burn research, the intricate and deeply complex nature of hair follicle morphogenesis has dictated that this has yet to be accomplished. After wounding, hair follicles form *de novo* in genetically normal adult

mice with nascent hair follicles arising from epithelial cells outside of the hair follicle stem cell niche suggesting that epidermal cells within the wound assume a hair follicle stem cell phenotype (Ito et al., 2007). To achieve *de novo* hair follicle morphogenesis it is necessary to recapitulate, in the correct sequence, the finely regulated contextual and molecular clues in the primitive human skin that result in embryological hair follicle formation.

1.3. Embryological hair follicle morphogenesis

As previously mentioned, embryological hair follicle morphogenesis relies on a complex series of mesenchymal-epithelial interactions (Hardy, 1992). In humans, the process is initiated in the 10th week of development with complete follicle formation obtained by the 22nd week (Sennett and Rendl, 2012). The reciprocal interaction between the mesenchyme and the epithelium is an evolutionary ancient process that is necessary for the development of all ectodermal appendages across all species including scales, feathers, nails and teeth (Wu et al., 2004).

Morphologically hair folliculogenesis may be broadly divided into induction, organogenesis and cytodifferentiation phases with these being further subdivided into at least eight distinct developmental stages (Muller-Rover et al., 2001). In the skin prior to folliculogenesis the ectoderm is an undifferentiated epithelium with gradients of inhibitors and activators establishing an inductive field (Millar, 2002). Between the 8th and the 10th week of development the first induction signal is relayed from the mesodermal mesenchyme (dermis) to the ectodermal epithelium (epidermis) through β-catenin, the degradation of which is prevented by Wnt signalling molecules (Fuchs, 2007)(Figure 1.2 i).

Understanding the patterning involved in hair follicle development has long presented a challenge to developmental biologists. Recent work by Glover et al. (2017) seems to confirm that a Turing diffusion-response signalling system exists where interacting signals diffusing from static cells first delineate a pre-pattern that then causes cell repositioning to create an anatomical structure. The signalling involved includes a network of fibroblast growth factor (FGF), wingless-related integrating site (WNT) and bone morphogenetic protein (BMP) signalling. In response to this signalling, a small collection of epithelial cells known as an 'epithelial placode' appear in the otherwise homogenous epithelium (Figure 1.2 ii).

Epidermal placodes now signal to the underlying dermis, causing aggregation of underlying mesenchymal cells creating the first dermal condensate using paracrine factors such as WNT signalling with subsequent downstream activation of Sonic Hedgehog (Huelsken et al., 2001)(Figure 1.2 iii). Fibroblast growth factor 20 (Fgf20) is one of the signalling molecules that is expressed in hair placodes and is induced by and functions downstream from epithelial ectodysplasin (Eda)/Edar and Wnt/b-Catenin signalling to initiate formation of the underlying dermal condensates (Huh et al., 2013). The epithelial placode together with the underlying dermal condensate of dermal fibroblasts is known as a hair germ. A second dermal signal, not yet clearly elucidated, stimulates and regulates proliferation and down-growth of the follicular epithelium into the dermis enveloping the dermal condensate forming the dermal papilla (St-Jacques et al., 1998). The structure is now known as the hair peg' which completes the stage of organogenesis (Figure 1.2 iv).

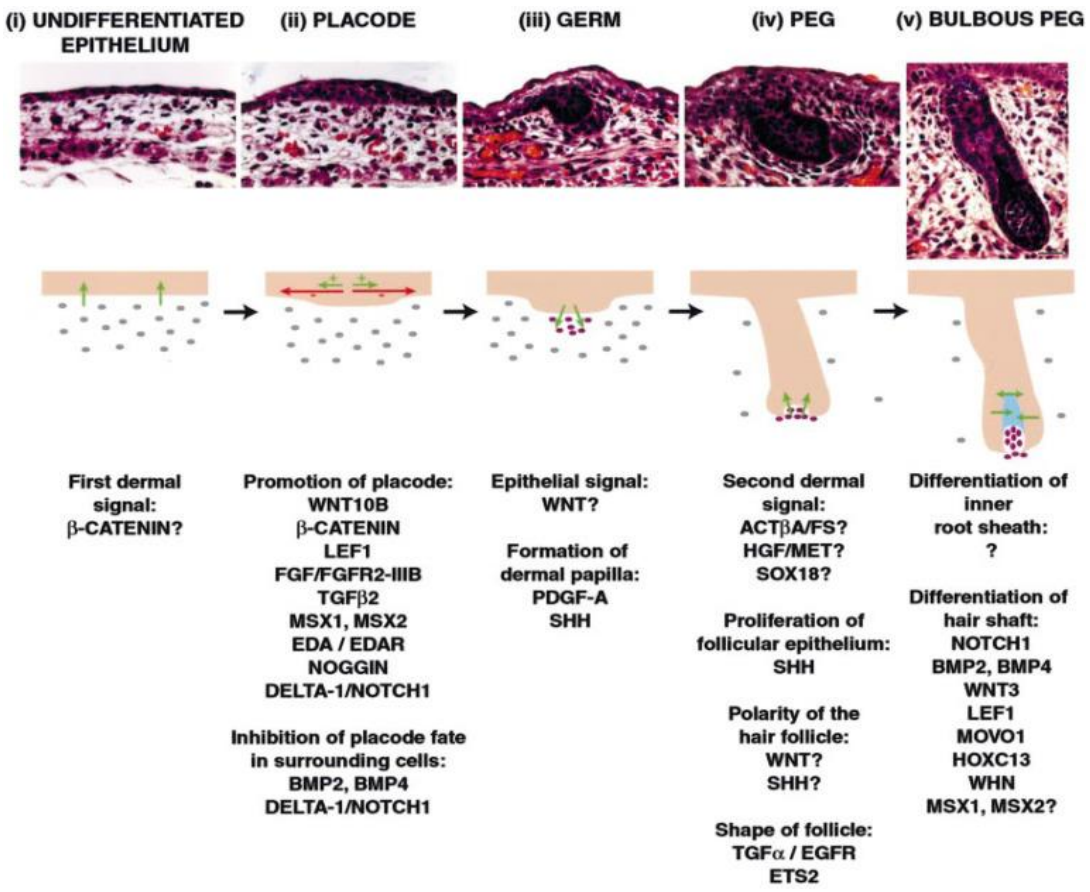

Figure 1.2: Embryological hair follicle signalling and morphogenesis. In the upper panels, haematoxylin and eosin staining of paraffin sections of primary mouse hair follicles at embryonic days 14.5 (undifferentiated epithelium and placode), 15.5 (germ and peg), and 18.5 (bulbous peg) are shown. The middle panels represent the developmental stages schematically, with intercellular signals depicted by coloured arrows, and molecules important for each stage listed below. (*i*) The first signal initiating hair follicle formation arises in the mesenchyme (grey dots) and instructs the overlying epithelium (pink stripe) to thicken, forming a placode. (*ii*) Placode formation is facilitated by promoting signals (+), shown as *green arrows*, and prevented in neighbouring epithelial cells by inhibitory signals (–), shown as *red arrows*. (*iii*) Signals from the epithelium result in the clustering of mesenchymal cells to form a dermal condensate (*purple dots*). (*iv*) the dermal condensate signals to the follicular epithelium to proliferate and grow down into the dermis. (*v*) The dermal condensate becomes surrounded by follicular epithelial cells to form the dermal papilla.(Image obtained from (Millar, 2002))

The final stage of folliculogenesis is cytodifferentiation which begins around the 13th week of gestation in humans. The superficial portions of the primitive hair follicles develop two distinct asymmetrical bulges of cells on the side of the follicle. The upper bulge will eventually form the sebaceous gland while the lower bulge will form the location of the presumptive follicular stem cells which will anchor the developing arrector pili muscle to the hair follicle. As the epidermal plug penetrates down into the dermis, mesodermal cells aggregate around it developing a fibrous follicular sheath, or collagen capsule, which encases the epidermal cells. The final stage of hair development is marked by significant growth of the hair itself. The hair fibre and the inner root

sheath elongate and the centre of the hair peg disintegrates and keratinizes allowing the cone of the central core of cells to move upwards, away from the bulb, with the hairs eventually erupting from the skin around the 22nd week of development (Paus et al., 1999).

1.4. Similarities between hair follicle morphogenesis and the hair cycle

The hair follicle undergoes regular cycles of growth (anagen) involution (catagen) and rest (telogen) throughout life (Hardy, 1992) with the anagen stage of hair follicle development mimicking embryological hair follicle induction. The formation of the new hair follicle at the initiation of each hair cycle begins with proliferation of secondary germ cells in the bulge of the hair follicle after inductive signals from the dermal papilla which moves upward during the telogen stage, coming to rest underneath the hair follicle bulge. So important is this translocation of the dermal papilla that if it fails to reach the bulge during this catagen stage, the follicle stops cycling and the hair is destroyed (Panteleyev et al., 1998).

As mentioned previously embryological hair follicle morphogenesis depends on intensive and reciprocal interactions between epithelial and mesenchymal components (Hardy, 1992). Currently, attempts to regenerate hair follicles centre on combining 'receptive' epithelial and 'trichogenic' dermal mesenchymal components and grafting them into an *in vivo* environment (Ohyama and Veraitch, 2013). Several models have been established for the study of dermal-epidermal interactions, as well as the reconstitution of hair follicles. Most hair reconstitution assays take place *in vivo* in immunodeficient host mice (Chuong et al., 2007). Despite these assays working well with mouse cells, regenerating human hair follicles is still a challenge that requires breakthroughs in several aspects. Obtaining epithelial cells for human hair follicle assays is relatively simple as epithelial cells have been shown to retain their responsiveness to dermal signalling into adulthood (Jahoda et al., 1984) and are readily expanded from donor sites. The current major challenge involves obtaining inductive dermal cells to model the trichogenic mesenchymal component of the hair follicle – dermal papillae (DP) and dermal sheath (DS) cells.

1.5. Dermal Papilla and Dermal Sheath

The dermal component of the hair follicle consists of the dermal papilla (DP) and the dermal sheath (DS). The DP is the mesenchymal cell condensation located at the proximal end of the hair follicle while the DS, or connective tissue sheath, lines the epithelium of the hair follicle from the bulge level, downward (Figure 1.3). The DP is contiguous with the base of the dermal papilla through a stalk and both cell populations are separated from the epithelial component of the hair follicle by a basement membrane. Both DP and DS cells are specialized fibroblasts. Fibroblasts in different body sites, and therefore DP, have different embryonic origins. Head and facial fibroblasts are derived from the neural crest, while trunk as ventral and dorsal trunk fibroblasts come from the dermomyotome of somitic and lateral plate origin respectively (Fernandes et al., 2004).

Hair follicle dermal papillae first arise as mesenchymal cell condensates in the dermis in response to epithelial placode formation and are termed hair follicle dermal papillae once encased by the epithelial cells at the base of the mature hair follicle (Yang and Cotsarelis, 2010). It is important to note that prior to dermal cells becoming morphologically identifiable as dermal condensates in the organogenesis stage, mesenchymal cells within the uniform dermis that will go to form part of the dermal condensate are responsible for the critical 'first dermal signal' initiating hair follicle formation.

Both hair follicle dermal papillae cells and dermal sheath cells possess distinctive morphology and display different properties *in vitro*. These properties include support for epidermal cell growth (Reynolds et al., 1991), aggregative behaviour in culture (Jahoda and Oliver, 1984) and upregulation of the same biomarkers. Critically, both dermal papillae cells and dermal sheath cells are 'trichogenic' or capable of inducing hair follicle formation in receptive epithelial cells.

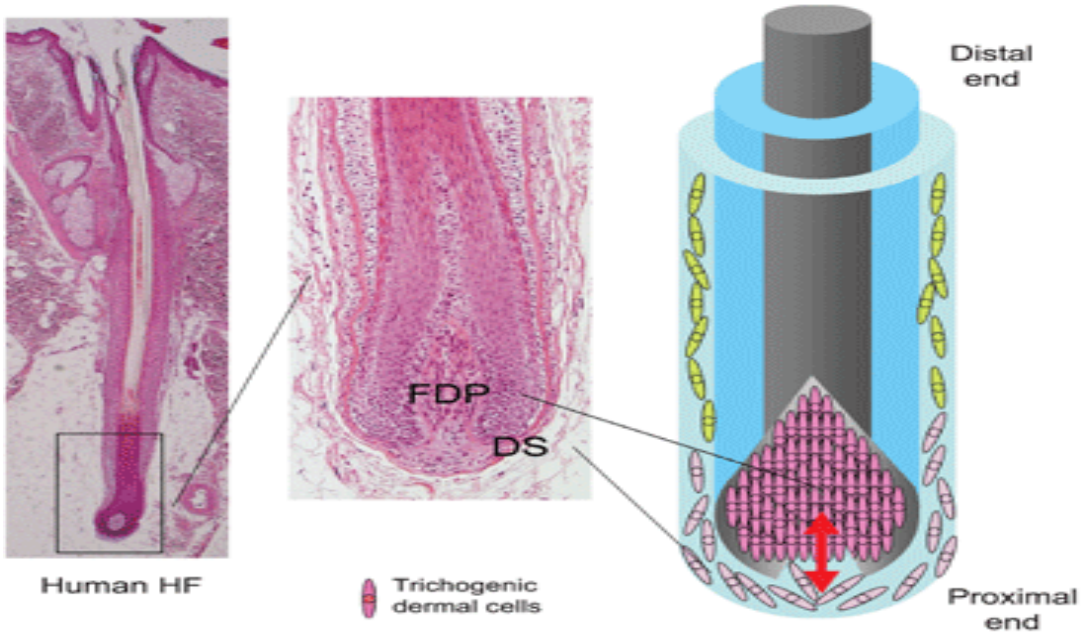

Figure 1.3: The trichogenic component of the hair follicle. A cluster of mesenchymal cells at the base of the hair follicle, the hair follicle dermal papilla (FDP) and a single layer of flattened mesenchymal cells contiguous with the FDP with a stalk, the dermal sheath (DS) retain the ability to induce hair follicle formation in responsive epithelial cells throughout life. Image from (Ohyama et al., 2010)

It has long been recognised that DP cells are capable of inducing hair follicle differentiation in epithelial cells and are required in hair reconstruction assays. The inductive property of dermal cells was first shown when DP were transposed beneath the upper half of amputated vibrissae hair follicles, without the bulb, and demonstrated regrowth of the whisker follicles (Oliver, 1967). Later, it was demonstrated that rat vibrissae DP, when implanted into the footpad of the adult rat, could induce *de novo* hair follicle neogenesis even in this afollicular epidermis (Oliver, 1970). In a landmark study, Reynolds et al. (1999) implanted DS from a male human scalp follicle into the arm of a female

recipient with the resultant formation of a new hair follicle. This allotransplant experiment was one of the first indications that DS and DP may enjoy a level of immune privilege and escape immune rejection (Paus et al., 2003). Further evidence for the inductive capability of dermal papilla cells was revealed in a skin reconstitution assay when keratinocytes and dermal cells are mixed and grafted onto a nude mouse host, hair follicles are formed in the reconstituted skin if active dermal papilla cells are included in the mixture. In their absence, smooth hairless skin is formed by the graft (Kamimura et al., 1997).

Although investigators have for many years sought the molecules that define the biological characteristics of hair follicle DP cells, with particular emphasis on those that confer their trichogenic capacity, the complexity of the hair inductive process has meant that a high throughput approach is required to fully elucidate the list of molecules that govern all of the events that are involved. Adopting differential screening of cDNA libraries, microarray analyses or proteonomics, several labs have identified the molecules up-regulated in rat (Sleeman et al., 2000) and human (Midorikawa et al., 2004, Rutberg et al., 2006) FDP cells. However a major limitation of these studies is that the cells studied have largely been cultured DP cells. The biological characteristics of cultured cells can be profoundly altered compared to DP cells residing in their natural environment (Ohyama et al., 2012). Another limitation is that the majority of these experiments have been conducted on adult hair follicle DP cells in the anagen stage of the hair cycle when cells from the dermal papillae initiate the formation of a new hair shaft from the epithelial bulge. While aspects of the hair cycle are similar to embryological hair follicle morphogenesis, the two processes are not identical and the markers for anagen hair follicle dermal papillae cells may not be helpful in identifying embryonic dermal cells. Therefore, while markers for hair follicle DP cells such as alkaline phosphatase (ALP) and markers for dermal sheath such as alpha smooth muscle actin (αSMA) have been identified in adult hair follicle dermal papilla cells in the anagen phase of the hair cycle little is known of gene expression in embryonic development and critically, little is known of how expression of these genes results in the ability of these cells to induce hair follicle formation. Recent elegant experiments co-isolated embryonic hair follicle placode and dermal condensate cells along with lineage related keratinocytes and fibroblasts and then used next generation RNA-sequencing to define gene expression patterns in the entire embryonic skin (Sennett et al., 2015). Through transcriptome cross comparisons they discovered genes in cell type specific signatures that create a molecular snapshot of hair follicle morphogenesis and will serve as the basis of future work in this area.

One of the most sensitive markers for adult hair follicle dermal papillae cells that are capable of inducing hair follicle formation is alkaline phosphatase (ALP). Alkaline phosphatase is a membrane-bound enzyme that catalyzes the hydrolysis of phosphate esters and occurs in almost all living organisms (Stefkova et al., 2015). A high level of ALP expression is traditionally a marker of pluripotent embryonic stem cells, which correlates with the fact that the inner cell mass is highly positive for ALP activity at the blastocyst stage (Tesar et al., 2007). ALP is highly expressed in the DP of the pilosebaceous unit (Handjiski et al., 1994). How the ALP enzyme functions within the DP, and

the reason for its increased expression in anagen, has not been elucidated. A linear relationship between hair inductive capability and ALP expression has been shown by *in vivo* hair induction experiments (McElwee et al., 2003, Rendl et al., 2008) where increased ALP expression is considered to be an accurate measure of the target cells' ability to induce hair follicle formation, and is considered one of the most reliable markers of trichogenicity in DP cells (Yang and Cotsarelis, 2010).

In human hair follicles Versican (VCAN) is expressed in DP during early anagen and is thought to play a vital role in anagen induction and maintenance (Kim et al., 2006). The protein encoded by the VCAN gene is a chondroitin sulphate proteoglycan mainly present in the extracellular matrix that plays a role in cell adhesion, migration, proliferation and differentiation (Lynn et al., 2004). VCAN is thought to be related to the aggregative growth characteristic of DP cells which is necessary to initiate hair follicle formation (Yang et al., 2012). Cells isolated by fluorescence-activated cell sorting (FACS), using green fluorescent protein (GFP) driven by the VCAN promoter to enrich for DP cells, showed behaviour and morphology consistent with DP cells and were able to induce hair neogenesis when combined with epidermal cells in engraftment assays (Kishimoto et al., 1999a).

The function of the chondroitin sulphate proteoglycans, of which versican is a member, remain elusive. All chondroitin sulphate proteoglycans contain G1 domains at their amino termini and G3 domains at their carboxyl termini and different domains are involved in different cellular processes (Zimmermann and Ruoslahti, 1989). Although the functional mechanism of versican in hair follicle development is still largely unknown, it has been suggested that it may function as an inhibitor of cell-cell or cell-extracellular matrix adhesion, selectively preventing the incorporation of dermal fibroblasts into the developing dermal papillae and maintaining the purity of the induced DP cell population (Lebaron, 1996). In leukocytes, P-selectin glycoprotein ligand-1 (PSGL-1), a glycoprotein expressed on the cell surface binds to the C-terminal (G3 domain) of versican which results in leukocyte aggregation as part of an immune response (Zheng et al., 2004) and it is possible that VCAN functions in a similar manner in hair follicle morphogenesis.

Another putative marker of hair follicle DP cells is the actin isoform α-smooth muscle actin (αSMA). This protein is an important part of the cytoskeleton in muscle cells and myofibroblasts, the contractile phenotype of fibroblasts. It has been shown to be present in the mid to lower DS in rat and human hair follicles but not in the DP (Jahoda et al., 1991). DP cells do however upregulate αSMA expression in culture. αSMA is therefore postulated to be a marker for DS *in vivo* and a marker for both DS and DP *in vitro* (Jahoda et al., 1991).

It is evident that DP cells are a primary target in the quest to generate *de novo* hair follicle morphogenesis however significant challenges are yet to be overcome regarding their use. The most widely used method to isolate DP is surgical micro-dissection which has been well established in both murine and human hair (Jahoda and Oliver, 1981), however the technique is labour-intensive and time-consuming. Critically, DP cells in culture gradually lose their inductivity with extended passage

number and are no longer able to induce hair follicle formation in overlying epithelial cells (Osada et al., 2007).

Considering the above information, the focus of many hair follicle engineering attempts has been that enriching and expanding hair inductive dermal cell populations in culture, while maintaining their properties, will establish an efficient hair reconstitution assay that could have therapeutic applications. Techniques used to maintain DP hair inductive properties in culture target the unique biological characteristics of DP cells and include spheroid cell culture (Higgins et al., 2010), co-culture with epithelial cells (Fujie et al., 2001) and exposure to Wnt signalling (Kishimoto et al., 2000).

1.6. Spheroid Culture of Dermal Papilla Cells

Since common culture conditions do not replicate the biological niche, the characteristic properties of most cells in tissue culture will be challenged, if not lost. Cultured DP cells were reported to lose their hair inductive capacity in culture with passage (Osada et al., 2007). The aggregative behaviour of DP in culture is one of their most defining features. This is analogous to the formation of the hair follicle dermal condensate in hair follicle morphogenesis (Schmidt-Ullrich and Paus, 2005). Analysis of global gene expression in human DP cells in culture reveals rapid and profound signature changes on transition from a 2-dimensional to a 3-dimensional environment, with early loss of their hair-inducing capacity (Higgins et al., 2013). Analysis of transcripts using PCR shows significantly decreased expression of transcripts implicated as important in embryological hair follicle morphogenesis including endothelin 3 (EDN3), low density lipoprotein receptor-related protein 4 (LRP4), Wnt inhibitory factor 1 (WIF1) and lymphoid enhancer-binding factor 1 (LEF1). Late-passage DP cells, that showed no trichogenic capacity as dissociated cells could induce hair follicle neogenesis after they were aggregated to form spheres (Osada et al., 2007). Higgins *et al*. demonstrated that intact dermal papilla transcriptional signature can be restored by growth of papilla in 3D spheroid culture and that this signature changes translates to a partial restoration of inductive capability (2013). The group further demonstrated that human dermal papilla cells, when grown as spheroids, are capable of inducing *de novo* hair follicles in human skin.

1.7. Co-culture of dermal papilla cells with epithelial cells

DP cells *in vivo* are in close contact via native extracellular matrix to the epithelial bulb. It was therefore postulated that co-culture of DP cells with epithelial cells should stabilize the trichogenic activity of the hair follicle-derived mesenchyme. Rat DP cells have been shown to sustain their trichogenic capacity for at least 70 passages when cultured in keratinocyte-conditioned medium (Inamatsu et al., 1998). A comprehensive list detailing keratinocyte-derived factors that are responsible for the maintenance of hair inductive potency has not been described however recent

reports suggest that WNT signalling molecules and BMP's may be among key factors necessary for maintenance of hair inductive capacity (Rendl et al., 2008).

1.8. Canonical Wnt Signalling Pathway

The Wnt signalling pathway regulates vital aspects of cell fate determination, cell migration and organogenesis during embryonic development. The name Wnt is derived from a combination of the name of the Drosophila segment polarity gene *wingless* and the name of the vertebrate homologue, *integrated* (Wodarz and Nusse, 1998). The extra-cellular Wnt signal stimulates several intracellular signal transduction cascades, one of which is the canonical or Wnt/β-catenin pathway which is involved in hair follicle morphogenesis. The Wnt3a gene, which is located on human chromosome1q42 (He et al., 2015), induces the canonical Wnt signalling pathway (Katoh and Katoh, 2005). Secreted Wnt3a glycoproteins act through two cell surface receptor proteins: Frizzled (Fz), a seven-transmembrane-span protein similar in structure to G-protein coupled receptors, and low-density lipoprotein-related protein5/6 (LRP5/6), a co-receptor that associates with Fz in a Wnt-signal-dependent manner. In the absence of Wnt signalling, cytoplasmic β-catenin is degraded by a complex including Axin, adenomatosis polyposis coli (APC), protein phosphatase 2A (PP2A) and glycogen synthase kinase 3 (GSK3). Phosphorylation of β-Catenin within this complex targets it for ubiquitination and subsequent proteolytic destruction (He et al., 2004). Binding of Wnt to its receptor complex triggers a series of events that disrupts the APC/Axin/GSK3 complex that is required for degradation of β-catenin resulting in its stabilization and accumulation in the cytoplasm (Mao et al., 2001). Stabilized β-catenin then translocates to the nucleus where it exerts its effect on gene transcription by functioning as a transcriptional co-activator. The LEF/TCF DNA family of DNA-binding proteins mediate the effects of Wnt signalling.

In hair follicle embryogenesis there is significant evidence to suggest that the initial signal arising from the dermis that causes the formation of epithelial placodes involves the Wnt signalling pathway. In the chick nuclear β-catenin is found transiently in the dense dermis underlying the feather tract 2 days before the appearance of molecular and morphologic signs of placode development (Noramly et al., 1999). Correspondingly, one day after the appearance of β-catenin in the dermis, nuclear β-catenin is detectable in the overlying epithelium indicating that the Wnt signalling pathway is activated in the epithelium (Noramly et al., 1999). Analysis of the transcripts of GFP positive cells in a transgenic mouse line that expressed GFP in dermal papilla cells in anagen demonstrated expression of many of the components of the Wnt signal transduction cascade including *frizzled7*, *disheveled2*, *GSK3β*, *β-catenin* and *Lef1* (Kishimoto et al., 2000). Culture in media with the addition of recombinant Wnt3a resulted in maintenance of hair inducing capability of DP cells with a dramatic increase in hair growth when co-cultured with keratinocytes and used in skin reconstruction assays in nude mice when compared with cells co-cultured with control feeders (Kishimoto et al., 2000).

Despite the fact that co-culture with epithelial cells, spheroid culture and exposure to Wnt-signalling have been shown to re-confer hair inducing capacity on cultured DP cells that have lost their trichogenicity in culture, these techniques do not overcome one of the main limitations of using adult hair follicle DP cells. This is the fact that hair follicle DP cells can only be isolated by microsurgical techniques that are time and skill intensive and result in so few cells that they have no true clinical utility. For this reason alternative cell sources such as stem cells represent an attractive solution in obtaining DP-like cells in larger numbers.

1.9. Generation of dermal papilla cells from stem cells

By definition, a stem cell is characterised by its ability to self-renew and its ability to differentiate along multiple lineage pathways. Stem cells have potential therapeutic applications in their ability to be directed towards multiple different cell lineages. The concept of using stem cells to generate DP-like cells is not a new one. Gnedeva *et al.* (2015) were able to direct human embryonic stem cells (hESCs) to generate first neural crest cells and then hair inducing-DP like cells in culture. The premise for this study was that DP cells of cephalic hairs are known to be derived from neural crest cells unlike the majority of other DP cells that are derived from mesoderm (Fernandes et al., 2004). To programme the embryonic stem cells into NC-like cells, neurospheres were generated by manual separation of hESC colonies, growing them in low adhesion dishes and as floating spheres. Following five days of culture neurospheres were plated on fibronectin and maintained with Neutralization Medium. To direct NC-like ESCs to DP like cells NC cells were cultured in DP medium, dissociated to a single cell suspension and plated onto uncoated culture dishes. The group was able to demonstrate that the hESC-derived DP-like cells expressed markers typically expressed in adult human DP cells such as VCAN, αSMA and ALP and were able to induce hair follicle formation when the cells were transplanted under the skin of immunodeficient NUDE mice. When engineered to express GFP, hESC-derived DP-like cells incorporated into the DP of newly formed hair follicles and expressed appropriate markers in their new location.

Recently, human induced pluripotent stem cells were shown to be capable of being programmed into hair follicle DP-like cells (Veraitch et al., 2017). The study used hiPSCs and differentiated them into induced mesenchymal stem cells (iMCs) with a bone marrow stromal cell phenotype. A LGFR(+)THY-1(+) subset of these iMCs that was demonstrated to be highly proliferative and plastic was then programmed using retinoic acid DP cell activating culture medium to confer DP properties to the cells. The cells that were generated exhibited increased expression of known DP markers, were able to upregulate HF related genes in keratinocytes when co-culture and when co-grafted with human keratinocytes *in vivo* formed fibre-like structures with a hair cuticle coat that resembled a hair shaft.

Ideally, a stem cell for regenerative medicinal applications should be found in abundant quantities, harvested by a minimally invasive procedure and differentiated along multiple cell lineage pathways in a regulatable and reproducible manner (Gimble, 2003). Stem cells generated or harvested from

host adult tissues circumvent the major limitations around embryonic stem cells including ethical issues and potential for immunological rejection.

Adipose tissue has been reported as a valuable source of adult stem cells (Hombach-Klonisch et al., 2008). A high yield of autologous adipose derived mesenchymal stem cells (ASCs) can be isolated from lipo-aspirates obtained with minimal discomfort under local anaesthesia using liposuction techniques (Casteilla and Dani, 2006). ASCs have significant proliferative capacity and are adherent in vitro, maintaining their mesenchymal phenotype and plasticity toward the mesenchymal lineage after many passages in culture. According to the International Society for Cellular Therapy (Dominici et al., 2006), three criteria must be fulfilled for the MSC phenotype: adherence to plastic, appropriate surface antigens and multipotent differentiation into adipocytes, chondrocytes, osteoblasts, cardiomyocytes, and vascular endothelial cells (Zuk et al., 2001). MSCs usually express CD73, CD90 and CD105, while lacking expression of CD11b, CD14, CD34, CD45 and CD79a (Koellensperger et al., 2014). They have been reported to be hypo-immunogenic or 'immune privileged', a property that is thought to enable them to be transplanted across major histocompatibility barriers and used in both allogeneic and autologous transplants (Lee et al., 2016).

In its native environment, the hair follicle DP is in close contact with the subcutaneous adipose tissue layer and the link between adipose tissue and hair follicle DP cells has been widely explored. There is a close correlation between subcutaneous adipose tissue and hair follicle formation and function with adipose lineage cell numbers observed to change with the hair cycle and being reported as skin niche cells that regulate hair follicle stem cell activity (Festa et al., 2011). To investigate whether $CD34^+$ ASCs are capable of participating directly in hair follicle morphogenesis, $CD34^+$ ASCs were grafted with mouse embryonic epidermal and dermal cells in a nude mouse model and the results showed that $CD34^+$ cells were detectable participating in forming hair follicles, blood vessels and fat tissue (He et al., 2013). Another *in vivo* study showed that, as evidenced by the darkening of shaved skin, the conditioned medium from ASCs (ASC-CM) could promote hair growth when injected subcutaneously into nude mice (Park et al., 2015). A recent study looked at the influence of ASC-CM on the hair-inducing ability of rat DP cells (Zhang et al., 2014). This study showed that culturing DP cells in ASC-CM could significantly enhance their proliferation in a concentration gradient manner and that it also increased the expression of alkaline phosphatase possibly increasing their hair-inducing capacity.

1.10. Research approach

To recapitulate the events of early hair follicle morphogenesis and achieve *de novo* hair follicle generation it is necessary to find a plentiful source of suitable 'inductive' mesenchymal cells. The aim of this project was to explore the suitability of human adipose-derived mesenchymal stem (ASCs) cells to utilise in such a re-engineering process. This study aims to generate hair inductive DP cells from ASCs which represent an easily available, minimally invasive source of stem cells from the

patients themselves. We will make use of existing evidence to suggest that spheroid cell culture and exposure to specific signalling molecules will direct ASCs towards a hair-inductive DP-like phenotype.

If this approach is successful, we believe that mesenchymal stem cell derived DP cells could be a valuable addition to current therapy for cutaneous burns, both with autologous keratinocytes and with split thickness skin grafts, through the induction of hair follicles that would contribute to a skin that much closer resembles the structure and the function of normal skin.

Aim

The broad aim of this project is to generate hair follicle dermal papilla-like cells from adipose derived mesenchymal stem cells.

Specific Objectives

The objectives of this research study are:

1) To characterise adipose derived mesenchymal stem cells with respect to known dermal papilla markers.
2) To evaluate the effect of exposure to Wnt signalling on adipose derived mesenchymal stem cells and assess for evidence of upregulation of dermal papilla markers.
3) To evaluate the effect of spheroid cell culture on adipose derived mesenchymal stem cells and assess for any evidence of up-regulation of dermal papilla markers.
4) To evaluate the effect of adipose derived mesenchymal stem cells cultured in Wnt conditioned medium on epithelial cells to assess for any evidence of upregulation of epithelial placode markers.

Chapter 2: Materials and Methods

2.1. Cell culture

2.1.1. General

All tissue culture was conducted in a Bio-Flow Biological Safety Cabinet Class II with a laminar air flow system. Cells were incubated at 37^{o}C, in 5% CO_2 with 95% humidity in a Forma Scientific water-jacketed incubator (Thermo Scientific, USA). Pre-packaged or autoclaved sterile instruments, pipette tips and culture dishes were used in the tissue culture hood. In addition, aseptic technique was practiced at all times including the use of gloves and laboratory coats and all surfaces, bottles tubes, instruments and vials were wiped with 70% ethanol.

2.1.2. Cell lines

2.1.2.1. Adipose derived mesenchymal stem cells

Adipose derived mesenchymal stem cells (ASCs) were generously donated by Professor Michael Pepper of the Institute for Cellular and Molecular Medicine at the University of Pretoria. These cells were utilised with the informed consent of the donors for use of these cells in this context. Ethical approval for this study was obtained from the University of Cape Town Ethics Committee. These cell lines were isolated enzymatically according to protocols described by Zuk (2001) from the lipoaspirates of three different healthy patients undergoing routine plastic or reconstructive surgery procedures with informed consent. ASC cultures were maintained under routine culture conditions (37^{o}C, 5% CO_2) in Dulbecco's Modified Eagles Medium (DMEM) (Highveld Biological, South Africa) supplemented with 10% Foetal Bovine Serum (FBS) (Gibco, USA), 100µg/ml penicillin (Sigma-Aldrich, USA) and 100µg/ml streptomycin (Sigma-Aldrich, USA). Cells were plated at a density of approximately 5000 cells/cm^2 and medium was changed every 48-72 hours. ASCs were passaged when 80-90% confluent which usually required 7-14 days in culture.

2.1.2.2. Wnt-3A producing and Control Cells

L Wnt-3a (ATCC® CRL-2647™) cells were kindly donated by Dr Carola Niesler from the School of Biochemistry, Genetics and Microbiology at the University of Kwa-Zulu Natal. These L-M(TK-) fibroblasts, obtained from the subcutaneous connective tissue

of male C3H/An mice, are stably transfected with a Wnt-3A expression vector containing the Wnt3a complementary DNA under the PGK promoter. Stable clones are selected in medium containing G418. These cells constitutively secrete biologically active Wnt-3A protein (Willert et al. (2003)). Control L Cells (ATCC® CRL-2648™) without the addition of the expression vector, were used as a control cell line for all experiments. Both L Wnt-3A and L cells were cultured under standard culture conditions in DMEM supplemented with 10% FBS, 100µg/ml penicillin and 100µg/ml streptomycin.

2.1.2.3. HeLa Cells, HaCaTs and Human Dermal Fibroblasts

Stocks of HeLa Cells (immortal cell line derived from cervical cancer cells) , HaCaT Cells (spontaneously transformed aneuploid immortal keratinocyte cell line from adult human skin, Boukamp et al. (1988)) and Human Dermal Fibroblasts (HDFs), harvested from the skin biopsies of patients already present in the Kidson Laboratory, were cultured under standard culture conditions in DMEM supplemented with 10% FBS, 100µg/ml penicillin and 100µg/ml streptomycin.

2.1.3. Passaging cells

Cells were cultured to 80-90 percent confluence. Growth medium was aspirated off cells. Dishes were rinsed twice with PBS (5mls for a 60mm dish). After ensuring that all excess PBS had been removed, 1.5mls (for 100mm culture dishes) of 0.05% trypsin-1mM EDTA was placed on each dish and the cells were incubated at 37^{o}C until cells had detached from the dish. Time taken for cells to detach varied (ASCs roughly 5 min, HaCaTs roughly 15 min, L Wnt 3A and Control Cells roughly 7mins). Once the majority of cells were visualised, rounded up and floating in the dish, trypsinization was stopped by adding 4mls of complete growth medium and a 5ml pipette was used to triturate the cells to ensure that all cells were in suspension. The cell suspension was transferred to a 15ml conical tube and centrifuged at 1000g for 5 minutes. Following centrifugation the supernatant was discarded and the cells were re-suspended in the appropriate volume of growth medium to facilitate the correct seeding density. Half of the growth medium required was added to the new culture dish after which the new cell suspension was added to the dish which was then manipulated to ensure even dispersal of the cells on the base of the dish prior to placement in the incubator.

2.1.4. Growth studies

Growth rates of cells were determined by setting up a growth curve and calculating doubling times. Cells seeded for the growth curve were harvested at around 70 percent confluence to ensure that they were still in the log phase of growth. A defined number of cells ($3x10^4$) were seeded onto fifteen 35mm culture dishes allowing for five time points on five days to be counted (in triplicate). Cells were counted on Day 1, 2, 3, 5 and 7. After 1-8 days of incubation the dishes for that day were harvested using 0.05% trypsin-1mM EDTA and triturated to make a single cell suspension. The cells in each dish were then counted by placing 10µl of the suspension into the haemocytometer counting chamber. Standard error of the mean was used as a statistical test of significance.

2.1.5. Microscopy and photography

Cultured cells were viewed occasionally on the Olympus CKX41 Microscope (Olympus, Japan). More commonly, the cells were viewed using the Evos XL Core Microscope (Life Technologies, USA) which is situated within the hood in tissue culture. All photographs during culture were taken using this microscope. ImageJ software (National Institutes of Health, USA) was used to process images.

2.2. Spheroid cell culture

2.2.1. Preparation of single cell suspension

Spheroid clusters of ASCs were generated using the 'hanging drop' cell culture protocol described by Foty (2011). Adherent ASC cultures were grown to 90% confluence after which cells were rinsed with PBS, trypsinized and collected as for passaging of cells (described above). Following centrifugation cells were re-suspended in 1ml of culture medium. Cells were counted using a haemocytometer, loading 10µl of the suspension onto the counting chamber, and volume of medium was adjusted to maintain a specific concentration (usually 2.5×10^6 cells/ml) to ensure spheroid cell cultures containing a specific number of cells (e.g. 25 000 cells in a 10µl droplet of a 2.5×10^6 cells/ml suspension).

2.2.2. Formation of hanging drops

Once the cell suspension was at the correct concentration, the lid from a 60mm culture dish was removed and 5mls of PBS was placed in the base of the culture dish to facilitate adequate hydration of the cultures. The lid of the 60mm dish was inverted and a 20µl pipette was used to place 10µl drops onto the underside. Approximately twenty 10µl drops were placed on each 60mm lid. The lid was carefully inverted and placed back onto the PBS-filled dish and the whole dish was incubated at 37^oC and 5% CO_2.

2.2.3. Monitoring and medium changes

Dishes were viewed daily and photographed using the Evos XL Core Microscope (Life Technologies, USA) in the hood. Most hanging drops were processed (RNA extraction/protein extraction/histology) after 24-30 hours. If hanging drops remained in culture for more than 30 hours, the medium was changed daily. To change the medium, the lid of the dish was removed, gently inverted and placed on the stand of the Evos XL Core Microscope in the tissue culture hood. Under direct vision, 5µl of medium was removed from each droplet with a 20µl pipette, ensuring that no cells were disrupted or removed. The medium was then replaced with 5µl of fresh growth medium which was pipetted onto each droplet.

2.2.4. Plating Spheroids on Matrigel

Corning® Matrigel® Growth Factor Reduced (GFR) Basement Membrane Matrix (Corning, USA) was thawed overnight on ice at 4^{o}C and kept on ice at all times. All work was done on ice in the hood using pre-frozen pipette tips that had been cut off at the end to increase the tip diameter. The Olympus VM Stereo Dissecting Microscope (Olympus, Japan) was used to visualise spheroids. All surfaces and equipment were sterilised using 70% ethanol. Spheroid cell clusters were plated the day before plating on Matrigel to allow 30 hours in culture using the method described previously. Dishes containing hanging drops were brought to the incubator. Under microscope guidance 3-4 spheroids were picked up with a mouth pipette (25ul capillary micropipettes (Drummond Scientific, USA)) and tubing and placed on the base of a new 30mm tissue culture dish. Once the spheroids had been placed on the culture dish the medium was aspirated off them using the mouth pipette. Around 12 spheroids, in 4 groups of 3-4 spheroids, were placed on each culture dish. 10µl of Matrigel was placed on top of each spheroid group using a P20 pipette with a pre-cut tip. The dish was tilted several times to ensure that all spheroids were evenly coated with Matrigel. The dish was then placed in the incubator at 37^{o}C for 5 minutes to facilitate hardening of the Matrigel. In some dishes the order was reversed with 10 µl of Matrigel being placed on the base of the culture dish first, then groups of 3-4 spheroids placed on top of it, and then the dish replaced in the incubator to allow the Matrigel to set. Once the Matrigel had set, the dish was flooded with 2ml growth medium and medium was changed daily.

2.3. L Wnt3A and Control L Conditioned medium

2.3.1. Generating L Wnt3A and Control L Conditioned medium

To obtain Wnt 3A Conditioned medium, L Wnt3A cells were seeded in T175 flasks with approximately 8.75-9x10^5 cells in each flask. Cells were cultured in 25mls growth medium of DMEM with 10% FBS, 100µg/ml penicillin and 100µg/ml streptomycin. The cells were allowed to grow for 3-4 days until they reached 80-90% confluency. The medium was then pipetted off the flask and centrifuged at 3000g for 10 minutes. The supernatant constituted the first batch of medium and was stored at 4^{o}C. 20ml of fresh growth medium was added to the flask and the cells were cultured for an additional 3 days. The medium was collected and centrifuged at 3000g for 10 minutes. The supernatant was the second batch of medium. The first and second batches of media were mixed, filtered through a 0.2µm syringe filter (PALL Supor Sterile Acrodisc Syringe Filter, PALL) and stored in small aliquots (10-20ml) at -80^{o}C. Control L cells were seeded on the same day as L Wnt3A cells and cultured concurrently following identical procedure to generate control L conditioned medium.

2.3.2. Treating cells with L Wnt3A and Control L Conditioned medium

ASCs were seeded evenly onto 3 separate 10cm dishes at around 30 x10^4 cells per dish and allowed to grow for 7-10 days until they reached 70 percent confluence. Once cells reached 70 percent confluence the three dishes were randomly allocated to a DMEM group, a L Wnt3A Conditioned Medium group and a control L conditioned medium group and dishes were labelled accordingly. Medium was aspirated off the dishes and the dishes were rinsed twice with 10 ml PBS. Once all of the PBS had been removed 10mls of the relevant medium was placed onto the dish (D0 of L Wnt3A Conditioned Medium Experiment). Cells were monitored daily using the Evos Core XL microscope with which pictures were also taken. Medium was changed on day 2 and day 4 and processing of cells for downstream application (RNA extraction, protein extraction) was done on day 5 following 5 days in culture. To compare Wnt-treated cells in a monolayer with Wnt-treated spheroids an identical process was followed as stated above, with the addition of a duplicate 100mm dish for each group (6 dishes in total). The cells were cultured in a monolayer until day 4 where upon 3 of the dishes had a routine medium change while the other three were trypsinized, collected, counted and resuspended at the correct concentration and ‘hanging drops’ were generated. The hanging drops were then allowed to remain for 30 hours in culture and both groups (monolayer and spheroid) were processed on day 5.

2.4. Histology

2.4.1. Fixing and Processing

Spheroid cell clusters generated by the 'hanging drop' culture method (described above) were fixed and processed for histological staining after 30 hours in culture. The culture dish lid containing the hanging drops was inverted and the medium was aspirated from each drop using a 20µl pipette, leaving the spheroid cell cluster on the lid. To fix the spheroids 10µl of 4% paraformaldehyde was pipetted onto the top of each cell cluster on the lid of the culture dish and the lids were then placed on ice at 4^{o}C for 1 hour. Once removed from the refrigerator, the lid was rinsed with 3mls PBS and the contents were collected in a 1,5ml Eppendorf tube (Eppendorf, Germany). The spheroid clusters were allowed to sink to the bottom of the Eppendorf tube and the supernatant of PBS was pipetted off using a P1000 pipette. 200µl of 50% ETOH was placed into each tube and the tubes were placed in the refrigerator for 2 days.

Once removed from the refrigerator, the 50% ETOH was pipetted off each tube. HistoGel (Richard-Allen Scientific, USA) was warmed using a microwave and 200µl was placed into each Eppendorf which was then agitated to ensure all spheroids were embedded. The HistoGel was allowed to air dry and set for 15 minutes at room temperature. Once set, the gel with spheroids suspended within it was removed from the Eppendorfs using a toothpick and placed within a filter paper cone which was then placed in a plastic cassette. The cassette was closed and placed in the Shandon Elliot Automatic Tissue Processor (Shandon Elliot, USA) and processed by dehydration in an ethanol series and clearing in Xylene (15 min 70% EtOH, 15 min 80% EtOH, 15 min 96% EtOH (x2), 15 min 100% EtOH (x3), 15 min Xylene (x3) and Paraffin 30 min (x2)).

The spheroids within the HistoGel were placed in a Tissue-Tek™ (Sakura, EU) mould and embedded in wax the following morning. The tissue was then sectioned at 4µm intervals using the Reichert-Jung 2040 Rotary Microtome (Reichert-Jung, Germany). The wax sections were floated out first in 30% EtOH and then in H_20 at 37% to minimise distortion of the tissue and then were placed onto glass slides. The slides were placed in a 60°C oven overnight. The next morning the sections were processed again by clearing in xylene and hydration in an ethanol series (5 min Xylene (x2), 2 min Absolute EtOH (x3), 2 min 96% EtOH (x2) and 2 min 70% EtOH (x2)) followed by washing in running tap water for 1 minute.

2.4.2. Fixing and Processing

Slides were placed in haematoxylin for 5 minutes and then washed in running tap water for 1 minute. They were then stained in Scott's solution for 1 minute, rewashed, stained in eosin for 4 minutes and then washed once again. All the slides were then dehydrated using an ethanol series. (A few quick dips in 96% EtOH followed by a few in absolute EtOH). Finally, sections were cleared in Xylene for 2 minutes and mounted with Entellan™ (Spectrum Chemical MFG Corp, USA) for visualisation.

2.4.3. Microscopy and Imaging

Slides of histology specimens were visualised using the Zeiss Axiovert 200M Microscope (Zeiss, Germany) and photographed with a Zeiss Axiocam HR monochrome camera. AxioVision 4.7 Software (Ziess, Germany) was used to process images.

2.5. Quantitative real time polymerase chain reaction

2.5.1. RNA extraction

RNA extraction was performed with strict aseptic technique using a two-step combination of RNA extraction from TriPure Isolation Reagent (Roche, Switzerland) homogenates in a phenol chloroform method of extraction and a column-based clean up with the High Pure RNA Isolation Kit (Roche, Switzerland). Cells grown in a monolayer were lysed directly in the cell culture dish. The medium was aspirated off, 1ml of TriPure was added per $10cm^2$ of culture dish area, cells were triturated thoroughly and then the cell-TriPure solution was collected in a 1,5ml Eppendorf® Safe-Lock microcentrifuge tube (Sigma-Aldrich, USA). For spheroid cell clusters generated by the 'hanging drop' cell culture method, medium was removed from each cell cluster. 1ml of TriPure was pipetted over the spheroids and the spheroid-TriPure solution was collected in the same 1,5ml Eppendorf® Safe-Lock microcentrifuge tubes. The spheroids were then manually homogenised within the Tripure using a glassTeflon tissue grinder pestle (Sigma-Aldrich, USA). Both cells and spheroids were additionally lysed by repeated trituration.

The lysate was then transferred into a 1,5ml Eppendorf tube at room temperature for 5 minutes to ensure dissociation of the nucleoprotein complexes. Pure chloroform (0.2ml chloroform per 1 ml of TriPure) was added to the lysate, the caps of the tubes were closed and sealed with PARAFILM®M (Sigma-Aldrich, USA) and the samples were shaken vigorously for around 15 seconds. Once shaken, the samples were stored at room temperature for 15 minutes and then centrifuged in a Labnet Prism™R Refrigerated Microcentrifuge (Labnet,

USA) at 12 000g for 15 minutes at 4^{o}C to ensure that no residual DNA remained sequestered in the aqueous phase. Following centrifugation the aqueous phase was transferred to a fresh 1.5ml tube. An equal volume of 70% ethanol was added to the aqueous phase and was mixed by pipetting up and down around 15 times.

The sample was was then passed through the High Pure RNA Isolation Kit (Roche, Switzerland) columns for clean-up according to the manufacturer's instructions. High Pure filter tubes were inserted into Collection tubes and the sample was placed in the upper reservoir of the Filter Tube. The sample then passed through multiple steps within the column including a DNase incubation step, as well as two washing steps following each of which the tube assembly was centrifuged and the flowthrough liquid discarded. In the final step the purified RNA was eluted into a new microcentrifuge tube.

2.5.2. Nanodrop quantification

The concentration of extracted RNA and level of contamination was determined using spectrophotometry with a NanoDrop ND-100 Spectrophotometer (NanoDrop Technologies, USA). The concentration of RNA was read at OD_{260} while the $OD_{260/280}$ and $OD_{260/230}$ ratio denoted the level of nucleic acid purity. For the former, a ratio of around 2.0 was accepted as pure RNA, relatively uncontaminated by protein or genomic DNA.

2.5.3. Gel visualization of RNA

The integrity of RNA was tested via electrophoresis through a 1% agarose gel made using SeaKem LE Agarose (Lonza, USA) added to 1x Tris/Borate/EDTA (TBE) (Appendix A) and containing 1mg/ml ethidium bromide at 100 V for around 45 minutes. 1ug of RNA was run on the gel with 2.5µl of 6x Orange Loading Dye (Thermo Fischer Scientific, USA) and RNAse-free water to a total volume of 15µl. RNA bands were then visualised using a Spectroline Transilluminator (Spectroline, USA) and KODAK EDAS 290 camera system (KODAK, USA).

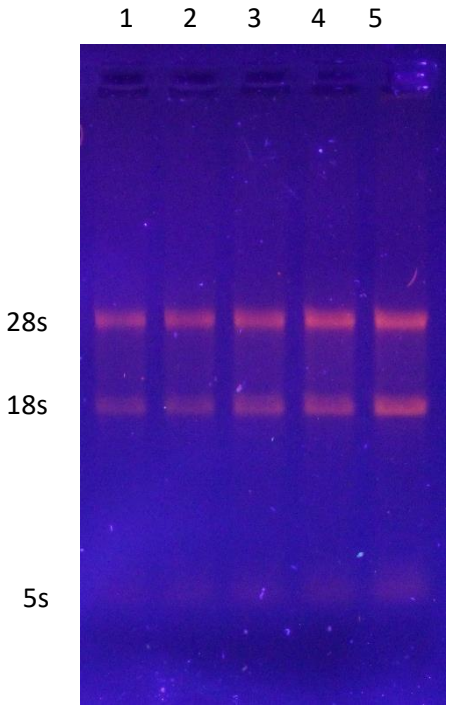

Figure 2.1 Example of agarose gel analysis (1% (w/v) agarose, 100V) indicating mRNA integrity of various experimental samples. The 28s, 18s and 5s ribosomal bands are shown.

Lane 1 – 10 ASC spheroids

Lane 2 – 20 ASC spheroids

Lane 3 – 30 ASC spheroids

Lane 4 – 40 ASC spheroids

Lane 5 – 50 ASC spheroids

2.5.4. Complementary DNA

Complementary DNA (cDNA) was synthesised according to standard laboratory protocol from 1 µg RNA using Maloney-Murine Leukaemia Virus Reverse Transcriptase (M-MLV RT)(Promega,UK), an RNA-dependent DNA polymerase. Gloves and lab coats were worn at all times, all surfaces were sprayed with 10% bleach and 70% ethanol and all work was done on ice to minimise degradation of RNA by RNases which are ubiquitously found. OligodT (1µl of a 61µM Oligo dT) was added to 1µg of RNA and Sabax water (Adcock Ingram, South Africa) to a total volume of 8.5µl. The samples were then incubated at 70°C for 5 minutes in a Labnet MultiGene Gradient Thermal Cycler (Labnet International Inc., USA) to allow for annealing of the Oligo dTs to the poly-A tails of the RNA. Samples were then transferred to slushy ice at

4°C for 10 minutes to ensure that tertiary RNA structures did not reform. The RNA sample was then combined with a cocktail containing 1x M-MLV RT buffer (Promega, USA), 1U/µl M-MLV RT (Promega, USA) and 20U/µl RNase Inhibitor (Promega, USA). A final concentration of 2.5 mM MgCl2 was provided by the RQ1 RNase free DNase buffer. Samples were incubated at 42°C for one hour in the Thermal Cycler, after which synthesised cDNA was stored at -20°C. Each run contained a negative control, with Sabax water instead of RNA, as well as a control for genomic DNA contamination with Sabax water replacing the reverse transcriptase.

2.5.5. Primer Design

Primers were generated using the Primer-BLAST program (http://blast.ncbi.nlm.nih.gov/Blast.cgi) to have melting temperatures between 50-60°C and be between 18-25 base pairs (bp) in length (Table 2.1). Where possible primer sets were designed to cross an exon-exon junction to eliminate the possibility of amplifying any contaminating genomic DNA. The estimated product size was calculated by aligning the primers on the gene of interest and counting the distance between them. The presence of secondary structures was tested for by using Integrated DNA Technologies OligoAnalyzer http://www.idtdna.com/analyzer/applications/oligoanalyzer/). Primers were synthesised by IDT (IDT, USA) and reconstituted according to the instructions of Whitehead Scientific (Whitehead Scientific, South Africa).

Table 2.1: RT-PCR and qRT-PCR Primer sequences and properties

Gene	Sequence (5′-3′)		GC Content (%)	T_M (°C)	Product Size (bp)
Glucuronidase B (GUSB)	F	Sequence intellectual property of Quiagen, USA	-	-	95
	R	Sequence intellectual property of Quiagen, USA	-	-	
Alkaline Phosphatase (ALP)	F	ATCTGACCCTCCCAGTCTC	57.9	57	165
	R	GAGTGAGTGAGTGAGCAAGG	55	56	
Versican (VCAN)	F	TGAGCATGACTTCCGTTGGACTGA	50	61	130
	R	CCACTGGCCATTCTCATGCCA	50	61	
β-Catenin (B-CAT)	F	AAAATGGCAGTGCGTTTAG	42.1	54	100
	R	TTTGAAGGCAGTCTGTCGTA	45	55	
αSMA	F	CCGACCGAATGCAGAAGGA	57.8	57.4	88
	R	ACAGAGTATTTGCGCTCCGGA	47.6	56.6	
Wnt3A	F	GCATCAAGATTGGCATCCAGGAGT	50	61.8	
	R	TGCACATGAGCGTGTCACTGC	50	59.5	100
Nuclear factor-kappa-B (NFkB)	F	CCTGGATGACTCTTGGGAAA	50	54.3	
	R	CTAGCCAGCTGTTTCATGTC	50	53.5	75
Keratin 10 (KRT10)	F	TTGGTGGAGGTAGCTTTCGTGGAA	50	60.3	
	R	AGAAGGCCATCTCCTCCAAAT	50	60.2	80
Keratin 5 (KRT5)	F	ACAAGGTTCTGGACACCAAGTGGA	50	60.3	
	R	AGGTCCTGCATGTTTCTCAGCTCT	50	60.2	100

2.5.6. Reverse transcription polymerase chain reaction (RT-PCR)

To evaluate the integrity of the cDNA, reverse transcription polymerase chain reaction (RT-PCR) was performed to determine the expression of human beta glucuronidase (GUSb)

[Qiagen]. The reaction mix (tabulated in Table 2.1) was created to a total volume of 20µl and contained 1µl of cDNA.

Table 2.2: RT-PCR Reaction Mix

Reagent	Volume (µl) (V_T = 20µl)	Final Concentration
10mM dNTP	0.4	0.2mM
50mM MgCl2	0.6	1.5mM
10x NH4 buffer (JMR Holdings, UK)	2	1x
hGUSb Primer	1	0.5µM
BIOTAQ™ DNA Polymerase (Bioline, UK)	0.2	1U
H20	4.8	

1µl of cDNA or water (no template control) was added to 19ul of mastermix in a PCR tube and incubated in a Labnet MultiGene Gradient Thermal Cycler (Labnet International Inc., USA) under the conditions seen in Table 2.3 below.

Table 2.3: Standard conditions for RT-PCR

	Number of Cycles	**Temperature (°C)**	**Time (min:sec)**
Initial denaturation	1	94	5:00
Cycling – Denaturation, Annealing, Extension	30	94 primer dependent 72	0:30 0:30 0:30
Final extension	1	72	7:00

To determine the best temperature for annealing, a gradient PCR was run for each primer set with a positive control sample and the temperature at which a single product of the correct size was visualised on a gel after electrophoresis was selected.

2.5.7. Quantitative real time polymerase chain reaction (qPCR)

Quantitative Real Time Polymerase Chain Reaction (qPCR) was used to quantify expression of genes of interest. Reactions were performed in a StepOnePlus™ Real-Time PCR System (ThermoFisher, USA) according to manufacturer's instructions. qPCR reactions containing 5µl of a 1xPowerUp™SYBR®Mastermix (Thermo Fisher Scientific,USA) and 0.4µM of each PCR primer in a total of 8µl were aliquoted into each well of a 0.1ml MicroAmp® Fast 96-well reaction plate (Applied Biosystems, USA). Two microlitres of a 1:2 dilution of cDNA were added per well to give a final reaction volume of 10µl. The plates were sealed and with a MicroAmp™ optical adhesive film (Applied Biosystems, USA), centrifuged at 2500 rpm for 20 seconds in an Eppendorf 5810R centrifuge (Eppendorf, Germany) and loaded into the StepOnePlus™ machine. The software provided by the supplier was used to generate the required conditions which entailed a comparative ΔΔCT program with 40 cycles and a melting temperature of 60^{o}C. Cycling conditions comprised denaturation (10mins at 95^{o}C) followed by annealing and amplification (15 sec at 95^{o}C and 1 min at 60^{o}C respectively). Lastly samples went through a final melting step (15 sec at 65^{o}C at a ramp rate of 2.8%) and a cooling step (30 seconds at 4^{o}C). Each cDNA sample was done in triplicate for each gene of interest and a negative (no template) control was included for each set of primers.

Table 2.4: qRT-PCR reaction mix

	Volume (µl)	Final Concentration
SABAX Water	2.6	-
Forward primer (10µM)	0.2	4µM
Reverse primer (10µM)	0.2	4µM
Power SYBR®Green PCR MasterMix	5	-
cDNA	2	50ng/µl

2.5.8. Gel visualisation of qRT-PCR products

Ten microlitres of each qRT-PCR product was visualised after electrophoresis on a 2% agarose gel as previously described to confirm the correct product size and specificity of the reactions

by comparing the bands to those of the O'Generuler 100bp DNA ladder molecular weight marker.

2.5.9. Analysis of qRT-PCR

Data from the qRT-PCR reactions was assessed to establish the relative expression of each gene using the comparative CT method according to the protocol developed by Livak (Livak and Schmittgen (2001)). The CT value or 'threshold cycle' is the cycle number at which the fluorescence generated within a reaction crosses the threshold line. An endogenous control, human beta glucuronidase (GUSb), was used as a reference gene to normalize experimental results by demonstrating the baseline signal generated as a result of PCR amplification. A calibrator sample (generally the control or untreated sample) was used as the basis for comparative expression results. The fold change of each gene was calculated as the value of 2-ΔΔ CT (see table 2.5 below).

Table 2.5 Calculation of relative expression of sample gene using fold change

ΔC_T	C_T of Target Gene - C_T of housekeeping Gene
$\Delta\Delta C_T$	ΔC_T of Sample - ΔC_T of Calibrator
Final normalised expression of target gene in sample	$2^{-\Delta\Delta CT}$.

Error bars on graphs represent the standard deviation on all the possible values of normalised expression calculated using the triplicate values of the target and housekeeping genes.

Statistical analyses on data was completed using GraphPad Prism 7 (developed by GraphPad Software, USA). Differences in expression were analysed using the Holm-Sidak method with p-values <0.05 considered as significant.

2.6. Western blot

2.6.1. Protein isolation from cell lysate

To prepare samples for running on a gel, cells were lysed to disrupt the cellular membrane and solubilize intracellular proteins to ensure individual migration through the gel. To minimise proteolysis, dephosphorylation and denaturation after lysis, all samples were kept on ice and appropriate inhibitors were added fresh to the lysis buffer. Culture dishes were placed on ice, growth medium was aspirated and the cells were washed three times with ice-

cold PBS. Radio Immunoprecipitation Assay buffer (RIPA buffer) (Appendix B) with the addition of phenylmethylsulfonyl fluoride (PMSF) (Sigma, USA) aprotinin (Sigma, USA), pepstatin (Sigma, USA) and complete protease inhibitor cocktail (CPIC)(Sigma, USA) were added to the culture dishes (500 µl for 10cm plate) which were incubated on ice for 10mins while intermittently scraping the adherent cells off the base of the dishes using a cold plastic cell scraper. The cell suspension was transferred gently to a pre-cooled microfuge tube to minimise foaming. Samples were then sonicated for approximately 1 second until foam was visible throughout the sample and then placed on ice until the foaming subsided. Samples were then centrifuged for 8 minutes at 10000g after which a pellet was visible in the base of the microfuge tube. The supernatant was aspirated and placed in a fresh tube and kept on ice.

2.6.2. Protein quantification

The Bicinchoninic Acid (BCA) Assay (Pierce™ BCA Protein Assay Kit, ThermoFisher Scientific, USA) was used for the calorimetric detection and quantitation of total protein in the extract. The total protein concentration was exhibited by a colour change of the sample solution from green to purple caused by the chelation of two molecules of BCA with one cuprous ion. This complex exhibits a strong absorbance at 562nm that is nearly linear with increasing protein concentrations over a broad working range. Protein concentrations are determined and reported with reference to standards of a common protein, bovine serum albumin (BSA). A series of dilutions of known concentrations are prepared from the protein and assayed alongside the samples prior to calculating the concentration of the samples using a standard curve.

Reference samples in the protein concentration ladder were formulated according to manufacturer's instructions using an unadorned RIPA buffer as a diluent. Dilutions of the unknown sample were also made using RIPA buffer to generate 1:2 and 1:4 dilutions to ensure accuracy. Twenty-five microlitres of each reference and unknown sample was pipetted, in duplicate, into a microplate well (Pierce™ 96-Well Polystyrene Plates, ThermoFisher Scientific, USA). Two hundred microliters of working reagent (WR) was added to each well and the plate was agitated on a plate shaker for 30mins. Once the samples were mixed the plate was covered and incubated at 37^{o}C for 30 minutes. Following cooling the absorbance of the sample was read on a plate reader (Rayto RT-2100C Microplate Reader)(Rayto, China). The average 562nm absorbance measurement of the blank standard replicates was subtracted from the 562nm measurements of all other individual standard and unknown sample

replicates and a standard was prepared by plotting the average blank-corrected 562nm measurement for each BSA standard versus its concentration in µg/mL. The standard curve was then used to determine the protein concentration of each unknown sample. Once the concentration of each sample had been determined the samples were frozen at -80^{o}C for later use.

2.6.3. Sodium dodecyl sulfate polyacrylamide gel electrophoresis

Sodium dodecyl sulfate polyacrylamide gel electrophoresis (SDS-PAGE) was used to separate proteins according to their molecular weight. A thin, 12% resolving gel (Appendix B) was made and loaded into the glass plates in the Loading Cassette (BIO-RAD, China) followed by a thin 5% stacking gel (Appendix B). To prepare samples for loading, 20µg of protein was combined in a 1:1 ration with 2x Laemmli Buffer (Appendix D), containing the anionic denaturing detergent sodium dodecyl sulfate to unfold the 3D conformation of the protein, ensuring access of the antibody to the epitope. The samples were then boiled for 5-10 minutes at 100^{o}C prior to loading onto the gel. A Thermo Scientific Page Ruler Prestained Protein Ladder (ThermoFisher Scientific, USA)(Appendix B) was loaded to enable determination of protein size and a loading control, p38 MAPK Antibody (Cell Signalling, USA), was used to demonstrate that lanes had been evenly loaded. The gel was placed in an electrophoresis tank (BIO-RAD MINI PROTEAN® Tetra System) which was filled with Running Buffer (Appendix B) and which was run at 100V for 10 minutes to ensure even compression of the samples within the resolving gel, and then at 120V until the proteins were adequately separated (+/- 2,5 hrs).

2.6.4. Transfer of protein from gel to nitrocellulose membrane

Following electrophoresis, proteins were transferred onto a nitrocellulose membrane using an electric current to 'blot' the protein from the gel under wet conditions. Gels were removed from the loading cassettes, trimmed and placed next to a nitrocellulose membrane within a transfer sandwich as demonstrated in Table 2.6 (below). The sandwiches were loaded into the tank with the red plates facing the positive electrode, submerged in transfer buffer and run overnight (16 hours) at 200mA.

Table 2.6. Transfer Sandwich for transfer of protein from gel to nitrocellulose membrane

Positive (red) plate	Flow of current 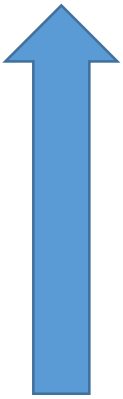
Transfer sponge (x3)	
Filter paper (x3)	
Nitrocellulose membrane	
Gel	
Filter paper (x3)	
Transfer sponge (x3)	
Negative (black) plate	

2.6.5. Visualizing proteins on the membrane

To check for the successful transfer of proteins to the membrane, the membrane was washed in TBST (Appendix B) and then submerged in Ponceau Red (Appendix B) and incubated on an agitator for 5 minutes. The membrane was then washed with distilled water to remove excess Ponceau and protein bands were examined to confirm successful protein transfer as presented in figure 2.2 (below).

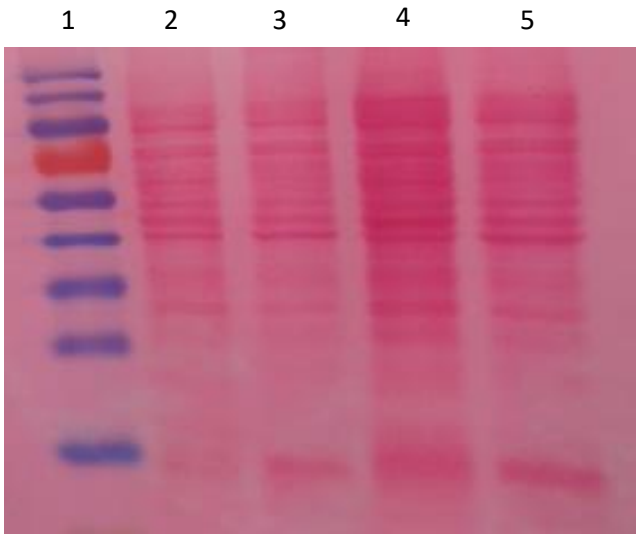

Figure 2.2: Example of Ponceau staining of nitrocellulose membrane post transfer showing protein bands.

Lane 1 – Thermo Scientific PageRuler Prestained Protein Ladder

Lane 2 – 10µg L Wnt-3A whole cell protein extract

Lane 3 – 10µg L whole cell protein extract

Lane 4 – 20µg L Wnt-3A whole cell protein extract

Lane 5 – 20µg L whole cell protein extract

2.6.6. Blocking

The nitrocellulose membrane was trimmed to the minimum required size ensuring that the areas of the protein ladder above and below the size of the protein of interest were retained. The membrane was then rinsed with TBS-T until all trace of Ponceau was removed. Next, the membrane was blocked for 1 hour in 5% non-fat dried milk to prevent non-specific background binding of primary and/or secondary antibody to the membrane. After blocking, the membrane was rinsed in TBST.

2.6.7. Detection

The primary antibody was diluted in TBST according to manufacturer's instructions, and then the transferred membrane was agitated overnight at 4^{o}C on a shaker. The following morning the membrane was rinsed by immersing it in a tray filled with TBST and agitating the tray for

five minutes, a process that was repeated five times. After rinsing, the membrane was incubated in the secondary antibody, diluted in TBST according to manufacturer's instructions for 1 hour on a shaker. Following incubation the membrane was rinsed once again in TBST. Working solution of the chemiluminescent substrate were made as described by the manufacturer in the SuperSignal™ West Pico Chemiluminescent Substrate (ThermoFisher Scientific, USA). Excess secondary antibody solution buffer was removed by touching the edge of the membrane onto tissue paper. The membrane was immersed for 1 minute in around 1ml of chemiluminescence. Following this the membrane was picked up with tweezers and placed between two transparencies. The membrane, within the transparencies, was placed on a film cassette with the transferred protein facing upwards and the casette was then closed and taken to the dark room. Once chemiluminescence was visible upon opening the cassette, an x-ray film was placed on top of the wrapped membrane and exposed for 1min initially and then varying time periods to optimise bands. The x-ray film was removed from the film cassette and immersed in developer until bands appeared. Once the bands appeared the films were rinsed and then immersed in fixer solution. Following immersion in fixative the x-ray films were once again washed in running water and then left to dry on a rack.

Table 2.7. Antibodies used in Western blot

Protein	Primary antibody	Secondary antibody	Protein size
Wnt3A	Wnt-3a (YY-7): sc-80457 (Santa Cruz Biotechnology, USA)	Anti-Rat IgG: A9037 (Sigma, USA)	39kDa
P38	P38 MAPK Antibody #9212 (Cell Signaling Technology, USA)	Anti-Rabbit IgG: A0545 (Sigma, USA)	41kDa

2.6.8. Analysis

Qualitative analysis of the protein bands was performed using the position of the bands relative to the protein ladder and the size of the bands in the control and experimental groups to assess the level of protein expression in the relevant samples.

Chapter 3: Results

Hair follicle morphogenesis occurs exclusively during embryogenesis and relies on a complex series of interactions between the mesenchymal dermis and the ectodermal epithelium (Hardy, 1992). The multipotent mesenchyme underlying the epidermis becomes clustered, the result of which is a triggering of a cascade of events that ultimately create hair follicle and adnexa formation. To date a method of recapitulating this process in regenerating adult skin and achieving *de novo* hair follicle morphogenesis has not been achieved.

Dermal papillae (DP) cells are a cluster of mesenchymal cells at the proximal end of the hair follicle. They have been shown to retain the ability to induce hair shaft formation in overlying epithelial cells throughout life but their use in trichogenic assays is limited by the labour intensive isolation technique required, and their loss of inductive potential in culture (Ohyama et al., 2010). A method of generating **hair** follicle DP cells from a readily available source is therefore required.

3.1. Comparison of adipose derived mesenchymal stem cells and human dermal fibroblasts

The ultimate aim of this project is to generate hair follicle DP-like cells from a readily available cell line. Adipose derived mesenchymal stem cells (ASCs) are multipotent and have the ability to differentiate into multiple different cell types and are obtainable through liposuction. Human dermal fibroblasts (HDFs), a fully differentiated cell line of mesenchymal origin, are frequently used in tissue culture and are readily obtainable via a skin biopsy, which is a simpler procedure than liposuction. As they are stem cells, ASCs should be the most suitable line to use in trying to obtain hair follicle DP-like cells. However if HDFs were also able to be directed towards a DP-like fate then this would be a simpler source of cells to use. The first experiment therefore, aimed to compare the baseline characteristics of ASCs and HDFs, including their morphology, growth kinetics and gene expression to determine which cell line would be best suited to becoming DP-like cells.

This experiment would provide a baseline set of characteristics from which to work and establish if there were any shared characteristics between ASCs or HDFs and those reported in DP cells. ASCs are characteristically adherent to culture-dish plastic, show an extensive proliferative ability and exhibit a fibroblast-like morphology in culture (Baer and Geiger, 2012).

ASCs obtained from the lipo-aspirates of patients undergoing liposuction that had been fully characterised with respect to known mesenchymal stem cell markers including CD73, CD105 and CD90 (van Vollenstee et al., 2016) were cultured to confluence under routine culture conditions and compared to HDFs, grown out from skin biopsies of adult human skin.

When observing the morphology of the two cell types in culture it was noted that fibroblasts were spindle shaped with lengthy cytoplasmic extensions, and tended to align into parallel arrays (Figure 3.1 A) when crowded. In contrast, ASCs in culture, while also displaying elongated cytoplasmic extensions, exhibited a more polygonal morphology (Figure 3.1 B).

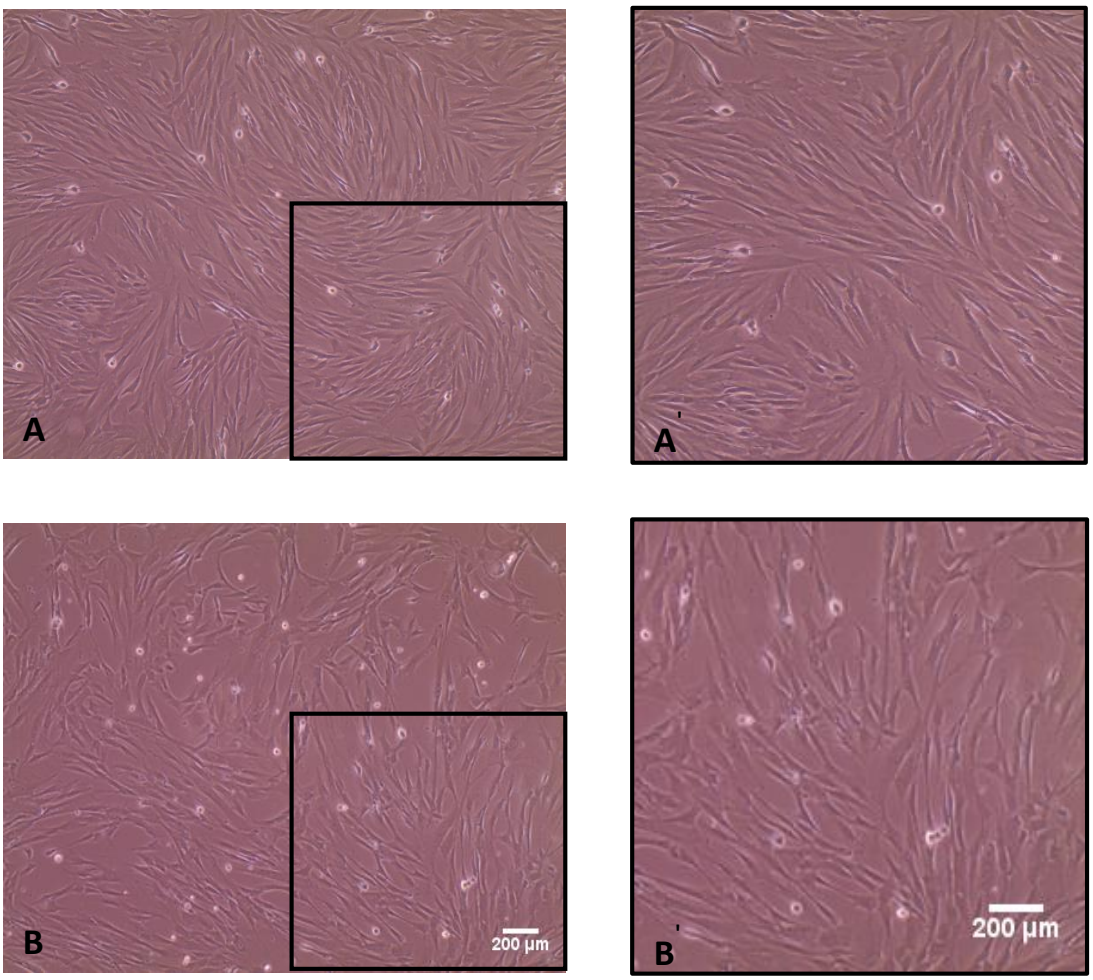

Figure 3.1: Comparison of human dermal fibroblasts (HDFs) (A, A') and human adipose derived mesenchymal stem cells (ASCs) (B,B') in culture. ASCs exhibit a more polygonal shape than spindle shaped fibroblasts. When grown to confluence fibroblasts tend to group into parallel sheaths while ASCs remain fairly dispersed. There is significant deposition of extracellular matrix material between cells in both groups.

The phenotype of ASCs in culture has previously been shown to change with increasing passage number with the cells ultimately becoming senescent (El Atat et al., 2016). To confirm that the ASCs in this study were not senescent, their growth kinetics under routine culture conditions were examined. Passage 9 (P9) ASCs and passage 16 (P16) HDFs were plated at a density of $3x10^4$ cells per 30mm culture dish and cultured for 7 days. Cell counts were performed in 3 separate dishes for each cell type at each time point. Calculated doubling time confirmed a slightly higher proliferation rate of

the HDFs with a mean doubling time of 43.5 hours for HDFs and 47.26 for the ASC cell line (Figure 3.2 B). The growth curve clearly demonstrates that ASCs, even at P9, are proliferative and have not become senescent, indicating that they are at an appropriate state for the current study.

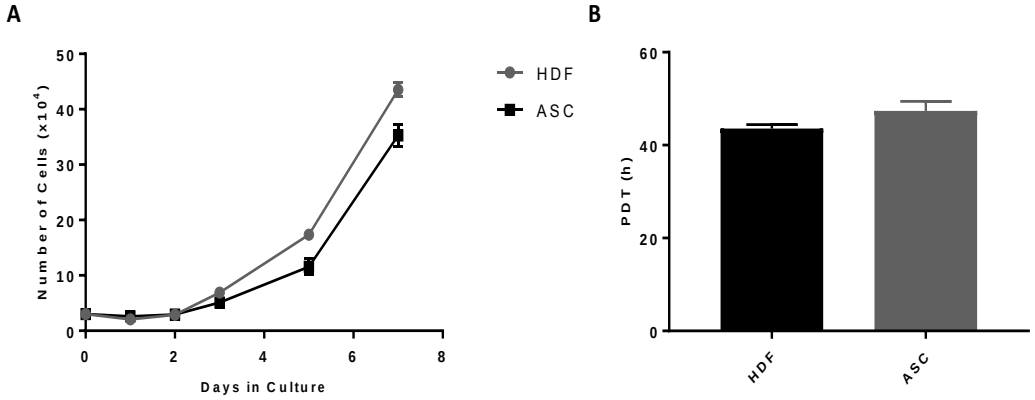

Figure 3.2: Growth curve of human dermal fibroblasts (HDFs) and human adipose derived mesenchymal stem cells (ASCs) (A) and calculated Population doubling time (PDT, measured in hours)(B). HDFs and ASCs grow at a similar rate under routine culture conditions with HDFs showing slightly accelerated growth after the first 48 hours (A) and a shorter doubling time (B). Results shown are for a single experiment using P16 HDFs and P9 ASCs. Cell counts were performed in triplicate for each cell type at each time point.

Several markers for hair follicle DP cells including versican, alkaline phosphatase, alpha smooth muscle actin and members of the Wnt signalling cascade, have been identified in previous studies. The understanding of how these genes function to confer the hair inductive capacity and stem-like properties of DP cells is, however, largely unknown. The objective of the next experiment was to evaluate whether genes known to be markers of hair follicle DP cells are expressed in ASCs cultured in routine culture conditions. To establish this baseline level of expression in ASCs, qPCR reactions were run on cDNA reverse transcribed from mRNA extracted from both ASCs and HDFs. Expression was analysed using the $2^{-\Delta\Delta C_T}$ method (Livak et al., 2001) and normalised to the reference gene Glucuronidase B (Gus).

The expression of ALP is used as a marker for dermal tissue that will have the ability to induce clustering and hair follicle formation in the overlying epithelium. ALP expression in ASCs was significantly less than that in HDFs when cultured under routine culture conditions ($P<0.001$) (Figure 3.3 A).

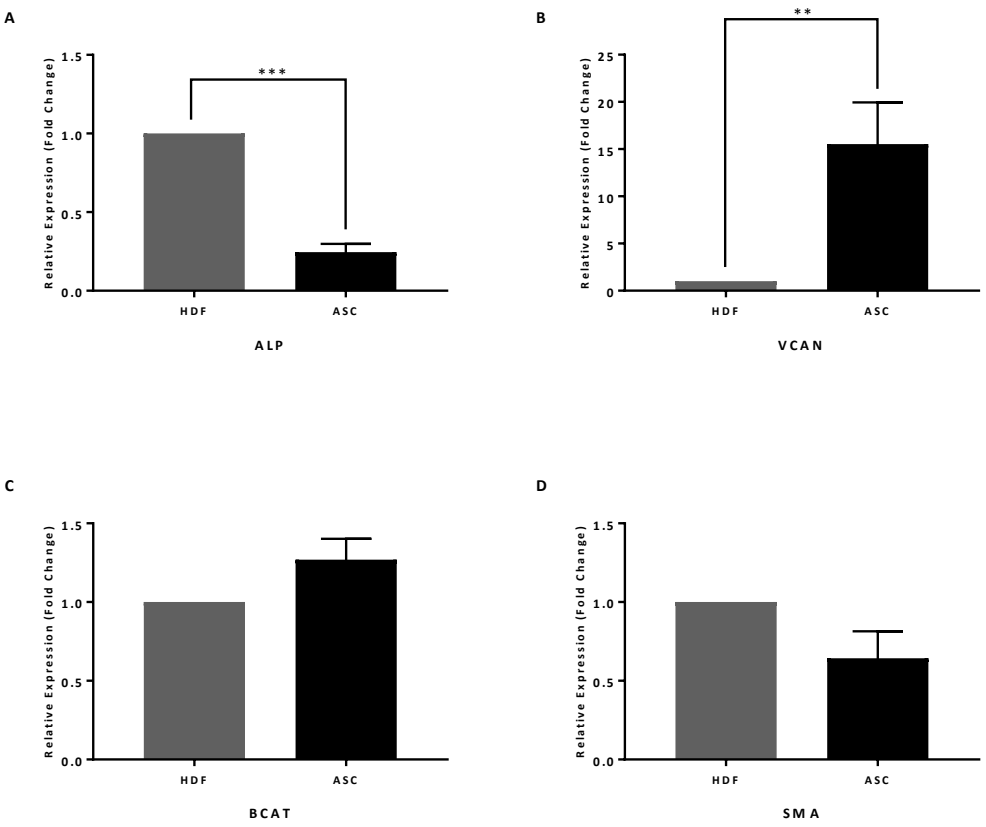

Figure 3.3: Analysis of differential mRNA expression of known DP genes *ALP*, *VCAN*, *BCAT*, *SMA* and *VIM* in HDFs and ASCs under routine culture conditions. Relative expression was analysed by qPCR and normalised to the reference gene *GUS*. The data represent the means ± SD of experiments conducted in duplicate and repeated in 2 different cell lines.* indicate statistical significance. ***p≤0.001.

In adult human hair follicles Versican is specifically expressed in DP during anagen and in development versican, an extracellular matrix protein is thought to be play an important role in the aggregative nature of DP cells (Soma et al., 2005). VCAN expression was significantly increased (P=0.008) (Figure 3.3 B) in ASCs when compared to HDFs. The Wnt/β-catenin signalling cascade is thought to provide the 'first dermal signal' that triggers aggregation of the overlying epithelial cells into placodes and begins the process of epithelial mesenchymal cross-talk that results in embryological hair follicle morphogenesis (Millar, 2002). β-catenin mRNA expression in ASCs was slightly elevated when compared to HDFs although this result was not significant (P=0.18)(Figure 3.3 C). α-Smooth muscle actin (αSMA), an actin isoform involved in cell motility and structure, is a marker for DP *in vitro* but not *in vivo* with the reason for this being poorly understood (Jahoda et al., 1991). αSMA expression was higher in ASCs than in HDFs in routine culture however this result was not significant either (P=0.07)(Figure 3.3 D).

These initial experiments to establish the baseline characteristics of ASCs demonstrate that they retain their proliferative capacity even at high passage numbers, and do express some of the genes known to be expressed in hair follicle DP cells, particularly Versican, when cultured under routine culture conditions. In order for these results to have been more meaningful, it would have been preferable to use a line of DP cells for comparison of gene expression. These results may indicate that ASCs have the potential to be directed to form the mesenchymal component of the hair follicle.

3.2. Comparison of Adipose derived mesenchymal stem cells in a monolayer and as spheroids

During early development (approximately 60 days post conception in humans (Holbrook and Minami, 1991)) dermal mesenchymal tissue begins to form clusters throughout the foetal skin. These mesenchymal-cell condensates, around 50 µm in diameter, are the first sign of follicle morphogenesis and trigger the cascade of subsequent reactions (Huang et al., 2013). During this process cells upregulate markers such as alkaline phosphatase, versican and members of the Wnt signalling cascade. The next step was to test whether 'clustering' of ASCs would result in changes in gene expression when compared to unclustered cells.

3.2.1. Morphology

ASCs cultured in a monolayer (Figure 3.4 A) were trypsinised, resuspended at specific concentrations and plated in 10µl droplets on the lid of a tissue culture dish (Figure 3.4 B) that was inverted. Gravity causes the cells within the droplet to sink to the bottom of the drop forming a cluster. To maintain the correct humidity PBS was placed in the culture dish (as described previously). To ascertain the best number of cells to use in each spheroid, ASCs were suspended in different concentrations to create spheroids of different cell numbers (50 000 cells, 25 000 cells, 12500 cells and 5000 cells) prior to generating hanging drops. After 24 hours in culture, clusters of cells were visible within all the droplets irrespective of cell number and the living clusters were photographed (see Figure 3.4 C).

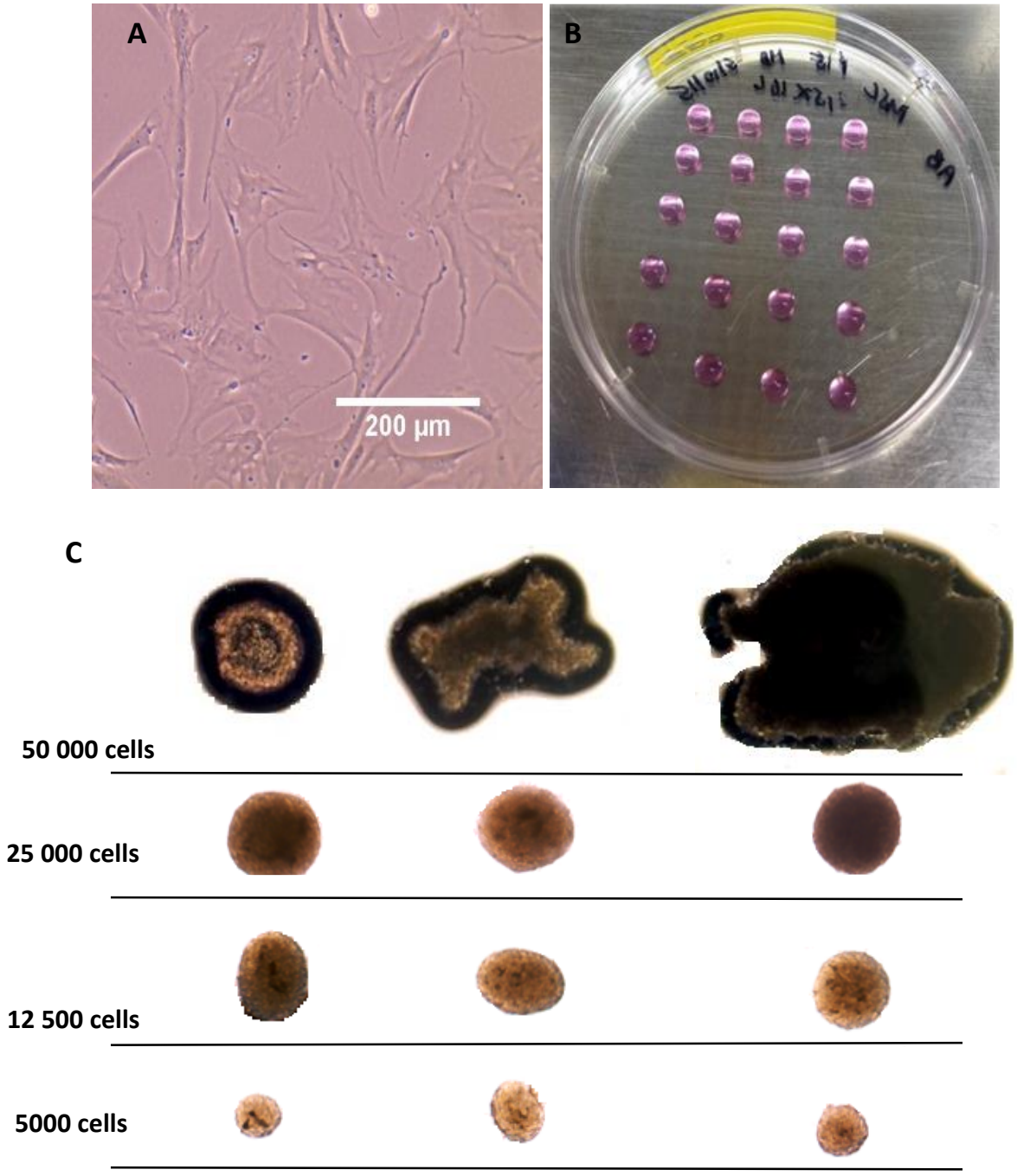

Figure 3.4: ASCs visualised in culture in a monolayer (A), immediately after being plated as 10µl drops prior to inversion of the culture dish lid (B) and viewed in culture after 24 hours. For each different size, 10 clusters were photographed and three examples are shown here. Clusters of 50 000 cells were irregular in shape while those of 25 000 cells were more regular.

Cell clusters generated from droplets containing 50 000 cells exhibited very irregular shapes (Figure 3.4 C) while the cell clusters generated from 25 000 cells were regular spheroids of almost identical size and shape (see the 3 examples in Figure 3.4 C). In addition, clusters generated from smaller numbers of cells (Figure 3.4) were also regular and spherical in nature and exhibited little variability between the different clusters, although they were not as uniform as in the 25 000-cell spheroid group.

3.2.2. Histology and measurement of spheroids

To examine the morphology and structure of cells within the spheroids as well as to determine the diameter of the spheroids, they were fixed, processed and stained with haematoxylin and eosin (see Materials and Methods). Sections were then viewed and photographed at high magnification to enable visualization of the morphology and structure of cells within the cluster.

As expected from visualization in culture prior to histology, cell clusters generated from 50 000 cells had irregular shapes and were not spheroid in nature (Figure 3.5 A1). Cell clusters generated from 25 000 cells had the most regular, spheroidal shape (Figure 3.5 B2), and clusters generated from 12 500 and 5000 cells respectively also formed spheroid structures (Figure 3.6 C1 & D1). ASCs situated at the periphery of the cell cluster were flattened and elongated and formed a border around all of the spheroids (Figure 3.5 and 3.6, see arrow). This flattened border was thickest in spheroids of 25 000 cells (Figure 3.5 B) where it appeared to comprise 2-3 cell layers. ASCs visible within the centre of the spheroids appeared smaller and more rounded than those on the border.

In all the cell clusters, normal looking nuclei (Figure 3.5 and 3.6) without evidence of pyknosis were visible. All spheroids exhibited significant deposition of homogenous pink extra-cellular matrix material between the cells (Figure 3.5 and 3.6). This material appeared much more dense and tightly arranged in the larger spheroids (Figure 3.6 C3 & D3) generated from 50 000 cells (Figure 3.5 A3) than in the smaller spheroids where the extra-cellular matrix material looked similar to loose areolar connective tissue. The ratio of extracellular matrix material to cell number appeared lowest in spheroids of 25 000 cells where the cell nuclei are seen to be tightly packed together with minimal space between them (Figure 3.5 B3). All spheroids showed some evidence of non-stained gaps (Figure 3.5 and 3.6) but this was more pronounced in spheroids of smaller cell numbers (Figure 3.5). This may reflect an artefact of shrinking arising from histological processing.

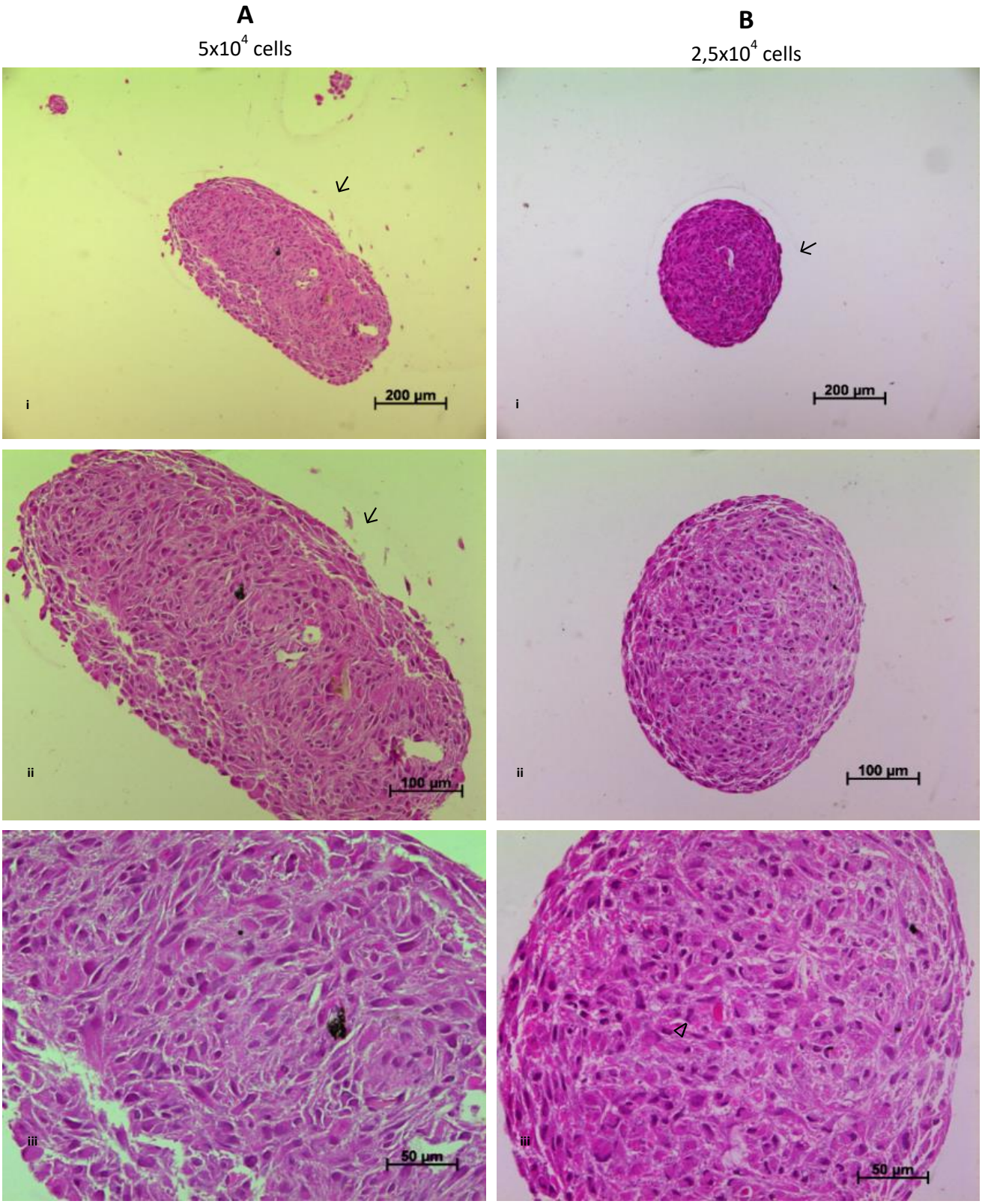

Figure 3.5: Haematoxylin and eosin staining of adipose derived mesenchymal stem cell spheroids generated from 50 000 cells (A) or 25 000 cells (B) viewed at the 10x (1), 20x (2) and 40x (3) objective. A smooth border is visible surrounding the spheroids formed by 2-3 layers of elongated layer of cells (see ↓). Rounded, normal-looking nuclei are visible throughout the structures including the centre. Abundant extra-cellular matrix material is visible in spheroids of both sizes, however more cell nuclei are visible relative to the extracellular matrix material in the spheroid generated from 25 000 cells (see Δ).

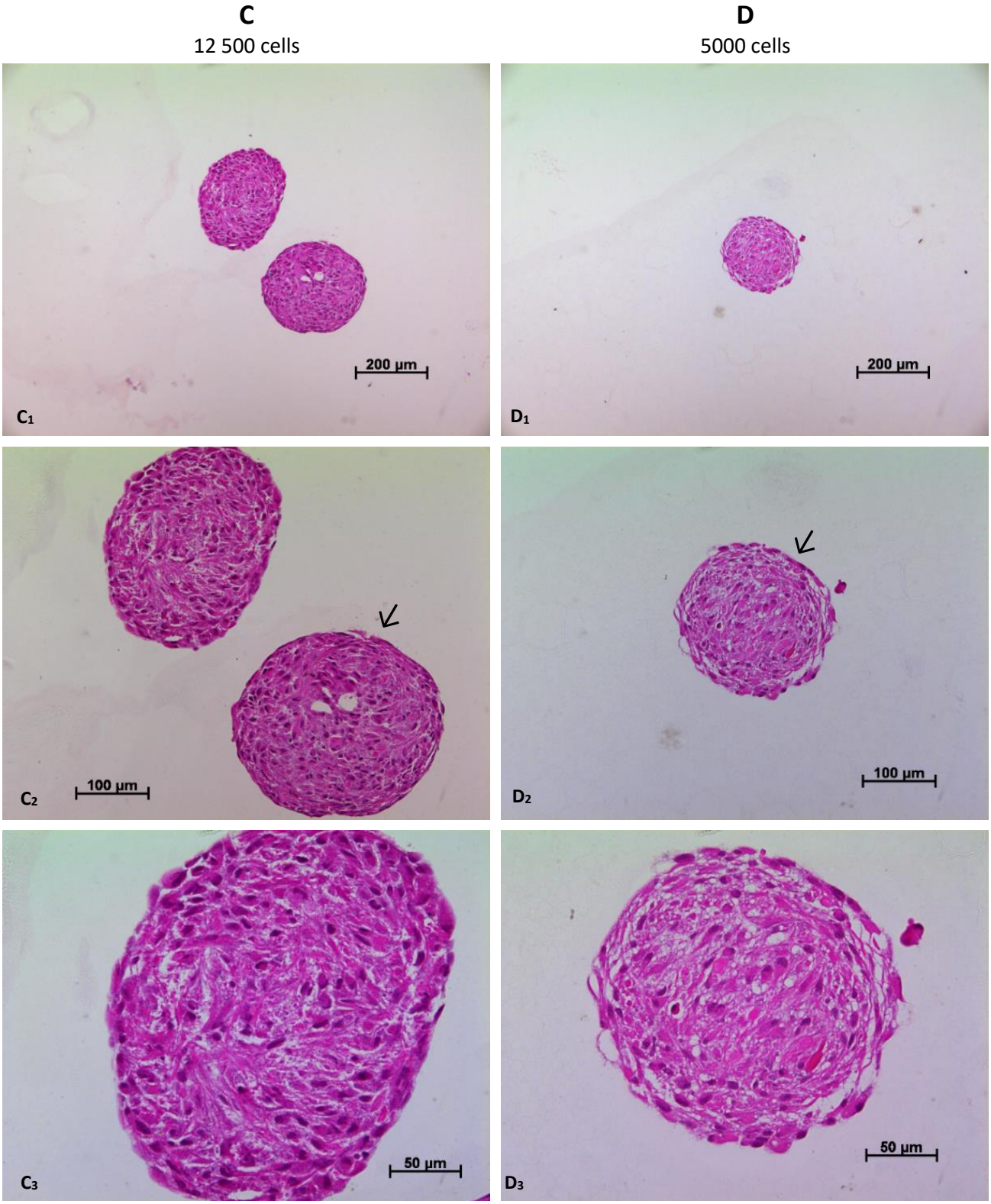

Figure 3.6: Haematoxylin and eosin staining of ASC spheroids generated from 12 500 cells (C) or 25 000 cells (D) viewed at the 10x (1), 20x (2) and 40x (3) objective. A border is visible surrounding the spheroids formed by an elongated layer of cells (see↑) Dark, normal looking nuclei are visible throughout the structures including the centre. Abundant, loosely arranged extra-cellular matrix material is visible in spheroids of both sizes with this material appearing most loosely arranged in the smaller spheroid (D).

To calculate the mean diameter of the spheroids generated from each different cell number, spheroids were measured using AxioVision 4.7 Software (Ziess, Germany) and the diameter calculated using the formula (horizontal diameter + vertical diameter)/2. Spheroids generated from 25 000 ASCs revealed the most reproducibility in terms of shape and size, although all spheroids in all groups were largely reproducible (Figure 3.7 A), and had an average diameter of 370 µm. Spheroids generated from 5000 cells had a diameter closest to that of the human scalp hair follicle with a mean diameter of 210 µm (Figure 3.7 B).

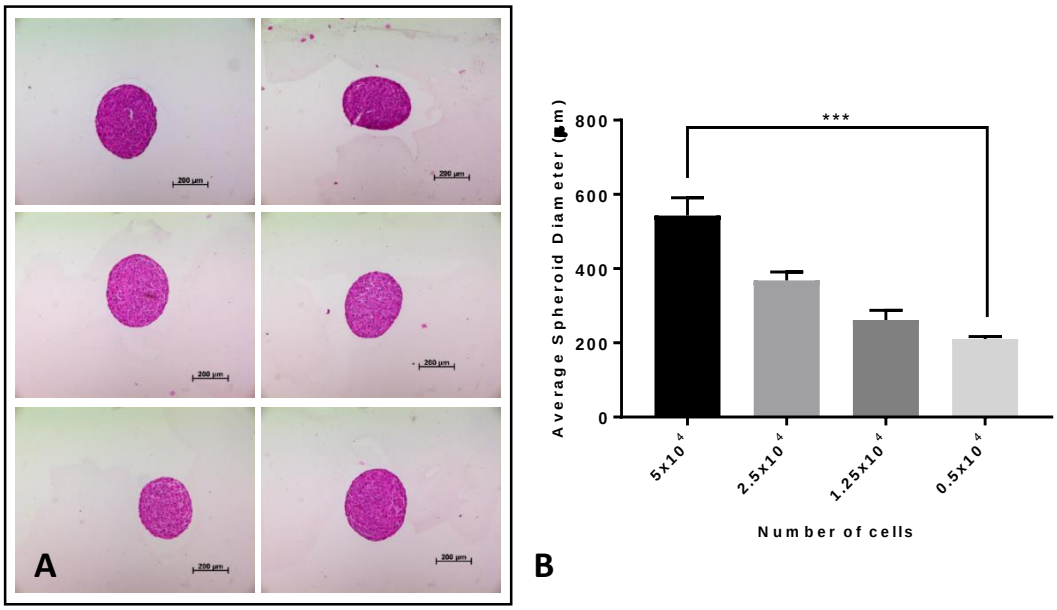

Figure 3.7: Haematoxylin and eosin staining of ASC spheroids generated from 25 000 cells showing uniformity of spheroid size (A) and average spheroid diameter of spheroids generated from different cell numbers (B).

3.2.3. Plating on Matrigel®

The next step was to determine if ASCs within the spheroid would survive and how they would behave once removed from within a droplet and replated in a new environment. If ASC spheroids were used in future hair follicle induction assays they would need to function within the dermal layer of a 3 dimensional skin-like model therefore Matrigel®, which has a composition similar to that of an early developmental extracellular matrix ,was used to generate an environment similar to embryonic mesenchyme. ASC spheroids of different sizes were placed on top of Matrigel®, set prior to spheroid being placed on it, or within Matrigel®, set after spheroid had been placed on it, and then observed in culture for 4 days.

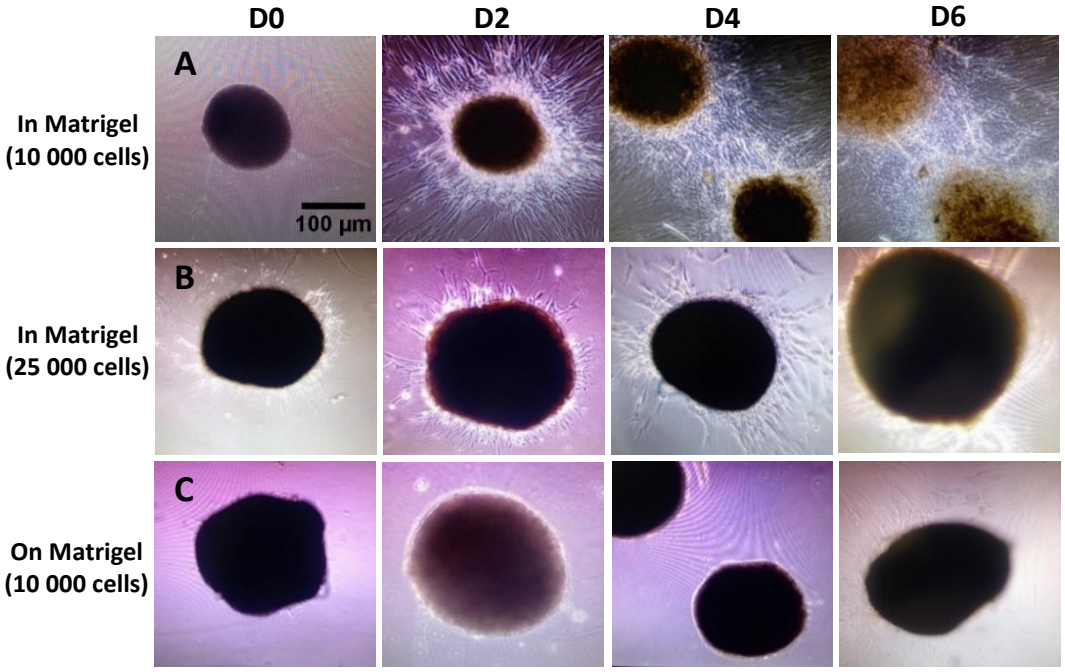

Figure 3.8: ASC spheroids placed within (A,B) or on top of (C) Matrigel® and observed for 4 days in culture. Multiple cells were observed growing out of 10 000 cell ASC spheroids within Matrigel® after 48 hours in culture and this continued for 6 days (A). Sparse numbers of cells grew out of 25 000 cell ASC spheroids placed within Matrigel® after 48 hours but this stopped after 4 days (B). No cells were observed growing out of 10 000 cell ASC spheroids placed on top of Matrigel®(C).

Large numbers of ASCs with elongated cytoplasmic extensions were observed growing out from spheroids generated from 10 000 cells after 48 hours within Matrigel®, and this continued for at least 6 days (Figure 3.8 A). As cells extended further out from the spheroids and came into contact with cells extending from neighbouring spheroids, the cells densified forming a reticulated network of ASCs. Spheroids of 25 000 cells placed within Matrigel® did exhibit cells extending out from them after 48 hours, however far fewer cells were observed and the outgrowth appeared to stop after 4 days in culture (Figure 3.8 B). No ASCs were visible extending out from ASC spheroids plated on top of Matrigel® with these spheroids retaining their original spheroid structure (Figure 3.8 C). This experiment proved that cells within the spheroids are still viable and are capable of growing out of the spheroid under certain conditions.

3.2.4. Alterations in gene expression resulting from spheroid culture of ASCs

Next it is was necessary to ascertain whether clustering ASCs as spheroids resulted in any changes in gene expression, in particular in those of known hair follicle DP cell markers. To assess changes in gene expression analysis of mRNA from three different ASC cell lines cultured in a monolayer and as spheroids was performed.

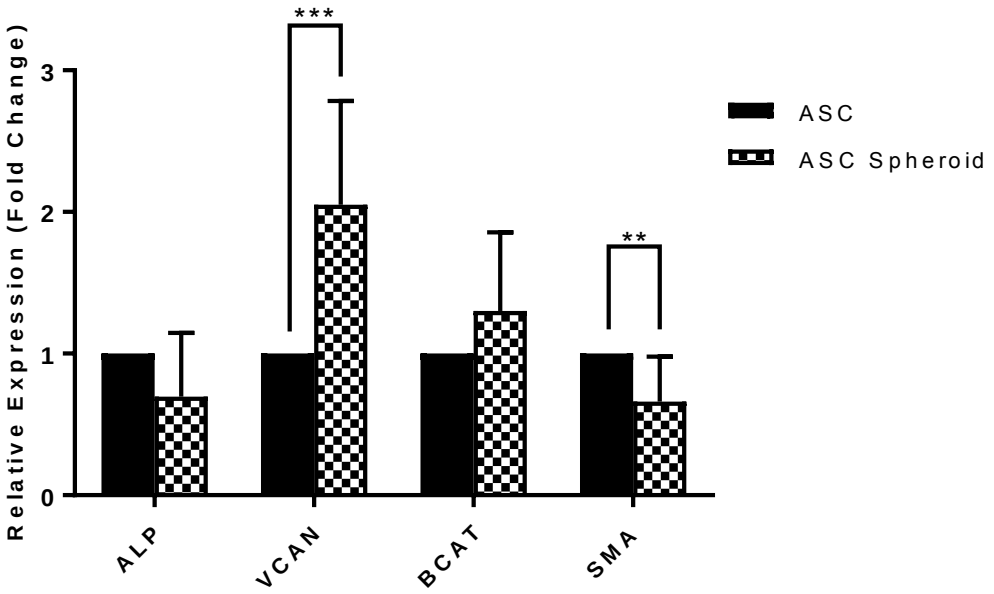

Figure 3.9: Differential mRNA expression of known DP genes in ASCs cultured in a monolayer or as spheroids. Relative expression was analysed by qPCR and normalised to the reference gene *GUS*. The data represent the means ± SD of experiments conducted in duplicate in 3 different cell lines. VCAN expression was significantly upregulated and αSMA significantly downregulated in ASC spheroids when compared to ASCs in monolayer culture.* indicate statistical significance. ***p≤0.001.

Clustering of ASCs resulted in a decrease in ALP expression when compared to ASCs in a monolayer, however this result was not significant (P=0.03) (Figure 3.9). The decrease in ALP expression in this experiment may not be meaningful as the relative expression compared to actual DP cells is not demonstrated. VCAN expression was more than double in spheroids as compared to ASCs in monolayer culture and this result was significant (P=<0.001) (Figure 3.9). This is consistent with the fact that VCAN expression is thought to be responisble for the aggregative nature of DP cells. By forcing the ASCs to cluster, this extracellular matrix component is upregulated possibly to maintain the integrity of the cluster. The expression of β-Catenin (BCAT) was increased in ASC spheroids when compared to ASCs in a monolayer but these results were not significant (P=0.07)(Figure 3.9). αSMA expression decreased signficantly in ASCs cultured as spheroids (P=0.001) when compared to ASCs in a monolayer. This result is interesting as in in vivo cells αSMA is highly expressed in the dermal sheath, a single layer of cells that is contiguous with the base of the DP, but not in the clustered cells of the DP themselves. This changes in culture with cells from both the DP and dermal sheath becoming αSMA positive in vitro. This experiment suggests that ASCs may respond to clustering similarly to DP cells, by downregulating αSMA expression.

In summary, it has been demonstrated that ASCs readily form spheroids when cultured using the hanging drop method and that cells within the cluster appear to be healthy and remain viable with the ability to grow out from the spheroid when replated in a different environment. Cell clusters of around 10 000 cells appear to form a spheroid closest in size to the dermal condensate. Analysis of gene expression shows that the DP marker VCAN is upregulated in spheroid cluster and that αSMA, a marker of DS cells that is known to drop with increasing inductivity, is reduced in spheroid cell clustering. These changes in gene expression may suggest that ASCs cultured in this manner develop the aggregative phenotype that is most characteristic of native DP cells.

3.3. Culture of ASCs in Wnt3a-conditioned medium

During hair follicle embryogenesis the initial signal arising from the dermis that causes the formation of epithelial placodes involves the Wnt signalling pathway (Millar, 2002). Exposure of stem cells to such key regulatory molecules is often sufficient to direct them towards a particular cell fate. The next experiment aimed to establish whether culturing ASCs in Wnt3a-conditioned medium would upregulate expression of the Wnt/β-catenin signalling cascade and thereby induce ASCs to adopt a phenotype closer to that of the hair follicle DP cells.

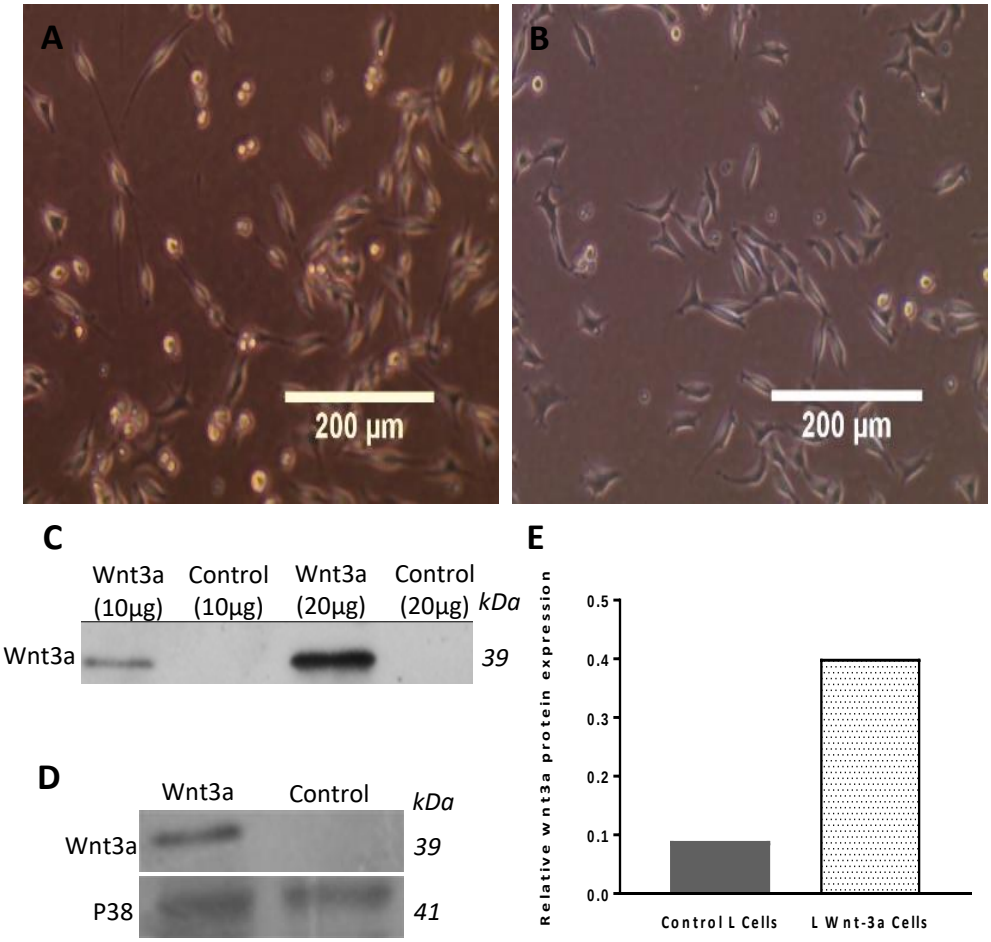

Figure 3.10: Comparison of Control L (A) and L Wnt-3a (B) cells in culture and qualitative (C,D) and semi-quantitative (E) analysis of wnt3a protein expression in the two cell lines. The morphology of L-Wnt-3a and Control L cells is identical in culture with both cell types being stellate with small centrally placed nuclei (A,B). Wnt3a protein is demonstrable in 10µg of the whole cell lysate of L-Wnt3a cells and much more pronounced in 20µg (C). Wnt3a protein is expressed more than four times higher in L Wnt-3a cells than in Control L cells(D,E).

Prior to initiating these experiments, L Wnt-3a (ATCC® CRL-2647™) cells that constitutively secrete biologically active Wnt-3A protein (Willert et al. (2003)) were used to generate Wnt3a conditioned medium (Wnt3a CM) as described in the Materials and Methods. ASCs were cultured in this medium

and evaluated for changes in morphology and gene expression. Control L Cells (ATCC® CRL-2648™), L-M(TK-) fibroblasts that do not contain the expression vector, were used to generate control conditioned medium (Control CM) for all experiments. There were no observed differences in the morphology of Wnt-3a cells and control cells in culture with both cell types exhibiting a stellate morphology with small centrally placed nuclei (Figure 3.10 A,B).

To confirm that the Wnt-3a cell line obtained from ATCC were secreting the Wnt3a protein, Wnt3a cells and control cells were cultured under routine culture conditions and a western blot performed on the whole cell lysate of both cell lines to determine the presence or absence of Wnt3a. The results clearly demonstrated the presence of Wnt3a protein in as little 10µg of the whole cell lysate and this protein expression was greatly enhanced in 20µg of the lysate (Figure 3.10 C). Wnt3a protein was very low even in 20µg of whole cell lysate of control cells (Figure 3.10 C). The presence of Wnt3a protein in Wnt3a cells and its absence in control cells was confirmed using p38 as a loading control (Figure 3.10 D). Semi-quantitative analysis of western blot results confirmed that wnt3a protein expression was four times higher in wnt3a secreting cells than in controls (Figure 3.10 E).

ASCs were then cultured in a monolayer for 5 days in Wnt3a or Control CM and the cells were evaluated for morphological changes as well as changes in protein and gene expression.

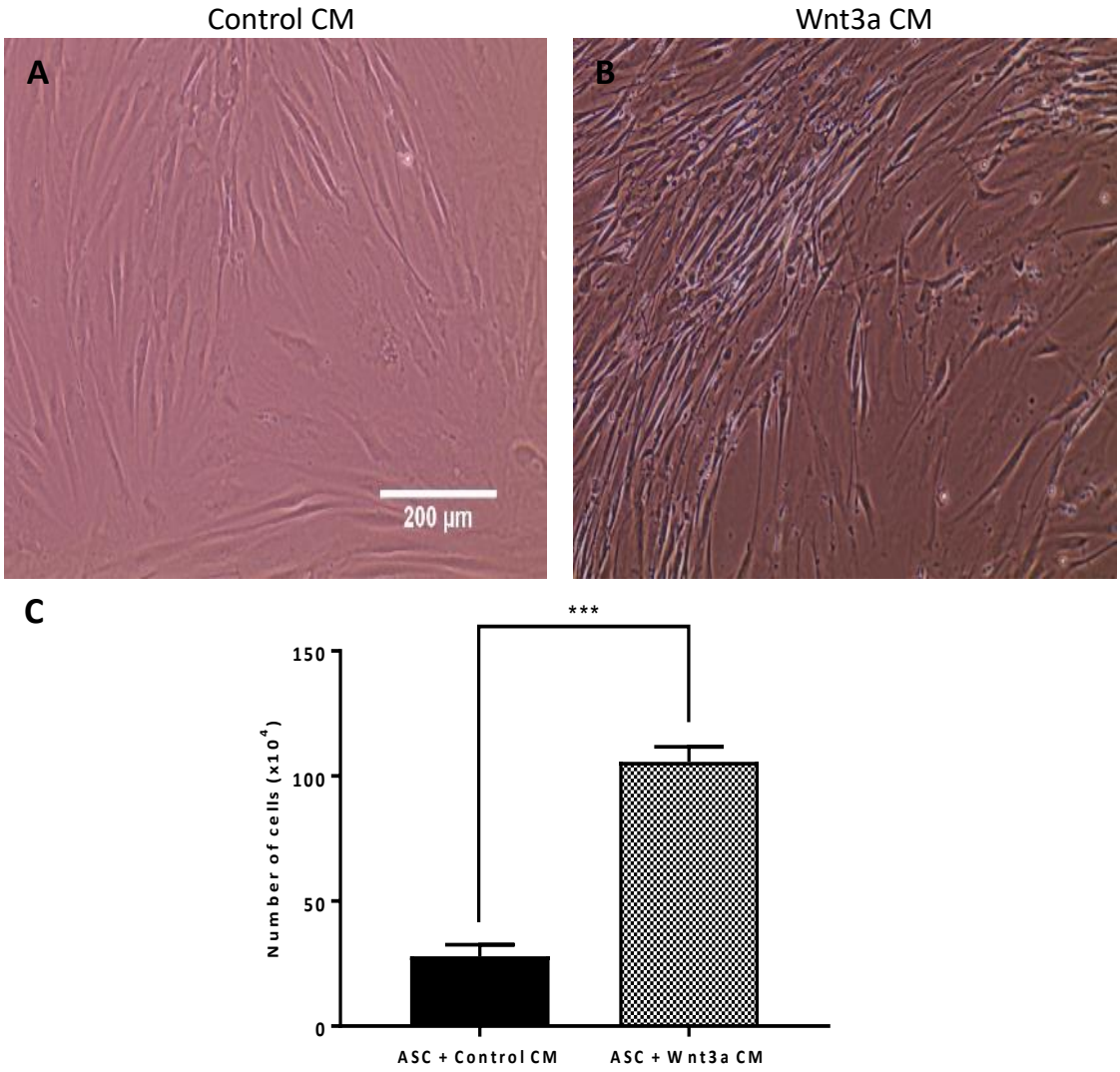

Figure 3.11: ASCs in control -conditioned medium (A) or Wnt3a-conditioned medium (B) and counted after 5 days in culture (C). ASCs cultured in Wnt3a conditioned medium showed definite evidence of altered morphology with the cytoplasmic extensions of the cells lengthening, and the cells clustering into parallel sheaths (B). The number of ASCs cultured in Wnt3a-conditioned medium was more than four times that of those cultured in control conditioned medium after 5 days in culture (C). * indicates statistical significance ($P<0.001$)

When cultured in Wnt-conditioned medium, the typical spindle shaped cytoplasmic extensions of the ASCs (Figure 3.11 A) appeared to elongate and the cells clustered together in parallel sheaths (Figure 3.11 B). Cell counts reveal that the number of ASCs in the Wnt exposed group was more than four times that of the those in the control group (Figure 3.11 C). This result echoes other studies that show that exposure to Wnt-signalling results in increased proliferation of mesenchymal cells (De Boer et al., 2004)

Since it is is known that exogenous Wnt signalling can stimulate expression of endogenous Wnt (Wodarz and Nusse, 1998), a western blot was performed on the whole cell lysate of Wnt -treated

and untreated ASCs after 5 days in culture. The results show that there is constitutive endogenous secretion of Wnt3a by ASCs and that there is an increase in this intra-cellular Wnt3a protein expression in the Wnt-treated cells relative to control cells(Figure 3.12 A). Semi-quantitative analysis of the western blot the relative expression of Wnt3a in cells cultured in Wnt3a conditioned medium was more than double that in control cells (Figure 3.12 B) however, given the strong exposure and background this quantification is not convincing.

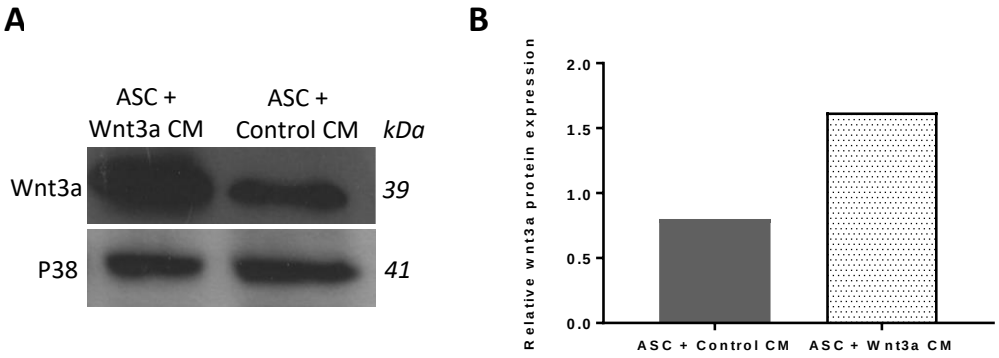

Figure 3.12: Comparison of Wnt3a protein expression levels in ASCs cultured in Wnt3a or control-conditioned medium. Western blot results (A); and semi-quantitative bar graph of A (B). Wnt3a protein expression was highly upregulated in ASCs treated with wnt3a conditioned medium compared to those treated with control medium (B).

It is known that in vivo, dermal clusters signal to the epithelium via, inter alia, Wnt-signalling therefore the next step was to determine if upregulation of Wnt signalling cascade would induce any change in expression of hair follicle DP associated genes in ASCs. In the first instance these experiments were conducted on ASCs cultured in a monolayer for 5 days in Wnt3a or control-conditioned medium and then lysed for RNA extraction and qPCR analysis.

The expression of the extra-cellular matrix proteoglycan versican quadrupled under the influence of Wnt3a-conditioned medium and this result was significant ($P<0.001$) (Figure 3.13).

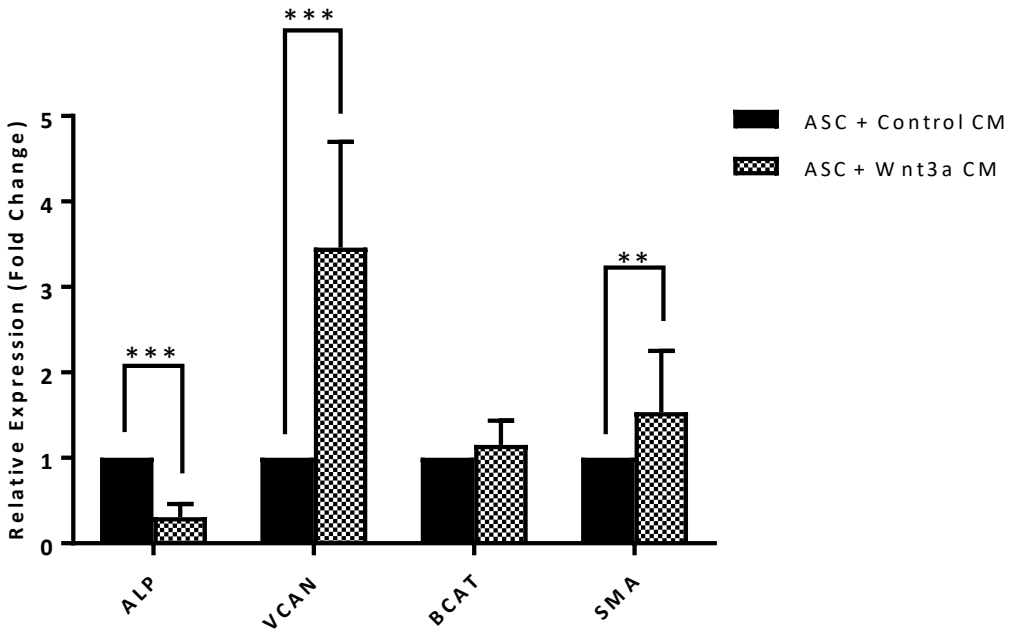

Figure 3.13 Differential mRNA expression of known DP genes in ASCs cultured in a monolayer in Wnt3a- or control-conditioned medium. expression was more than two fold higher in ASCs exposed to Wnt3a than in controls and this was significant. Alpha smooth muscle actin expression in ASCs increased significantly and alkaline phosphatase expression decreased significantly upon treatment with Wnt3a-conditioned medium. B-catenin expression appeared to increase in ASCs exposed to Wnt3a but this was not significant.* indicate statistical significance. ***p≤0.001.

αSMAAlpha smooth muscle actin expression increased significantly (P=0.02) upon treatment with Wnt3a conditioned medium while alkaline phosphatase expression decreased significantly (P<0.001). β-catenin expression appeared to increase slightly under the influence of Wnt3a but this result was not significant (P=0.07).

In summary, exposure to Wnt3a -conditioned medium has a significant effect on cultured ASCs. It causes them to proliferate more rapidly and upregulate the expression of both versican and α smooth muscle actin.

3.4. Culture of adipose derived mesenchymal stem cells as spheroids with Wnt3a -conditioned medium

In early hair follicle morphogensis, mesenchymal cells within the unifom dermis cluster together to form the dermal condensate, a process which is initiated by Wnt signalling. The next objective of this project was to establish the combined effect of culture as spheroids and exposure to Wnt3a-conditioned medium on DP gene expression in ASCs. ASCs were cultured in either Wnt3a- or control-

conditioned medium, first in a monolayer for 5 days and then as spheroid clusters. ASCs within the hanging drops remained in the relevant medium for 24 hours.

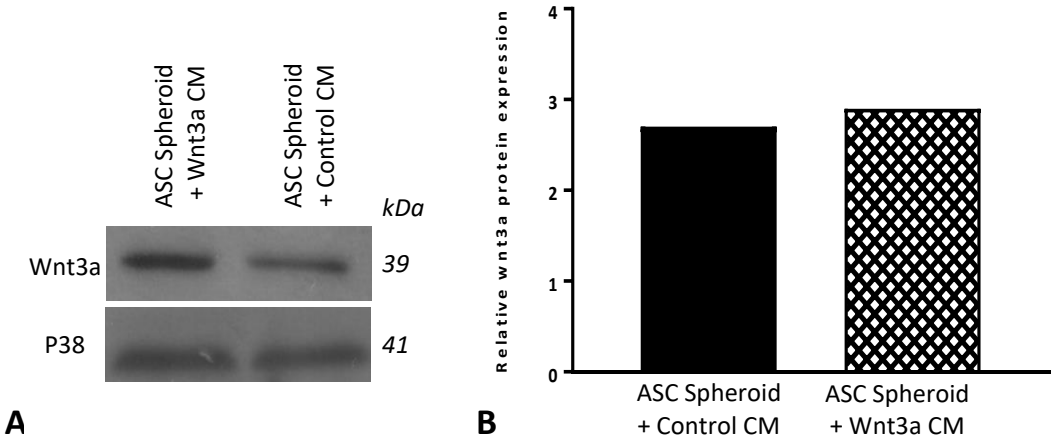

Figure 3.14: Comparison of Wnt3a protein expression levels in ASCs cultured as spheroids in Wnt3a- or control-conditioned medium. Western blot results (A); and semi-quantitative bar graph of A (B). Wnt3a protein levels did appear to be higher in the whole cell lysates of ASC spheroids treated with Wnt3a -conditioned medium than in those treated with control-conditioned medium however this difference was not particularly marked.

A western blot performed on the cell clusters after 6 days confirmed that the presence of the Wnt3a protein was slightly higher in Wnt3a treated spheroids than in controls (Figure 3.14 A). Semi-quantitative analysis of western blot results revealed the relative expression of the Wnt3a protein was only slightly higher in the Wnt3a spheroids than in controls with a ratio of 2.7:2.9 (Figure 3.14 B). Analysis of differential mRNA expression in Wnt3a treated and untreated spheroids was then performed to evaluate the effect of a combination of treatment with Wnt3a and spheroid culture on ASCs (Figure 3.15).

The results showed that the addition of Wnt3a to ASCs causes a decrease in alkaline phosphatase expresssion and that this remains true if they are cultured as a monolayer or as a cluster (Figure 3.15 A). Alkaline phosphatase expression was lowest in Wnt3a -treated ASC spheroids and this result was significant ($P<0.001$). This may reflect that ASCs within Wnt-treated cell clusters are in a more differentiated state.

There is no additional increase in versican expresssion in ASCs in a cluster when they are exposed to Wnt3a-conditioned medium (Figure 3.15 B). ASCs have been shown in this project to express

endogenous Wnt. Clustering cells together may increase the local concentration of Wnt which results in the addition of exogenous Wnt under these circumstances having no effect.

Beta-catenin mRNA remains unaltered in ASCs exposed to Wnt-signalling whether they are cultured as a monolayer or in clusters (Figure 3.15 C).

The expression of αSMA in ASCs treated with Wnta3a-conditioned medium was increased compared to those treated with control-conditioned medium whether they were cultured as spheroids or in a monolayer (Figure 3.15 D).

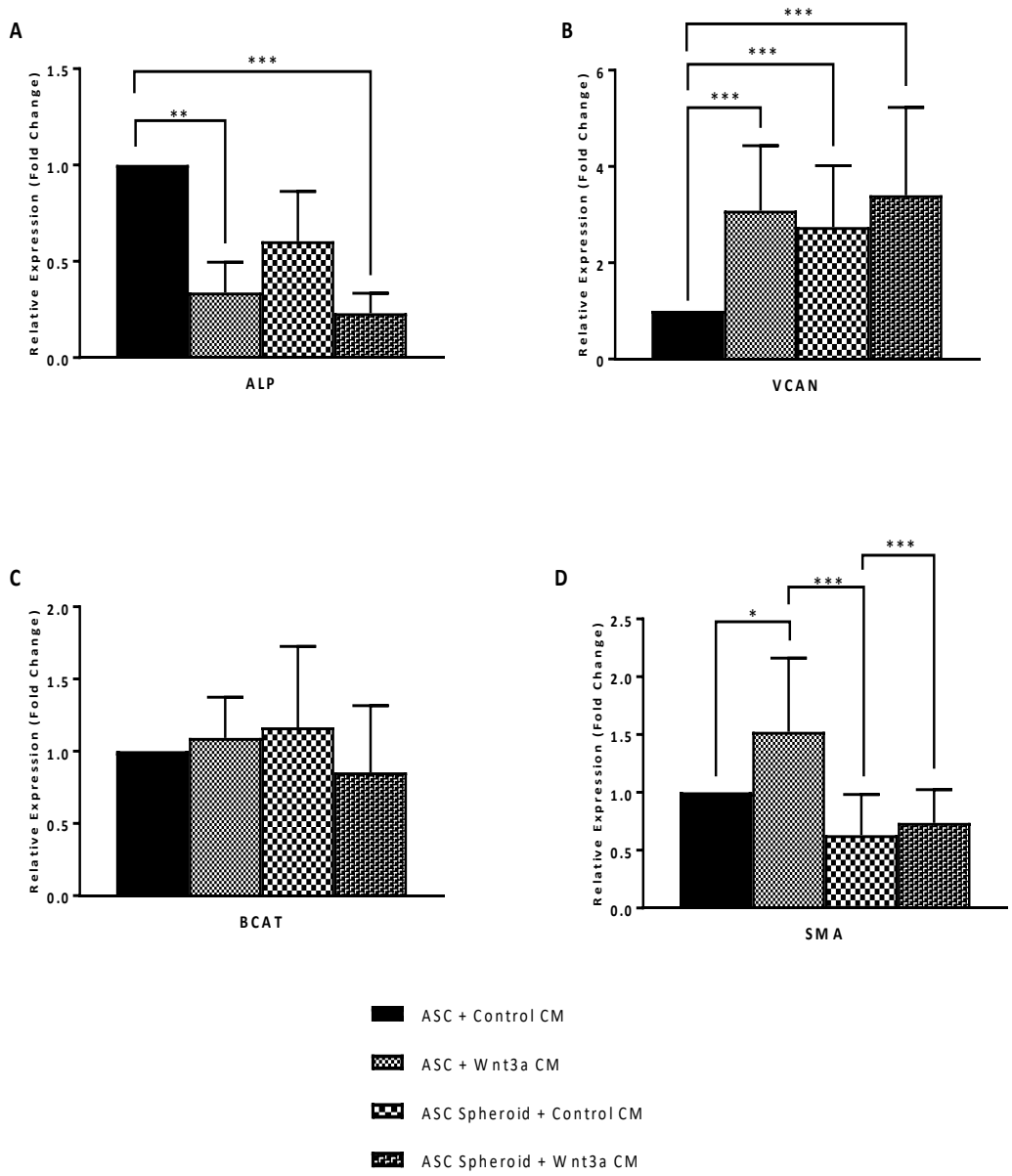

Figure 3.15: Analysis of differential mRNA expression of known dermal papillae genes in adipose derived mesenchymal stem cells cultured in wnt3a- or control-conditioned medium and clustered to form spheroids. Alkaline phosphatase expression was lowest in ASC spheroids treated with wnt3a-conditioned medium and this result was significant ($P<0.001$). Versican expression was highest in ASCs treated with wnt3a-conditioned medium and clustered as spheroids ($P<0.001$). β-catenin mRNA levels, while increasing in ASCs treated with wnt3a-conditioned medium and clustered as spheroids in the absence of wnt3a; decreased in ASCs that were both treated with wnt3a and clustered as spheroids, however these trends were not significant. α-smooth muscle actin expression increased slightly in ASCs exposed to wnt3a irrespective of monolayer or spheroid culture but this increase was more marked in monolayer culture ($P=0.04$). * indicate statistical significance. ***$p\leq0.001$.

The results of this set of experiments reveal that the combination of exposure to Wnt signalling and spheroid cluster have different effects on the expression of each of the genes examined in this study and do not neccesarily have an additive effect in directing ASCs to adopt a DP-cell like phenotype.

3.5. Culture of HaCaTs in Wnt3a-conditioned medium

As mentioned previously, the critical 'first dermal signal' in hair follicle morphogenesis that results in the aggregation of palisade-like epithelial cells to form an epithelial placode is thought to be Wnt-signalling. To enable assessment of inductive capability of DP-like ASC clusters that were generated in the future, they would need to be combined with epithelial cells, and a response in the overlying epithelial cells suggesting that the series of reciprocal epithelial-mesenchymal interactions had been triggered would have to be seen. The first question asked was whether exposure to Wnt3a-conditioned medium alone would have any effect on epithelial cells.

HaCaTs, a spontaneously transformed aneuploid immortal keratinocyte cell line from adult human skin (Boukamp et al., 1988) were therefore cultured in Wnt3a-conditioned medium and changes in morphology or gene expression were evaluated to establish whether Wnt3a exposure alone would result in HaCaTs adopting a phenotype more simliar to that of primitive epithelial placodes. HaCaTs were cultured for 5 days in Wnt3a- and control-conditioned medium and then RNA was extracted to analyse gene expression.

There were no discernable differences betweeen the cell morphology and size of HaCaTs between the Wnt3a treated and untreated groups after 5 days in culture in the centre of the culture dish (Figure 3.16 A&B). This was unlike the obvious change in morphology induced in
ASCs when exposed to Wnt3a (Figure 3.11). In the centre of the culture dish, cells cultured in both Wnt3a- and control-conditioned medium had the polygonal shape, horizonatal, oval-
shaped nuclei and abundant cell junctions common to sqaumous epithelial cells while the cobblestone morphology of the cell sheet was characteristic of an epithelial layer (Figure 3.16 A&B). There was no apparent difference in cell number in the Wnt3a-treated HaCaTs, which was also unlike in ASCs where wnt3a exposure significantly increased the proliferation rate and cell number (Figure 3.11).

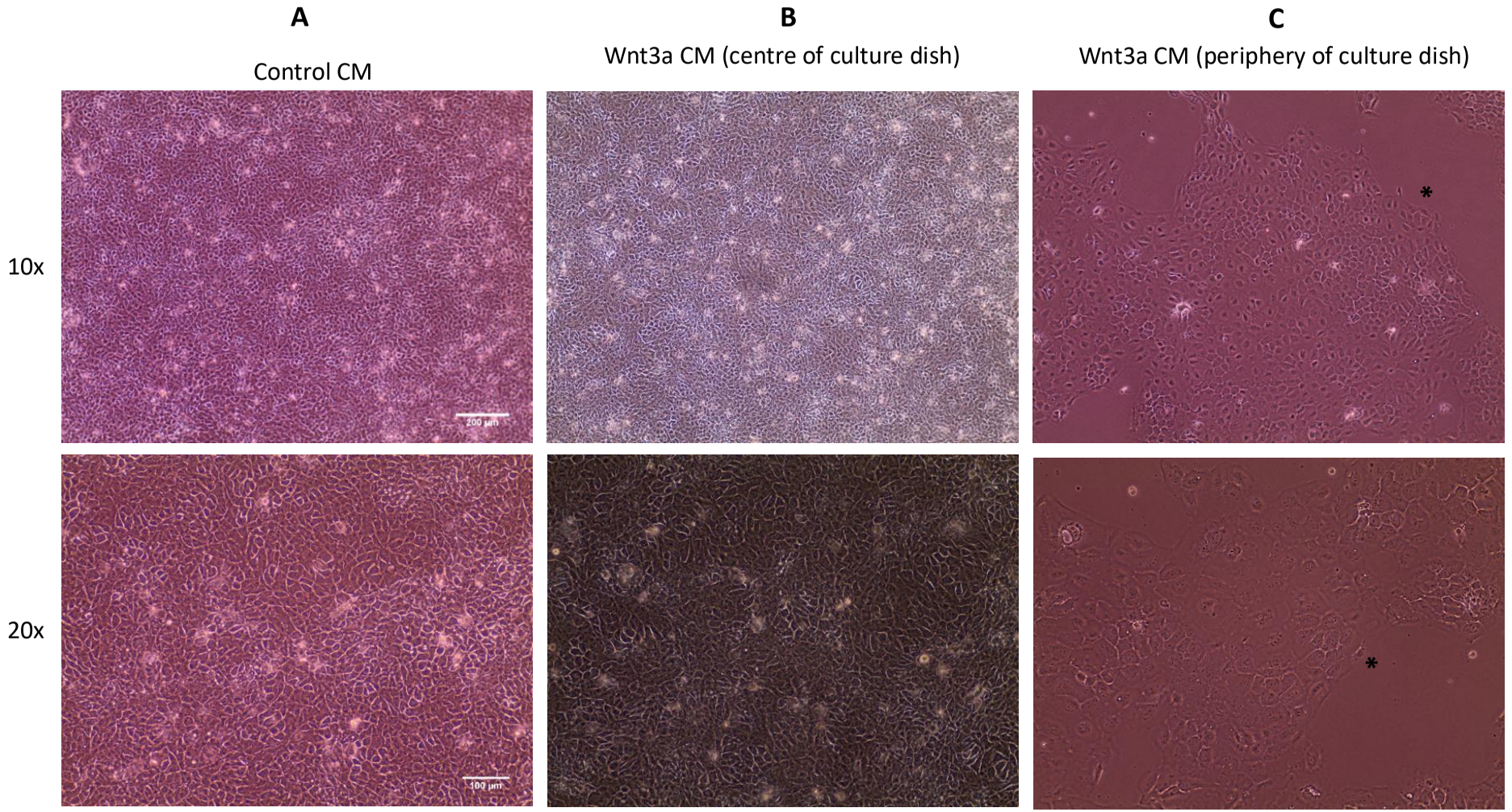

Figure 3.16: HaCaTs cultured in wnt3a- or control conditioned medium for 5 days and viewed the 10x (A) and 20x (B) objective at both the centre and periphery of the cell culture dish. There is very little difference in the observed cell morphology and cell number in the wnt3a treated and control group at the centre of the cell culture dish (A,B) where the cobblestone morphology of an epithelium is evident. At the edge of the cell culture dish, HaCaTs cultured in wnt3a-conditioned medium appear larger, and more flattened and are seen to form a distinct border with the base of the cell culture dish visible beyond it (C*).

Interestingly, the morphology of Wnt3a -treated HaCaTs around the periphery of the dish did appear to be slightly different to that of the cells in the centre. Cells closer to the edges of the culture dish were observed to be larger and flatter than those in the centre (Figure 3.16 C).

At the perpiphery of the culture dish in the Wnt3a-treated HaCaTs, the cells came together at the edge of the cell mass to form a sharply demarcated border that appeared to be slightly raised from the base of the cell culture dish and the base of the culture dish was visible beyond this (Figure 3.16 C*). The changes observed appeared to suggest that the HaCaTs at the outermost area of the culture dish were preferentially proliferating upwards into layers instead of laterally under the influence of Wnt3a. This may reflect the cells transitioning from a simple to a stratified squamous epithelium. Analysis of expression of genes demonstrating the response of epithelial cells to dermal signalling and the initiation of epithelial hair shaft formation appeared to corroborate this.

HaCaTs exposed to Wnt3a signalling showed significant decreases in the expression of keratin 5 and keratin 10 ($P=<0.001$)(Figure 3.17). These keratins, are upregulated in the epithelial placodes of the nascent hair follicle and their expression co-incides with the initiation of epithelial hair shaft formation. The decrease in their expression may suggest that, as reflected in the altered cell morphology (Figure 3.16 C), the cells are not assuming the phenotype of keratinocytes within the developing hair follicle, but rather assuming the phenotype of mature keratinocytes within a stratified sqaumous epithelium. The Wnt signaling casacde genes Wnt3a, beta-catenin and nuclear factor kappa b all demonstrate a trend of increasing slightly in Wnt3a treated HaCaTs however this was not significant ($P=0.65$, 0.11 and 0.30 respectively)(Figure 3.17). Exposure to Wnt3a signalling did not appear to elicit any response in HaCaTs to suggest that they were responding and beginning to initiate the process of hair shaft formation. However, as HaCaTs are a fully differentiated cell line of epithelial origin, there is a good chance that they would not be capable of responding to inductive dermal cells. It is possible that if a more primitive, embryonic epithelial cell line had been used, such as human neonatal foreskin keratinocytes, the effect of Wnt3a-exposure could have been quite different.

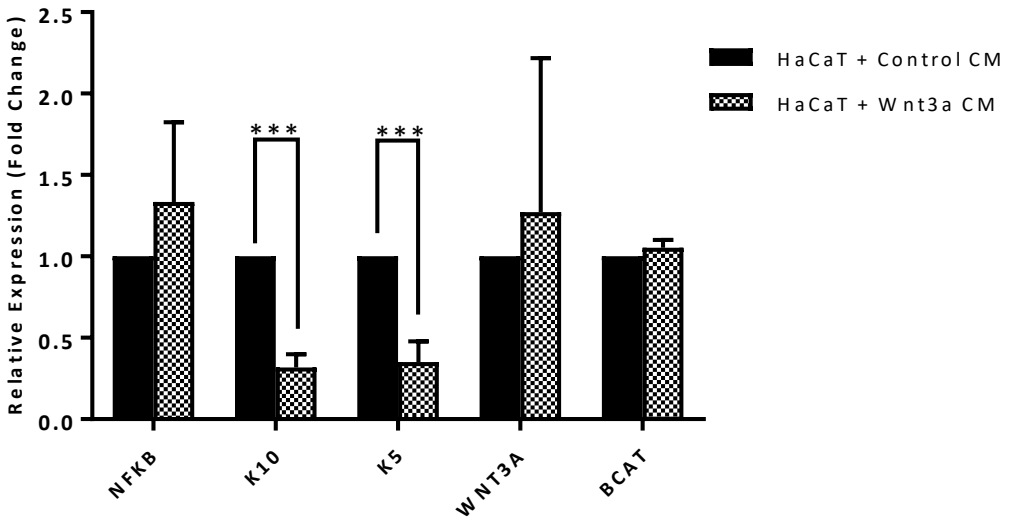

Figure 3.17: Analysis of differential mRNA expression of genes expressed in the epithelium that demonstrate response to dermal signalling and initiation of hair follicle formation in HaCaTs cultured in wnt3a- or control-conditioned medium. The expression of the immature hair follicle keratinocyte markers keratin 5 and keratin 10 was significantly decreased on exposure to wnt suggesting that the cells were adopting a phenotype consistent with a mature, stratified epithelium and not of a primitive hair follicle. Although genes suggesting activation of the wnt signalling cascade including nuclear factor ƙappa b, beta-catenin and wnt3a did appear to show a trend of increased expression this was not significant and did not suggest marked upregulation of the wnt-signalling cascade.* indicate statistical significance. ***p≤0.001.

Chapter 4: Discussion

Embryological hair follicle morphogenesis relies on a complex series of reciprocal interactions between the 'inductive' mesenchyme and the 'receptive' epithelium of the primitive skin (Figure 4.1)(Hardy, 1992). Despite the importance of the hair follicle in the aesthetics and functioning of human skin the challenge of de novo hair follicle morphogenesis from human cells has yet to be achieved. To generate a hair follicle, suitable 'inductive' mesenchymal cells and 'receptive' epithelial cells need to be combined within a model that allows them to interact and eventually differentiate to form a hair follicle. Fortunately epithelial cells have been shown to retain their responsiveness to dermal signalling into adulthood (Jahoda et al., 1984) and can be readily expanded from donor sites; therefore obtaining and preparing suitable epithelial cells is not the challenge to achieving hair follicle formation. The major challenge has been and remains the need to find suitable mesenchymal cells that will be capable of triggering the induction cascade leading to hair follicle formation.

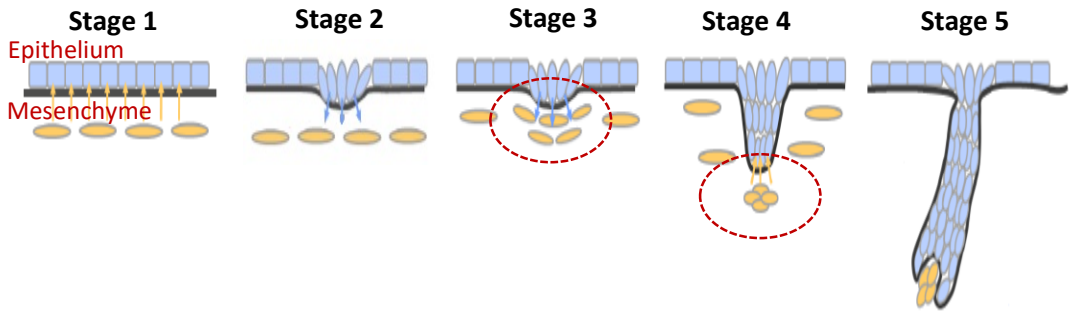

Figure 4.1: Early stages in embryonic hair follicle morphogenesis. In hair follicle embryogenesis specific dermal mesenchymal cells provide the 'first dermal signal' that results in aggregation and palisading of epithelial cells above them (Stage 1). In what is likely related to a 'dose response' these aggregations of epithelial cells, referred to as epithelial placodes, then signal back to underlying dermal cells triggering aggregation of these dermal cells and dermal condensate formation (Stage 2 & 3). The dermal condensate then triggers proliferation, downgrowth and differentiation of overlying epithelial cells resulting in hair shaft formation (Sage 4 & 5). The epithelial cells at the base of the hair follicle will grow to encase the cells of the dermal condensate which will form the dermal papillae, responsible for hair follicle cycling throughout life. This study aims to recapitulate the events of mesenchymal condensation and dermal condensate formation demonstrated in Stage 3 and 4 (encircled). Adapted from Liu et al. (2002).

The aim of this project was to explore the suitability of human adipose-derived mesenchymal stem cells to utilise in such a hair follicle re-engineering process i.e. to attempt to direct adipose derived mesenchymal stem cells to adopt a hair follicle DP cell fate. Specifically, the project aimed to use extrinsic factors (as opposed to endogenous transcription factors) mimicking the steps of early embryonic hair

follicle morphogenesis using enforced aggregation and exposure to Wnt-signalling (see Figure 4.1 Stage 3&4) to see if these interventions would direct ASCs to adopt a hair follicle DP cell like-phenotype.

Ideally, whether extrinsic or intrinsic factors are used, direct reprograming of cells should involve techniques such as genome wide RNAi screening with integrated transcriptome analysis to identify key genes and cellular events required at the transition steps in reprogramming, evaluation of multiple markers to compare with the expression and phenotype of the target cell as well as functional assays to demonstrate the capability of the reprogrammed cells to perform the same role as the target cell. As metioned, one of the methods to establish whether a multi-potent cell is successfully being directed to a new cell fate is the upregulation in expression of genes known to be markers of the target cell (and/or to check that non relevant genes are down regulated). In the case of hair follicle morphogenesis this presents a number of challenges. One of the challenges is that in hair follicle morphogenesis, as in all embryological organ formation, specific genes are often expressed on a changing continuum, being highly expressed at one development stage and then expressed at low levels at specific time points or in specific places in a tightly regulated process. This makes it hard to accurately interpret different expression levels in a transient structure such as DP. In addition, there is an absence of reliable markers for hair follicle DP and a rather poor understanding of the function of markers in the developmental process itself.

4.1. The effect of Wnt3a signalling on gene expression and mesenchymal condensation

The 'first dermal signal' that causes mesenchymal cell condensation thereby triggering hair follicle morphogenesis is Wnt-signalling (Millar, 2002). The first objective of this project was to try to explore the effect of exposure to Wnt3a signalling on ASCs cultured in a monolayer and understand how Wnt-signalling may result in clustering of mesenchymal cells by examining changes in the expression of known DP genes. One of the few genes identified in embryonic hair follicle formation subsequent to the activation of Wnt-signalling when mesenchymal cells cluster together to form dermal condensates is versican (Kishimoto et al., 1999b). This chondroitin sulphate proteoglycan that is mainly found in the extracellular matrix and is thought to be responsible for the ability of mesenchymal cells to aggregate, and for maintaining aggregation.

The baseline expression of versican in ASCs was shown to be significantly higher than in adult dermal fibroblasts, another cell line of mesenchymal origin, in this project, by at least 15 fold (Figure 3.3, B). The higher expression of versican in ASCs compared to fibroblasts suggests that at baseline they may have greater potential to aggregate than HDFs. When ASCs in a monolayer were exposed to Wnt3a-conditioned medium, the expression of versican mRNA revealed a more than three-fold increase

(Figure 3.13). This result proves that ASCs, like hair follicle DP cells, respond to exposure to the WNT-signalling cascade by upregulating versican expression. This suggests that the Wnt/β-catenin signalling cascade may regulate hair follicle DP cell aggregative growth through modifying versican expression which in turn results in them clustering together to form the dermal codensate.
This result is consistent with a study by Yang et al (2012) who used DP cells isolated from adult human scalp follicles and showed that with increasing passage number DP cells lost their aggregative ability. This loss in aggregative property corresponded to a gradual decline in versican mRNA and protein levels, while the mRNA and protein levels of β-catenin remained relatively constant. The mRNA of both β-catenin and versican reduced simultaneously after β-catenin siRNA transfection. They concluded that the Wnt/β-catenin signalling cascade regulates hair follicle DP cell aggregative growth through modifying versican expression.

Previous studies have shown that in vascular smooth muscle cells versican transcription is mediated by the glycogen synthase kinase, GSK-3β pathway via the β-catenin-TCF transcription factor complex where such regulation contributes to the formation of a provisional matrix (Rahmani et al., 2005). The canonical Wnt signalling pathway acts by preventing degradation of β-catenin which translocates to the nucleus and binds to the LEF-TCF family of DNA binding factors and it is therefore likely that in this study the upregulation in versican expression resulting from Wnt-signalling may be as a result of transactivation of the versican promoter by binding of β-catenin to the TCF transcription factor complex in this manner.

Another gene known to be highly expressed in hair follicle DP cells, although not in embryological hair follicle morphogenesis, is the actin isoform α smooth muscle actin (αSMA). This protein has been shown to be a marker for the dermal sheath (DS) in vivo and a marker for both DS and DP in vitro (Jahoda et al., 1991). As with other putative dermal papilla markers the function of αSMA within the dermal sheath remains unclear. In this study the level of αSMA mRNA expression in ASCs was lower than in human dermal fibroblasts under routine culture conditions (Figure 3.3). This slightly elevated level of αSMA expression in HDFs correlates with the fact that HDFs are known to adopt the contractile migratory myofibroblast type phenotype in culture (Sappino et al., 1990).

Exposing ASCs in monolayer culture to wnt3a conditioned medium resulted in a significant upregulation in αSMA expression (Figure 3.13). This result is similar to previous research that showed that exposing human dermal fibroblasts to recombinant wnt3a significantly increased α smooth muscle actin expression and incorporation of this contractile protein into stress fibres which in turn

increased cell migration of fibroblasts (Carthy et al., 2011). The increase in expression of α smooth muscle actin mRNA in ASCs exposed to wnt3a suggests that the Wnt/β catenin signalling cascade may promote the migration of mesenchymal cells, possibly promoting the ability of mesenchymal cells in a monolayer within the dermis to migrate together to form the dermal condensate.

The results of this project suggest that the Wnt/β-catenin signalling cascade may result in mesenchymal cell condensation by increasing the ability of mesenchymal cells to migrate towards each other through the upregulation of the contractile protein α smooth muscle actin which results in a migratory phenotype. Furthermore, increased Wnt signalling regulates the expression of versican which is mediated through binding of β-catenin to the TCF family of transcription factors. This increased expression of versican functions to promote aggregation of mesenchymal cells possibly through the provision of the extracellular matrix and adhesion molecules between them.

4.2. The effect of spheroid culture on the phenotype of adipose derived mesenchymal stem cells

The next objective of this study was to attempt to mimic mesenchymal condensation in early hair follicle morphogenesis by enforcing ASCs to aggregate and to evaluate whether this enforced clustering of ASCs would result in any changes in gene expression. Cultured ASCs were induced to form spheroids in hanging drop cultures for 24 hours. In embryological limb development, mesenchymal condensation is a critical transitional stage that precedes cartilage formation (Ghone and Grayson, 2012) and a concern in this study was that enforced aggregation of ASCs may result in the initiation of chondrogenesis. The short term culture of this experiment would not have enabled chondrogenesis to occur as this takes a few weeks in culture (Stromps et al., 2014). Histology of ASC clusters however did not appear to demonstrate any evidence of cartilage formation, although this was not confirmed with staining or gene analysis (Figures 3.5 and 3.6). This result correlates with a study performed by Zhang et al. (1998) who investigated the role of versican in mesenchymal condensation and chondrogenesis in a model using mesenchymal stem cells obtained from chick embryos at developmental stage 22 that were exposed to conditioned medium from COS-7 cells transfected with a mini versican gene and reported that this gene product inhibited mesenchymal chondrogenesis. It appears that ASCs, when clustered together are not directed to form cartilage which may have prevented them from being directed toward hair follicle DP-like cells.

The culture of ASCs as spheroid clusters, even in the absence of Wnt3a-conditioned medium, resulted in a significant increase in versican expression (more than two-fold) compared to ASCs grown in a monolayer (Figure 3.9). Of the genes examined in this study, versican was the most evidently altered

by spheroid culture. These results appear to suggest that even in the absence of epithelial Wnt-signalling, enforced aggregation with mechanical cues from surrounding cells is sufficient to upregulate versican expression. This result may suggest that versican is both causal and necessary for maintaining the integrity of dermal cell condensates. It is possible that the consistently elevated expression of versican within cell clusters functions to ensure that cells that do not have inductive potential, such as dermal fibroblasts, are unable to develop into DP cells.

Interestingly, went ASC cell clusters were exposed to Wnt3a conditioned medium there was no significant upregulation of versican expression (Figure 3.15). As ASCs have been shown in this study to express Wnt3a constitutively (Figure 3.12), clustering of ASCs may result in an increased expression of endogenous Wnt3a in a concentration related manner. It is possible that this elevated level of Wnt3a expression may generate a negative feedback loop, directly attenuating the effect of exogenous Wnt secretion. As versican expression has been shown to be regulated by Wnt/β-catenin signalling, the consequence of this negative feedback loop is that there is no significant increase in versican expression which is already highly expressed within the cluster.

When ASCs were cultured as spheroids the expression of αSMA decreased significantly (Figure 3.9). These results suggest that enforced aggregation and immobility result in a decrease in αSMA expression which may correspond to the fact that the cells are no longer migratory, being held in position within the cell cluster. Cells of the lower outer root sheath of the hair follicle exist as a single layer of flattened cells while cells of the DP in their native environment are tightly clustered as spheroids similar to the 3D cell clusters generated in this project.

Hair follicle dermal sheath cells have been shown to be able to migrate down from the lower dermal sheath to become the source of regenerated DP after papillae removal or lower follicle amputation (Oliver, 1966). The results obtained in this study suggest that the rapid switch on of α-SMA expression by cultured DP cells may be explainable by the fact that in monolayer culture hair follicle DP cells loose the contextual and positional cues from their native environment and adopt a more 'migratory' DS like-phenotype as they spread out along the culture dish.

4.3. Evaluating the expression of β-Catenin mRNA in ASCs exposed to Wnt and cultured as spheroids

In this study, no significant changes in β-catenin mRNA expression resulted from culturing ASCs as spheroids or from exposing them to Wnt3a-conditioned medium. The rationale for examining β-catenin expression came from other studies that examined the role of β-catenin gene expression in

hair follicle morphogenesis and demonstrated that β-catenin activity in the DP mediates the inductive effect of the DP on keratinocytes (Enshell-Seijffers et al., 2010) Although β-catenin mRNA may function within the DP of the hair follicle it is an inaccurate marker to quantify the effect of exposure to Wnt3a-conditioned medium as performed in this study and to thereby demonstrate activation of the Wnt-signalling cascade. Visualising or quantifying nuclear localization of the β-catenin protein in ASCs after exposure to Wnt might have given a more accurate picture of their response to the Wnt signalling cascade. There are also other β-catenin target genes such as Axin1, EP2 and LEF1 (Kwack et al., 2013) that would be far more sensitive in demonstrating a response. Therefore, while this study was unable to demonstrate any changes in β-catenin mRNA induced by spheroid culture or exposure to Wnt3a-conditioned medium this does not necessarily reflect inactivity of the Wnt-signalling cascade and no further conclusions can be drawn from these results.

4.4. Alkaline phosphatase mRNA expression as a marker of embryonic hair follicle morphogenesis

Alkaline phosphatase is used as the most reliable indicator of trichogenicity of hair follicle DP cells and has been demonstrated to be highly expressed in the DP of hair follicles in the anagen (inductive) phase of the hair cycle, and in in vivo hair induction assays where the level of alkaline phosphatase expression corresponds to the ability of dermal components to induce de novo hair follicle formation. When the baseline level of alkaline phosphatase gene expression in ASCs was examined in this study it was shown to be almost a quarter that of its expression in human dermal fibroblast (HDFs) (Figure 3.3). HDFs are known to express minimal levels of ALP under routine culture conditions (Hee and Nicoll, 2009). The results of this study are in keeping with other research that has demonstrated that mesenchymal stem cells derived from adipose tissue exhibit significantly lower levels of TNAP transcript and activity than embryonic stem cells, and even than other mesenchymal stem cell lines (Stefkova et al., 2015).

In this project culture of ASCs as spheroids, in Wnt3a conditioned medium or in a combination of the two produced no significant change in alkaline phosphatase mRNA expression. Although the expression of alkaline phosphatase is thought to be a suitable marker of differentiation processes in embryonic tissue (Stefkova et al., 2015), the exact mechanism by which it functions within the mature hair follicle DP to confer increased trichogenicity is unknown. Importantly, increased alkaline phosphatase expression has not been demonstrated in dermal or epithelial elements in embryonic hair follicle morphogenesis. It may be that as this project aims to recapitulate very early events in embryonic hair follicle morphogenesis, alkaline phosphatase expression is not an appropriate marker to use as it is specific for mature anagen hair follicles. Another consideration is that further

manipulations and steps would need to be taken before the expression of alkaline phosphatase mRNA becomes obviously elevated. In addition, further experiments would be needed to confirm whether the lack of significant increase in alkaline phosphatase expression in ASCs that have been clustered and exposed to Wnt in this study can be translated to whether or not these ASC cell clusters would be capable of inducing hair follicle formation in overlying skin.

4.5. Technical difficulties and limitations of this study

Certain technical elements of this project could have been refined to enhance the accuracy of results. As mentioned previously, as yet there is no definitive set of markers specific for hair follicle DP cells. Despite this, it is possible that the markers chosen to evaluate the transition of ASCs to DP cells could have been more specific for hair follicle DP cells. As mentioned, alkaline phosphatase, although considered to be a marker of the inductive capacity of hair follicle dermal papillae cells is widely expressed in embryonic tissue and is therefore not exclusive to the DP (Moss, 1982). Versican has also been shown to be widely expressed throughout the dermis in embryological development and as such is not localised to the DP and a reliable marker thereof (Lebaron, 1996). Furthermore, to increase the reliability of the qPCR reactions to demonstrate expression of DP genes it would have been preferable to have a DP control. This would aid in assessing whether gene expression levels in ASCs were very low and therefore irrelevant and not meaningful.The specific concentration of the Wnt3a protein in the Wnt3a-conditioned medium could have been measured using repeat Bradford assays to give a more accurate indication of how much of this signalling molecule the ASCs were being exposed to. This would have also allowed a spectrum of different concentrations to be tested in order to try and establish the concentration that most closely resembles the Wnt signalling in vivo. As mentioned previously immunocytochemistry to evaluate nuclear β-catenin concentrations and western blotting to quantify the amount of nuclear β-catenin present in ASCs may have been a more accurate method of assaying active WNT-signalling. Choosing other known downstream target genes of the Wnt-signalling cascade, including LEF-1, may also have provided a clearer picture of increased Wnt-signalling.

The events directing hair follicle morphogenesis are so tightly regulated and controlled in terms of physical and spatial queues, interaction between different tissue components and activation and inhibition of specific signalling molecules that to recreate this process in a culture dish is incredibly challenging. With specific reference to hair follicle morphogenesis and the prototypic series of mesenchymal-epithelial interactions, the absence of epithelial cells and a 3D model in which to not only measure epithelial responsiveness but also to trigger the cascade of reciprocal interactions necessary to generate a hair follicle severely limits the extent of hair follicle DP modelling possible.

More research will need to be done in developing human skin and hair follicles to elucidate the specific genes upregulated in embryological hair follicle morphogenesis and try to uncover their specific function in order to provide a clearer picture of the way forward.

4.6. Future work and progress from this study and concluding remarks

Despite the technical difficulties experienced in this project much has been shown that can be used as a foundation for further research. This research demonstrates that human ASCs cultured as spheroids and exposed to Wnt3a conditioned medium generate spheroids with morphological and phenotypic similarities to primary hair follicle DP. Exposure to Wnt and enforced aggregation result in an increase in the expression of versican in ASCs. Versican is the most reliable marker of hair follicle DP cells capable of inducing new follicle formation (Kishimoto et al., 1999a) and therefore its elevated expression may be an indication that ASCs cultured in this way could become capable of combining with epithelial components to induce hair follicle formation. Importantly, the approach used in this project required minimal manipulation and time in culture and as a result of this could potentially be rapidly translatable to clinical trials.

Amazingly, the potential success of using ASCs to generate DP-like cells capable of inducing de novo hair follicle generation was recently proven by Lee et al. (2016). The group isolated and cultured ASCs from canine adipose tissue, and differentiated them into DP- like cells by culturing them in DP forming media. When injected subcutaneously into athymic nude mice these DP-like tissues (DPLTs) exhibited a compact aggregated structure, formed extracellular matrix and highly expressed versican. Critically these DPLTs were able to induce de novo hair follicle formation in the mouse skin and enhanced vascularization in the wound bed which was thought to be due to the effect of vascular endothelial growth factor secreted by DPLTs *in vitro* and *in vivo*. The results of this study suggest that engineered canine DPLTs have characteristics of DP and have a positive effect on hair regeneration by secreting growth factors. This study will need to be repeated using human cells but provided exciting proof of the ability of ASCs to be directed to a DP cell-like fate.

The ability to generate DP-like tissues from ASCs has many obvious advantages. ASCs are readily available from the lipo-aspirates of patients undergoing liposuction, a minimally invasive procedure that can be done under local anaesthetic. Not only would ASCs be readily available from the lipo-aspirates of the index patient, but as ASCs are immunomodulatory and enjoy a degree of 'immune-privilege', there is the potential that ASCs from all patients undergoing liposuction could be harvested and stored for use in allogeneic transplants (Cawthorn et al., 2012). A further significant advantage

to using ASCs is that the secretome of ASCs including growth factors such as vascular endothelial growth factor (VEGF), transforming growth factor-β (TGF-β) and platelet –derived growth factor (PDGF). These molecules mediate a wide range of skin-regenerative effects including, but not limited to an angiogenic capacity and the ability to induce tissue neovascularization that could contribute a macroenvironment with abundant blood supply for hair follicles to regenerate (Cawthorn et al., 2012).

A very exciting first application for the DP-like ASC-spheroids generated in this project would be to seed them in the spaces between the enmeshed split-thickness graft that is placed upon the wound bed following a cutaneous burn wound in current burn wound management. It is likely that the ASC-spheroids would be able to not only facilitate healing of the wound through their secretome but also possibly to interact with epithelial cells migrating from the graft to close the wound bed to possibly induce hair follicle formation. This enhanced healing and hair follicle would hopefully make a significant contribution to regenerating a skin that more closely resembles, in aesthetic appearance and function, normal human skin.

In conclusion, the steps taken in this project provide exciting insight into the use of ASCs to generate hair follicle DP cells by demonstrating that short term spheroid cluster and exposure to Wnt signalling direct ASCs to assume a hair follicle DP-like fate. This is a novel method of DP-like cell generation that uses cells that are readily obtainable from patients, requires minimal time and manipulation in culture and may work synergistically with current burn wound therapies and could therefore potentially be rapidly translatable to clinical trials.

Chapter 5: Appendices

Appendix A – Recipes and Reagents

A.1 1x PBS

Dissolve 8g NaCl, 1.26g Na2HPO4, 0.2g KCl, and 0.2g KH2PO4 in 800ml of distilled water. pH to 7.4 and make up to 1 litre. Autoclave to sterilise and store at 4°C.

A.2 0.05% trypsin/EDTA

Dissolve 0.05g trypsin (Sigma-Aldrich, USA) in 100ml 1xPBS. Add 0.02g EDTA (Sigma-Aldrich, USA) and stir to dissolve. Filter sterilize through 0.22µm filter and aliquot into 50ml tubes. Store at -20°C.

A.3 4% Paraformaldehyde in PBS

Add 4g PFA (Merck, Germany) to 80ml of 1xPBS in fume hood. While in fume hood dissolve by heating and pH to 7.4. Make up to 100 ml and store at 4°C.

A.4 1x TBE

Dissolve 10.8g tris (Merck, Germany), 5.5g boric acid (Sigma-Aldrich, USA), and 0.75g EDTA (Sigma-Aldrich, USA) in 900ml distilled H20. Adjust pH to 8.0. Adjust volume to 1 litre and store at room temperature.

A.5 RIPA Buffer

NaCl 1.5ml, Triton X-100 500µl, SDS 500µl Tris (pH7.5) 1ml and deoxycholate 0,5g were added to 46.5 ml of double distilled H_20 to a final volume of 50ml. The solution was filter-sterilized through a 0.45µm filter and stored in 10ml aliquots at 4^oC.

A.6 12% Resolving Gel for SDS PAGE

40% Acrylamide 3ml, 1.5M Tris (pH8.8) 2.5ml, and 100µl 10% SDS were added to 4.3ml double distilled H20 in a glass beaker and mixed. Ammonium Persulphate (APS) 10% was made up fresh by adding 0.1g Ammonium persulphate powder (Promega, USA) to 1ml sterile ddH20. 10µl TEMED and 100µl 10% APS were added to the solution in the beaker to a final volume of 10ml.

A.7 5% Stacking Gel for SDS PAGE

40% Acrylamide 625µl, 1.5M Tris (pH6.8) 630µl, and 100µl 10% SDS were added to 7.27ml double distilled H20 in a glass beaker and mixed thoroughly. 10µl TEMED and 100µl 10% APS were added to the solution in the beaker to a final volume of 5ml.

A.8 Running Buffer

To make 10x running buffer stock 144g of glycine, 30g of Tris and 10g of SDS were dissolved in 1l double distilled H_20. To make 1x running buffer the 10x solution was diluted 10x with double distilled H_20. Running buffer was stored at 4^oC.

A.9 Transfer Buffer

To make 10x transfer buffer stock 144g of Glycine and 30g of Tris were dissolved in 1l of double distilled H_20. To make 1x transfer buffer the 10x solution was diluted 10x with double distilled H_20. Transfer buffer was stored at 4^oC.

A.10 Tris-buffered saline – 0.1% Tween 20 (TBS-T)

2.42g of Tris Base, 8g of NaCl, 3,8ml of 1M HCl were added to double distilled H_20 to a final volume of 1l to create Tris-buffered saline. The pH was set to 7.6. To generate TBS-T, 1ml of Tween 20 was added to 1l of TBS to a final concentration of 0.1%.

A.11 Ponceau S solution

Ponceau S (Sigma, USA) 1g was added to 50ml 10% Acetic Acid and made up to one litre with double distilled H_20.

Appendix B – Molecular Weight Marker and Protein Ladder

B.1. Molecular Weight Marker – O'Generuler 100bp DNA ladder

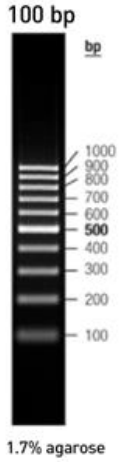

B.2 Protein Ladder – Thermo Scientific PageRuler Prestained Protein Ladder

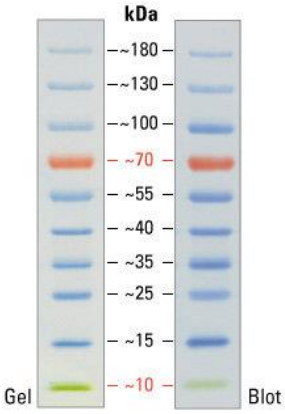

Appendix C – Additional Methods

C.1 Freezing down cells

Cells were lifted with 0.05% trypsin/EDTA, re-suspended in freezing medium (DMEM with 20% FBS and 10% dimethyl sulfoxide (Merck, Germany)), placed in cryogenic tubes and transferred to -80°C overnight. The following day they were placed in liquid nitrogen storage.

C.2 Testing for *Mycoplasma* infection

The presence of a *Mycoplasma* infection in cell lines was tested for by using a Hoechst nuclear stain and standard operating procedure (Chen 1977). Stained cells were visualised using a Zeiss Axiovert 200M fluorescent microscope (Carl Zeiss, Germany). Although treatment with antimycotics for *mycoplasma* is possible, for the purposes of this study all cells found to be contaminated with *mycoplasma* were discarded.

References

ALBERTYN, R., BICKLER, S. W. & RODE, H. 2006. Paediatric burn injuries in Sub Saharan Africa--an overview. *Burns,* 32**,** 605-12.

ANDL, T., REDDY, S. T., GADDAPARA, T. & MILLAR, S. E. 2002. WNT signals are required for the initiation of hair follicle development. *Dev Cell,* 2**,** 643-53.

BAER, P. C. & GEIGER, H. 2012. Adipose-derived mesenchymal stromal/stem cells: tissue localization, characterization, and heterogeneity. *Stem Cells Int,* 2012**,** 812693.

BISHOP, G. H. 1945. Regeneration after experimental removal of skin in man. *American Journal of Anatomy,* 76**,** 153-181.

BOUKAMP, P., PETRUSSEVSKA, R. T., BREITKREUTZ, D., HORNUNG, J., MARKHAM, A. & FUSENIG, N. E. 1988. Normal keratinization in a spontaneously immortalized aneuploid human keratinocyte cell line. *J Cell Biol,* 106**,** 761-71.

CARTHY, J. M., GARMAROUDI, F. S., LUO, Z. & MCMANUS, B. M. 2011. Wnt3a Induces Myofibroblast Differentiation by Upregulating TGF-β Signaling Through SMAD2 in a β-Catenin-Dependent Manner. *PLoS One,* 6.

CASTEILLA, L. & DANI, C. 2006. Adipose tissue-derived cells: from physiology to regenerative medicine. *Diabetes Metab,* 32**,** 393-401.

CAWTHORN, W. P., SCHELLER, E. L. & MACDOUGALD, O. A. 2012. Adipose tissue stem cells: the great WAT hope. *Trends Endocrinol Metab,* 23**,** 270-7.

CHUONG, C. M., COTSARELIS, G. & STENN, K. 2007. Defining hair follicles in the age of stem cell bioengineering. *J Invest Dermatol,* 127**,** 2098-100.

CRAMER, L. M., MC, C. R. & CARROLL, D. B. 1962. Progressive partial excision and early graftin in lethal burns. *Plast Reconstr Surg Transplant Bull,* 30**,** 595-9.

DE BOER, J., WANG, H. J. & VAN BLITTERSWIJK, C. 2004. Effects of Wnt signaling on proliferation and differentiation of human mesenchymal stem cells. *Tissue Eng,* 10**,** 393-401.

DOMINICI, M., LE BLANC, K., MUELLER, I., SLAPER-CORTENBACH, I., MARINI, F., KRAUSE, D., DEANS, R., KEATING, A., PROCKOP, D. & HORWITZ, E. 2006. Minimal criteria for defining multipotent mesenchymal stromal cells. The International Society for Cellular Therapy position statement. *Cytotherapy,* 8**,** 315-7.

EL ATAT, O., ANTONIOS, D., HILAL, G., HOKAYEM, N., ABOU-GHOCH, J., HASHIM, H., SERHAL, R., HEBBO, C., MOUSSA, M. & ALAAEDDINE, N. 2016. An Evaluation of the Stemness, Paracrine, and Tumorigenic Characteristics of Highly Expanded, Minimally Passaged Adipose-Derived Stem Cells. *PLoS One,* 11.

ENSHELL-SEIJFFERS, D., LINDON, C., KASHIWAGI, M. & MORGAN, B. A. 2010. β-catenin activity in the dermal papilla regulates morphogenesis and regeneration of hair. *Dev Cell,* 18**,** 633-42.

FERNANDES, K. J., MCKENZIE, I. A., MILL, P., SMITH, K. M., AKHAVAN, M., BARNABE-HEIDER, F., BIERNASKIE, J., JUNEK, A., KOBAYASHI, N. R., TOMA, J. G., KAPLAN, D. R., LABOSKY, P. A., RAFUSE, V., HUI, C. C. & MILLER, F. D. 2004. A dermal niche for multipotent adult skin-derived precursor cells. *Nat Cell Biol,* 6**,** 1082-93.

FESTA, E., FRETZ, J., BERRY, R., SCHMIDT, B., RODEHEFFER, M., HOROWITZ, M. & HORSLEY, V. 2011. Adipocyte lineage cells contribute to the skin stem cell niche to drive hair cycling. *Cell,* 146**,** 761-71.

FORJUOH, S. N. 2006. Burns in low- and middle-income countries: a review of available literature on descriptive epidemiology, risk factors, treatment, and prevention. *Burns,* 32**,** 529-37.

FOTY, R. 2011. A simple hanging drop cell culture protocol for generation of 3D spheroids. *J Vis Exp*.

FUCHS, E. 2007. Scratching the surface of skin development. *Nature,* 445**,** 834-42.

FUJIE, T., KATOH, S., OURA, H., URANO, Y. & ARASE, S. 2001. The chemotactic effect of a dermal papilla cell-derived factor on outer root sheath cells. *J Dermatol Sci,* 25**,** 206-12.

GHONE, N. V. & GRAYSON, W. L. 2012. Recapitulation of mesenchymal condensation enhances in vitro chondrogenesis of human mesenchymal stem cells. *J Cell Physiol,* 227**,** 3701-8.

GIMBLE, J. M. 2003. Adipose tissue-derived therapeutics. *Expert Opin Biol Ther,* 3**,** 705-13.

GLOVER, J. D., WELLS, K. L., MATTHAUS, F., PAINTER, K. J., HO, W., RIDDELL, J., JOHANSSON, J. A., FORD, M. J., JAHODA, C. A. B., KLIKA, V., MORT, R. L. & HEADON, D. J. 2017. Hierarchical patterning modes orchestrate hair follicle morphogenesis. *PLoS Biol,* 15**,** e2002117.

GNEDEVA, K., VOROTELYAK, E., CIMADAMORE, F., CATTAROSSI, G., GIUSTO, E., TERSKIKH, V. V. & TERSKIKH, A. V. 2015. Derivation of hair-inducing cell from human pluripotent stem cells. *PLoS One,* 10**,** e0116892.

HANDJISKI, B. K., EICHMULLER, S., HOFMANN, U., CZARNETZKI, B. M. & PAUS, R. 1994. Alkaline phosphatase activity and localization during the murine hair cycle. *Br J Dermatol,* 131**,** 303-10.

HARDY, M. H. 1992. The secret life of the hair follicle. *Trends Genet,* 8**,** 55-61.

HE, J., DUAN, H., XIONG, Y., ZHANG, W., ZHOU, G., CAO, Y. & LIU, W. 2013. Participation of CD34-enriched mouse adipose cells in hair morphogenesis. *Mol Med Rep,* 7**,** 1111-6.

HE, S., LU, Y., LIU, X., HUANG, X., KELLER, E. T., QIAN, C. N. & ZHANG, J. 2015. Wnt3a: functions and implications in cancer. *Chin J Cancer,* 34.

HE, X., SEMENOV, M., TAMAI, K. & ZENG, X. 2004. LDL receptor-related proteins 5 and 6 in Wnt/beta-catenin signaling: arrows point the way. *Development,* 131**,** 1663-77.

HEE, C. K. & NICOLL, S. B. 2009. Endogenous Bone Morphogenetic Proteins Mediate 1α,25-Dihydroxyvitamin D(3)-Induced Expression of Osteoblast Differentiation Markers in Human Dermal Fibroblasts. *J Orthop Res,* 27**,** 162-8.

HIGGINS, C. A., CHEN, J. C., CERISE, J. E., JAHODA, C. A. & CHRISTIANO, A. M. 2013. Microenvironmental reprogramming by three-dimensional culture enables dermal papilla cells to induce de novo human hair-follicle growth. *Proc Natl Acad Sci U S A,* 110**,** 19679-88.

HIGGINS, C. A., RICHARDSON, G. D., FERDINANDO, D., WESTGATE, G. E. & JAHODA, C. A. 2010. Modelling the hair follicle dermal papilla using spheroid cell cultures. *Exp Dermatol,* 19**,** 546-8.

HOLBROOK, K. A. & MINAMI, S. I. 1991. Hair follicle embryogenesis in the human. Characterization of events in vivo and in vitro. *Ann N Y Acad Sci,* 642**,** 167-96.

HOMBACH-KLONISCH, S., PANIGRAHI, S., RASHEDI, I., SEIFERT, A., ALBERTI, E., POCAR, P., KURPISZ, M., SCHULZE-OSTHOFF, K., MACKIEWICZ, A. & LOS, M. 2008. Adult stem cells and their trans-differentiation potential--perspectives and therapeutic applications. *J Mol Med (Berl),* 86**,** 1301-14.

HUANG, Y. C., CHAN, C. C., LIN, W. T., CHIU, H. Y., TSAI, R. Y., TSAI, T. H., CHAN, J. Y. & LIN, S. J. 2013. Scalable production of controllable dermal papilla spheroids on PVA surfaces and the effects of spheroid size on hair follicle regeneration. *Biomaterials,* 34**,** 442-51.

HUELSKEN, J., VOGEL, R., ERDMANN, B., COTSARELIS, G. & BIRCHMEIER, W. 2001. beta-Catenin controls hair follicle morphogenesis and stem cell differentiation in the skin. *Cell,* 105**,** 533-45.

HUH, S. H., NARHI, K., LINDFORS, P. H., HAARA, O., YANG, L., ORNITZ, D. M. & MIKKOLA, M. L. 2013. Fgf20 governs formation of primary and secondary dermal condensations in developing hair follicles. *Genes Dev,* 27**,** 450-8.

INAMATSU, M., MATSUZAKI, T., IWANARI, H. & YOSHIZATO, K. 1998. Establishment of rat dermal papilla cell lines that sustain the potency to induce hair follicles from afollicular skin. *J Invest Dermatol,* 111**,** 767-75.

ITO, M., LIU, Y., YANG, Z., NGUYEN, J., LIANG, F., MORRIS, R. J. & COTSARELIS, G. 2005. Stem cells in the hair follicle bulge contribute to wound repair but not to homeostasis of the epidermis. *Nat Med,* 11**,** 1351-4.

ITO, M., YANG, Z., ANDL, T., CUI, C., KIM, N., MILLAR, S. E. & COTSARELIS, G. 2007. Wnt-dependent de novo hair follicle regeneration in adult mouse skin after wounding. *Nature,* 447**,** 316-20.

JAHODA, C. & OLIVER, R. F. 1981. The growth of vibrissa dermal papilla cells in vitro. *Br J Dermatol,* 105**,** 623-7.

JAHODA, C. A., HORNE, K. A. & OLIVER, R. F. 1984. Induction of hair growth by implantation of cultured dermal papilla cells. *Nature,* 311**,** 560-2.

JAHODA, C. A. & OLIVER, R. F. 1984. Vibrissa dermal papilla cell aggregative behaviour in vivo and in vitro. *J Embryol Exp Morphol,* 79**,** 211-24.

JAHODA, C. A., REYNOLDS, A. J., CHAPONNIER, C., FORESTER, J. C. & GABBIANI, G. 1991. Smooth muscle alpha-actin is a marker for hair follicle dermis in vivo and in vitro. *J Cell Sci,* 99 (Pt 3)**,** 627-36.

JIMENEZ, F., POBLET, E. & IZETA, A. 2015. Reflections on how wound healing-promoting effects of the hair follicle can be translated into clinical practice. *Experimental Dermatology,* 24**,** 91-94.

KAMIMURA, J., LEE, D., BADEN, H. P., BRISSETTE, J. & DOTTO, G. P. 1997. Primary mouse keratinocyte cultures contain hair follicle progenitor cells with multiple differentiation potential. *J Invest Dermatol,* 109**,** 534-40.

KATOH, M. & KATOH, M. 2005. Comparative genomics on Wnt8a and Wnt8b genes. *Int J Oncol,* 26**,** 1129-33.

KIM, S. R., CHA, S. Y., KIM, M. K., KIM, J. C. & SUNG, Y. K. 2006. Induction of versican by ascorbic acid 2-phosphate in dermal papilla cells. *J Dermatol Sci,* 43**,** 60-2.

KISHIMOTO, J., BURGESON, R. E. & MORGAN, B. A. 2000. Wnt signaling maintains the hair-inducing activity of the dermal papilla. *Genes Dev,* 14**,** 1181-5.

KISHIMOTO, J., EHAMA, R., WU, L., JIANG, S., JIANG, N. & BURGESON, R. E. 1999a. Selective activation of the versican promoter by epithelial- mesenchymal interactions during hair follicle development. *Proc Natl Acad Sci U S A,* 96**,** 7336-41.

KISHIMOTO, J., EHAMA, R., WU, L., JIANG, S., JIANG, N. & BURGESON, R. E. 1999b. Selective activation of the versican promoter by epithelial– mesenchymal interactions during hair follicle development. *Proc Natl Acad Sci U S A,* 96**,** 7336-41.

KOELLENSPERGER, E., BOLLINGER, N., DEXHEIMER, V., GRAMLEY, F., GERMANN, G. & LEIMER, U. 2014. Choosing the right type of serum for different applications of human adipose tissue-derived stem cells: influence on proliferation and differentiation abilities. *Cytotherapy,* 16**,** 789-99.

KWACK, M. H., KIM, M. K., KIM, J. C. & SUNG, Y. K. 2013. Wnt5a attenuates Wnt/β-catenin signalling in human dermal papilla cells. *Experimental Dermatology,* 22**,** 229-231.

LEBARON, R. G. 1996. Versican. *Perspect Dev Neurobiol,* 3**,** 261-71.

LEE, A. 2016. Hair growth promoting effect of dermal papilla like tissues from canine. 78**,** 1811-8.

LEE, H. J., KANG, K. S., KANG, S. Y., KIM, H. S., PARK, S. J., LEE, S. Y., KIM, K. D., LEE, H. C., PARK, J. K., PAIK, W. Y., LEE, L. & YEON, S. C. 2016. Immunologic properties of differentiated and undifferentiated mesenchymal stem cells derived from umbilical cord blood. *J Vet Sci,* 17**,** 289-97.

LIVAK, K. J. & SCHMITTGEN, T. D. 2001. Analysis of relative gene expression data using real-time quantitative PCR and the 2(-Delta Delta C(T)) Method. *Methods,* 25**,** 402-8.

LYNN, A. K., YANNAS, I. V. & BONFIELD, W. 2004. Antigenicity and immunogenicity of collagen. *J Biomed Mater Res B Appl Biomater,* 71**,** 343-54.

MAO, J., WANG, J., LIU, B., PAN, W., FARR, G. H., 3RD, FLYNN, C., YUAN, H., TAKADA, S., KIMELMAN, D., LI, L. & WU, D. 2001. Low-density lipoprotein receptor-related protein-5 binds to Axin and regulates the canonical Wnt signaling pathway. *Mol Cell,* 7**,** 801-9.

MCELWEE, K. J., KISSLING, S., WENZEL, E., HUTH, A. & HOFFMANN, R. 2003. Cultured peribulbar dermal sheath cells can induce hair follicle development and contribute to the dermal sheath and dermal papilla. *J Invest Dermatol,* 121**,** 1267-75.

MIDORIKAWA, T., CHIKAZAWA, T., YOSHINO, T., TAKADA, K. & ARASE, S. 2004. Different gene expression profile observed in dermal papilla cells related to androgenic alopecia by DNA macroarray analysis. *J Dermatol Sci,* 36**,** 25-32.

MILLAR, S. E. 2002. Molecular Mechanisms Regulating Hair Follicle Development. 118**,** 216-225.

MOSS, D. W. 1982. Alkaline phosphatase isoenzymes. *Clin Chem,* 28**,** 2007-16.

MULLER-ROVER, S., HANDJISKI, B., VAN DER VEEN, C., EICHMULLER, S., FOITZIK, K., MCKAY, I. A., STENN, K. S. & PAUS, R. 2001. A comprehensive guide for the accurate classification of murine hair follicles in distinct hair cycle stages. *J Invest Dermatol,* 117**,** 3-15.

NIEMANN, C. & HORSLEY, V. 2012. Development and homeostasis of the sebaceous gland. *Semin Cell Dev Biol,* 23**,** 928-36.

NORAMLY, S., FREEMAN, A. & MORGAN, B. A. 1999. beta-catenin signaling can initiate feather bud development. *Development,* 126**,** 3509-21.

OHYAMA, M., KOBAYASHI, T., SASAKI, T., SHIMIZU, A. & AMAGAI, M. 2012. Restoration of the intrinsic properties of human dermal papilla in vitro. *J Cell Sci,* 125**,** 4114-25.

OHYAMA, M. & VERAITCH, O. 2013. Strategies to enhance epithelial-mesenchymal interactions for human hair follicle bioengineering. *J Dermatol Sci,* 70**,** 78-87.

OHYAMA, M., ZHENG, Y., PAUS, R. & STENN, K. S. 2010. The mesenchymal component of hair follicle neogenesis: background, methods and molecular characterization. *Exp Dermatol,* 19**,** 89-99.

OLIVER, R. F. 1966. Histological studies of whisker regeneration in the hooded rat. *J Embryol Exp Morphol,* 16**,** 231-44.

OLIVER, R. F. 1967. The experimental induction of whisker growth in the hooded rat by implantation of dermal papillae. *J Embryol Exp Morphol,* 18**,** 43-51.

OLIVER, R. F. 1970. The induction of hair follicle formation in the adult hooded rat by vibrissa dermal papillae. *J Embryol Exp Morphol,* 23**,** 219-36.

OSADA, A., IWABUCHI, T., KISHIMOTO, J., HAMAZAKI, T. S. & OKOCHI, H. 2007. Long-term culture of mouse vibrissal dermal papilla cells and de novo hair follicle induction. *Tissue Eng,* 13**,** 975-82.

PANTELEYEV, A. A., VAN DER VEEN, C., ROSENBACH, T., MULLER-ROVER, S., SOKOLOV, V. E. & PAUS, R. 1998. Towards defining the pathogenesis of the hairless phenotype. *J Invest Dermatol,* 110**,** 902-7.

PARK, I. S., CHUNG, P. S. & AHN, J. C. 2015. Enhancement of Ischemic Wound Healing by Spheroid Grafting of Human Adipose-Derived Stem Cells Treated with Low-Level Light Irradiation. *PLoS One,* 10**,** e0122776.

PAUS, R., ITO, N., TAKIGAWA, M. & ITO, T. 2003. The hair follicle and immune privilege. *J Investig Dermatol Symp Proc,* 8**,** 188-94.

PAUS, R., MULLER-ROVER, S., VAN DER VEEN, C., MAURER, M., EICHMULLER, S., LING, G., HOFMANN, U., FOITZIK, K., MECKLENBURG, L. & HANDJISKI, B. 1999. A comprehensive guide for the recognition and classification of distinct stages of hair follicle morphogenesis. *J Invest Dermatol,* 113**,** 523-32.

PLIKUS, M. V., GAY, D. L., TREFFEISEN, E., WANG, A., SUPAPANNACHART, R. J. & COTSARELIS, G. 2012. Epithelial stem cells and implications for wound repair. *Semin Cell Dev Biol,* 23**,** 946-53.

RAHMANI, M., READ, J. T., CARTHY, J. M., MCDONALD, P. C., WONG, B. W., ESFANDIAREI, M., SI, X., LUO, Z., LUO, H., RENNIE, P. S. & MCMANUS, B. M. 2005. Regulation of the versican promoter by the beta-catenin-T-cell factor complex in vascular smooth muscle cells. *J Biol Chem,* 280**,** 13019-28.

RENDL, M., POLAK, L. & FUCHS, E. 2008. BMP signaling in dermal papilla cells is required for their hair follicle-inductive properties. *Genes Dev,* 22**,** 543-57.

REYNOLDS, A. J., LAWRENCE, C., CSERHALMI-FRIEDMAN, P. B., CHRISTIANO, A. M. & JAHODA, C. A. 1999. Trans-gender induction of hair follicles. *Nature,* 402**,** 33-4.

REYNOLDS, A. J., OLIVER, R. F. & JAHODA, C. A. 1991. Dermal cell populations show variable competence in epidermal cell support: stimulatory effects of hair papilla cells. *J Cell Sci,* 98 (Pt 1)**,** 75-83.

RUTBERG, S. E., KOLPAK, M. L., GOURLEY, J. A., TAN, G., HENRY, J. P. & SHANDER, D. 2006. Differences in expression of specific biomarkers distinguish human beard from scalp dermal papilla cells. *J Invest Dermatol,* 126**,** 2583-95.

SAPPINO, A. P., SCHURCH, W. & GABBIANI, G. 1990. Differentiation repertoire of fibroblastic cells: expression of cytoskeletal proteins as marker of phenotypic modulations. *Lab Invest,* 63**,** 144-61.

SCHMIDT-ULLRICH, R. & PAUS, R. 2005. Molecular principles of hair follicle induction and morphogenesis. *Bioessays,* 27**,** 247-61.

SCHNEIDER, M. R., SCHMIDT-ULLRICH, R. & PAUS, R. 2009. The hair follicle as a dynamic miniorgan. *Curr Biol,* 19**,** R132-42.

SENNETT, R. & RENDL, M. 2012. Mesenchymal-epithelial interactions during hair follicle morphogenesis and cycling. *Semin Cell Dev Biol,* 23**,** 917-27.

SENNETT, R., WANG, Z., REZZA, A., GRISANTI, L., ROITERSHTEIN, N., SICCHIO, C., MOK, K. W., HEITMAN, N. J., CLAVEL, C., MA'AYAN, A. & RENDL, M. 2015. An Integrated Transcriptome Atlas of Embryonic Hair Follicle Progenitors, their Niche and the Developing Skin. *Dev Cell,* 34**,** 577-91.

SLEEMAN, M. A., MURISON, J. G., STRACHAN, L., KUMBLE, K., GLENN, M. P., MCGRATH, A., GRIERSON, A., HAVUKKALA, I., TAN, P. L. & WATSON, J. D. 2000. Gene expression in rat dermal papilla cells: analysis of 2529 ESTs. *Genomics,* 69**,** 214-24.

SOMA, T., TAJIMA, M. & KISHIMOTO, J. 2005. Hair cycle-specific expression of versican in human hair follicles. *J Dermatol Sci,* 39**,** 147-54.

ST-JACQUES, B., DASSULE, H. R., KARAVANOVA, I., BOTCHKAREV, V. A., LI, J., DANIELIAN, P. S., MCMAHON, J. A., LEWIS, P. M., PAUS, R. & MCMAHON, A. P. 1998. Sonic hedgehog signaling is essential for hair development. *Curr Biol,* 8**,** 1058-68.

STEFKOVA, K., PROCHAZKOVA, J. & PACHERNIK, J. 2015. Alkaline phosphatase in stem cells. *Stem Cells Int,* 2015**,** 628368.

STROMPS, J. P., PAUL, N. E., RATH, B., NOURBAKHSH, M., BERNHAGEN, J. & PALLUA, N. 2014. Chondrogenic differentiation of human adipose-derived stem cells: a new path in articular cartilage defect management? *Biomed Res Int,* 2014**,** 740926.

TESAR, P. J., CHENOWETH, J. G., BROOK, F. A., DAVIES, T. J., EVANS, E. P., MACK, D. L., GARDNER, R. L. & MCKAY, R. D. 2007. New cell lines from mouse epiblast share defining features with human embryonic stem cells. *Nature,* 448**,** 196-9.

VAN VOLLENSTEE, F. A., JACKSON, C., HOFFMANN, D., POTGIETER, M., DURANDT, C. & PEPPER, M. S. 2016. Human adipose derived mesenchymal stromal cells transduced with GFP lentiviral vectors: assessment of immunophenotype and differentiation capacity in vitro. *Cytotechnology,* 68**,** 2049-60.

VERAITCH, O., MABUCHI, Y., MATSUZAKI, Y., SASAKI, T., OKUNO, H., TSUKASHIMA, A., AMAGAI, M., OKANO, H. & OHYAMA, M. 2017. Induction of hair follicle dermal papilla cell properties in human induced pluripotent stem cell-derived multipotent LNGFR(+)THY-1(+) mesenchymal cells. *Sci Rep,* 7**,** 42777.

WILLERT, K., BROWN, J. D., DANENBERG, E., DUNCAN, A. W., WEISSMAN, I. L., REYA, T., YATES, J. R., 3RD & NUSSE, R. 2003. Wnt proteins are lipid-modified and can act as stem cell growth factors. *Nature,* 423**,** 448-52.

WODARZ, A. & NUSSE, R. 1998. Mechanisms of Wnt signaling in development. *Annu Rev Cell Dev Biol,* 14**,** 59-88.

WU, P., HOU, L., PLIKUS, M., HUGHES, M., SCEHNET, J., SUKSAWEANG, S., WIDELITZ, R., JIANG, T. X. & CHUONG, C. M. 2004. Evo-Devo of amniote integuments and appendages. *Int J Dev Biol,* 48**,** 249-70.

YANG, C. C. & COTSARELIS, G. 2010. Review of hair follicle dermal cells. *J Dermatol Sci,* 57**,** 2-11.

YANG, Y., LI, Y., WANG, Y., WU, J., YANG, G., YANG, T., GAO, Y. & LU, Y. 2012. Versican gene: regulation by the beta-catenin signaling pathway plays a significant role in dermal papilla cell aggregative growth. *J Dermatol Sci,* 68**,** 157-63.

ZHANG, P., KLING, R. E., RAVURI, S. K., KOKAI, L. E., RUBIN, J. P., CHAI, J. K. & MARRA, K. G. 2014. A review of adipocyte lineage cells and dermal papilla cells in hair follicle regeneration. *Journal of Tissue Engineering,* 5.

ZHANG, Y., CAO, L., KIANI, C. G., YANG, B. L. & YANG, B. B. 1998. The G3 domain of versican inhibits mesenchymal chondrogenesis via the epidermal growth factor-like motifs. *J Biol Chem,* 273**,** 33054-63.

ZHENG, P. S., VAIS, D., LAPIERRE, D., LIANG, Y. Y., LEE, V., YANG, B. L. & YANG, B. B. 2004. PG-M/versican binds to P-selectin glycoprotein ligand-1 and mediates leukocyte aggregation. *J Cell Sci,* 117**,** 5887-95.

ZIMMERMANN, D. R. & RUOSLAHTI, E. 1989. Multiple domains of the large fibroblast proteoglycan, versican. *Embo j,* 8**,** 2975-81.

ZUK, P. A., ZHU, M., MIZUNO, H., HUANG, J., FUTRELL, J. W., KATZ, A. J., BENHAIM, P., LORENZ, H. P. & HEDRICK, M. H. 2001. Multilineage cells from human adipose tissue: implications for cell-based therapies. *Tissue Eng,* 7**,** 211-28.